CHIRAL POLYMER PHOTODETECTOR

by

Yiwei Zhang

A thesis submitted to the Department of Chemistry

In conformity with the requirements for

the degree of Master of Science

Queen's University

Kingston, Ontario, Canada

(March, 2014)

Abstract

A polymer photodetector is fabricated using polythiophene with chiral alkyl side chains. The Cotton effect is observed in the CD spectrum of the photodetector, indicating an unequal absorbance of left- and right-handed circular polarized light (CPL). The photodetector is proven to be able to identify incident left- and right-handed CPL.

Polymer photodetectors that are made from R- and S-limonene induced achiral polymers are fabricated. A "hot spin-coating" process is introduced to cast uniform limonene induced polymer films. As a result of chirality transfer, Cotton effects are also observed in these photodetectors' CD spectra.

A model is suggested to explain the chirality generation of the polythiophene with chiral alkyl side chains and limonene induced achiral polymers.

Acknowledgements

It has been a very interesting experience to study as a graduate student in Queen's University. My life and research in past two years, in this adorable town, Kingston, was just a grace. My supervisor, Dr. Jean-Michel Nunzi, is not only a knowledgeable and creative mentor in science, but also a great and kind-hearted mentor of life to me. The completion of the thesis would not have been possible without his valuable advices, kind help and lots of supports in all stages of my study.

I would like to thank my co-supervisor Dr. Erwin Buncel, for his guidance on research and kind support on the thesis. His knowledge in organic chemistry is a treasury of mine. I also want to thank my supervisory committee members, Dr. Guojun Liu for his expert advice on polymer science and Dr. Hans-Peter Loock for his great help on optical physics. Dr. Loock's lecture very helpful in my research. I would specifically like to thank Dr. Ribal Georges Sabat for his very valuable advices on physics and his kind support for the laser experiment.

I am thankful for Dr. Gabriela Aldea-Nunzi and Dr. Feng Liu's help for teaching me experimental skills. Matthew Schuster, Konrad Piskorz, Thomas Meredith Kraft, Yue Tao, Sanyasi Rao, Yolène Sacchettini, Nam Musterer, Somayeh Mirzaee, Leila Mazaheri, Tham Adhikari and Jimmy Zhan all gave me kind help on research, I would like to thank them all for being great lab mates.

I would like to thank my father Zhang Qiang, my mother Li Hong and my step mother Lu Weimin. I would never have finish my study without their endless love and support.

Table of Contents

List of Figures

List of Tables

List of Abbreviations

CPL	**Circular polarized light**
CuPc	Copper phthalocyanine
DCV	Dicyanovinyl
DPP	Diketopyrrolopyrrole
E_g	Band gap
F8T2	Poly[(9,9-dioctylfluorenyl-2,7-diyl)-co-bithiophene]
gCD	Kuhn's g-factor
HOMO	Highest occupied molecular orbital
ITO	Indium Tin Oxide
LUMO	Lowest unoccupied molecular orbital
MDMO-PPV	Poly[2-methoxy-5-(3,7-dimethyloctyloxy)-1,4-phenylene vinylene]
MEH-PPV	poly[2-methoxy-5-(20-ethylhexyloxy)-1,4-phenylene vinylene]
MO	Molecular orbital
ORD	Optical rotatory dispersion
P3HT	Poly(3-hexylthiophene-2,5-diyl)
PCBM	Phenyl-C61-butyric acid methyl ester
PEM	Photo-elastic modulator
PIN-PD	p-i-n photodetector

PPV	Polyphenylenevinylenes
QWP	Quarter wave plate

Chapter 1

Introduction

1.1 Introduction of photodetector

1.1.1 Definition and application of photodetector

1.1.1.1 Definition of Photodetector

A photodetector is a sensor of light or other electromagnetic energies. [1] In most cases, a photodetector is a solid-state transducer that is used for converting light energies into electrical energies. However, there are some kinds of photodetectors that convert light energy to energies other than electrical energy, like kinetic energy. For example, Crooks and Nichols radiometers, which detect light by sensing light pressure.

1.1.1.2 Application of photodetectors

A major application of photodetectors is in the optical fiber communication system. Fiber-optic communication systems include an optical transmitter, a cable containing bundles of multiple optical fibers, as the transmission medium, and a photo-receiver to recover the signal as an electrical signal. (**Figure 1-1**)

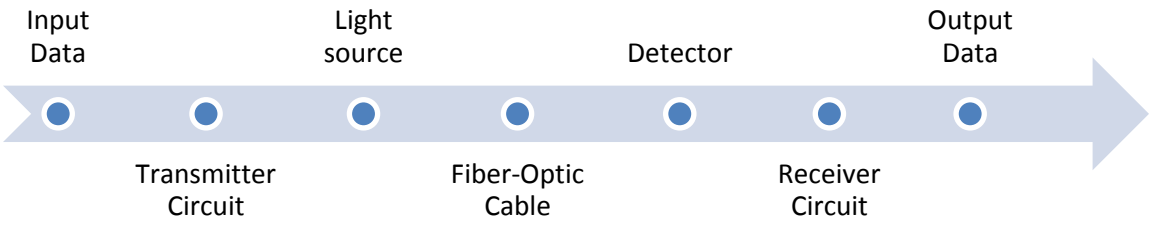

Figure 1-1 Schematic diagram of optical fiber communication

Figure 1-1 describes the basic scheme of fiber-optic communication systems. The detector (photodetector) is a key component of the system. A better performance photodetector, for example, a photodetector with higher sensitivity, can contribute to a transmitting system with fewer signal repeaters; faster response of the photodetector can contribute to a wider bandwidth, as a higher frequency can be used in the communication system.

Imaging sensors are another important application of photodetectors; the most currently used types are digital charge-coupled device (CCD) and complementary metal–oxide–semiconductor (CMOS) active pixel sensors. They are now widely used in cameras, scanners, bar code scanners and other imagers.

Other than fibre-optic communication systems and image sensing, photodetectors are also widely used in scientific research, such as particle detectors and photomultipliers for photon detection.

1.1.2 Conventional photodetector

1.1.2.1 Photoconductor

A photoconductor, or a photoresistor is a resistor for which resistance changes with the change of incident light intensity; in other words, it exhibits photoconductivity.

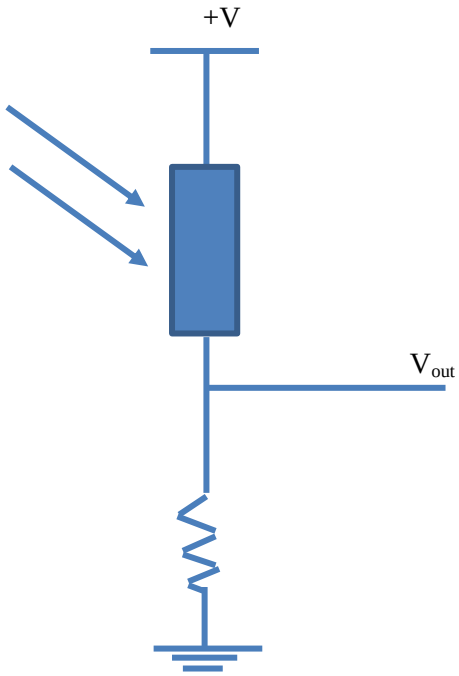

Figure 1-2 Scheme of a photoconductor

Figure 1-2 is a basic scheme of a photoconductor. A bias voltage +V is applied to the device. Photocurrent generated by the incident photons is detected by the output voltage.[2] The absorbed photons excite a carrier to a higher energy level, and result in a change of conductivity of the material; thus a change of resistance of the device happens.

There are two types of photoconductors: intrinsic and extrinsic. In an intrinsic photoconductor, carriers are excited from the valence band to conduction band, creating an electron-hole pair, which changes the conductivity.

In an extrinsic photoconductor, the material is doped. Carriers are excited from an impurity level, which is usually higher than its valence band, to the conduction band. So

the band gap (E_g) of extrinsic photoconductors are much lower than that of intrinsic photoconductors. (**Figure 1-3**)

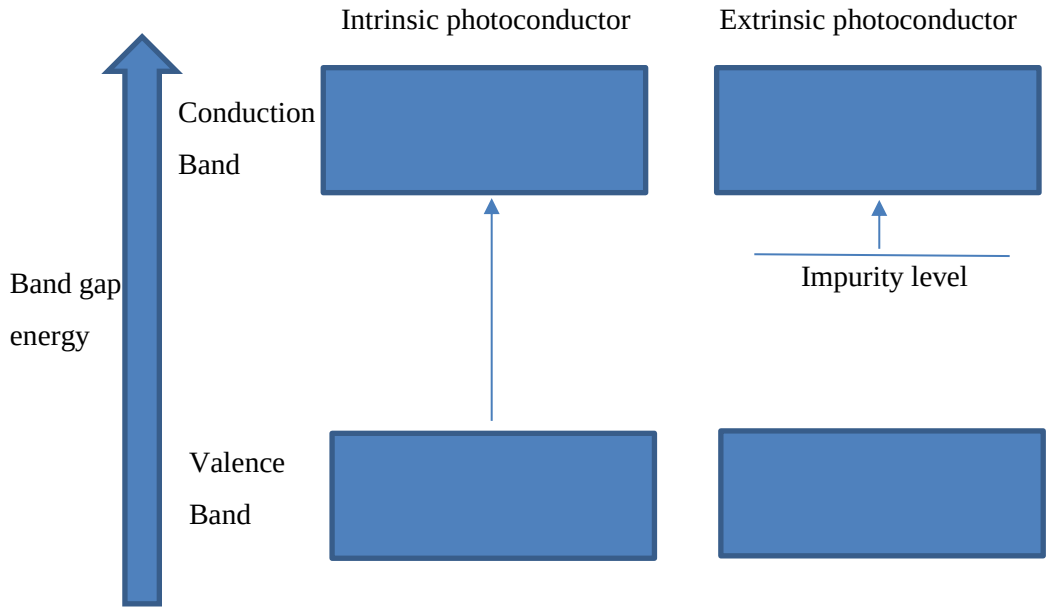

Figure 1-3 Energy level of intrinsic and extrinsic photoconductors

As the excitation of a carrier in intrinsic photoconductors calls for photon energy that is higher than the band gap, its sensitivity depends on the wavelength. An extrinsic photoconductor can have a smaller E_g so it can be used to detect long wavelength light (beyond 5μm). However, they suffer from low sensitivity and slow response speed, as well as high noise under room temperature. These extrinsic photodetectors need to be cooled in liquid nitrogen temperature when operated.[2]

1.1.2.2 Junction photodiode

A basic junction photodiode is a p-n junction diode that works under a reverse bias voltage. The bias voltage creates a depletion region with high electric field. Photons

absorbed in the depletion region create electron-hole pairs, which separated by the electric field, contribute to photocurrent.

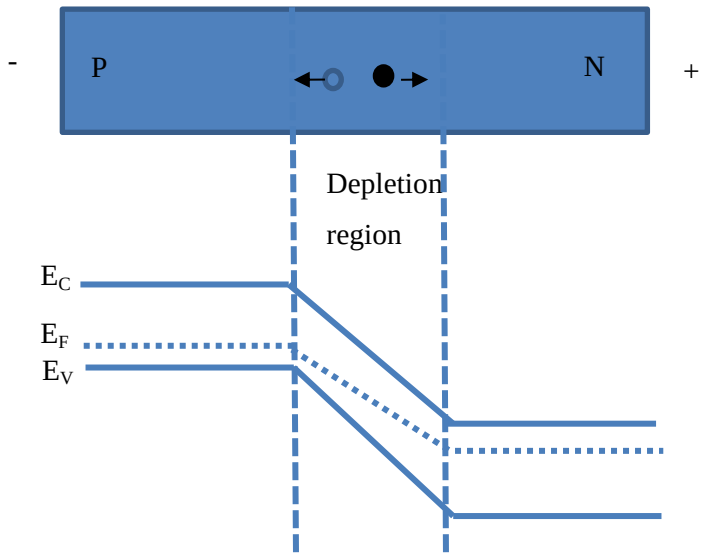

Figure 1-4 Energy-band diagram of a reverse biased p-n junction

A p-i-n photodetector (PIN-PD) has a similar structure of basic junction photodiodes. Other than the p layer and n layer, an intrinsic or very low n- or p-doped middle layer is sandwiched between them, where the photon absorption mostly happens. **Figure 1-5** shows the structure of a PIN-PD. The middle i-layer offers high resistance, so a large electric field exists in i-layer. The incident light is mostly absorbed by the i-region of the photodiode. [3] These photodetectors are used in fibre-optic communication because of their high bandwidth (The difference between the upper and lower frequencies using for the communication), and high detectivity.

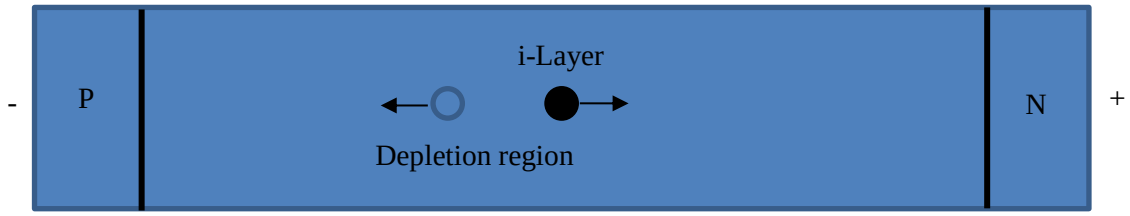

Figure 1-5 Structure of p-i-n photodiode

1.1.2.3 Avalanche photodiode

An avalanche photodiode is a photodiode with avalanche multiplication. With a structure similar to that of a junction photodiode, an avalanche photodiode provides internal current gain in a similar way as photomultiplier tubes.[3]

Avalanche multiplication is a result of impact ionization of carriers. When a carrier is injected into an electric field, it can be accelerated and gain kinetic energy. When this fast carrier hits a lattice, another electron-hole pair is generated. Then the new carrier can be accelerated again and allows impact ionization to happen more times. The gain is thereby achieved.

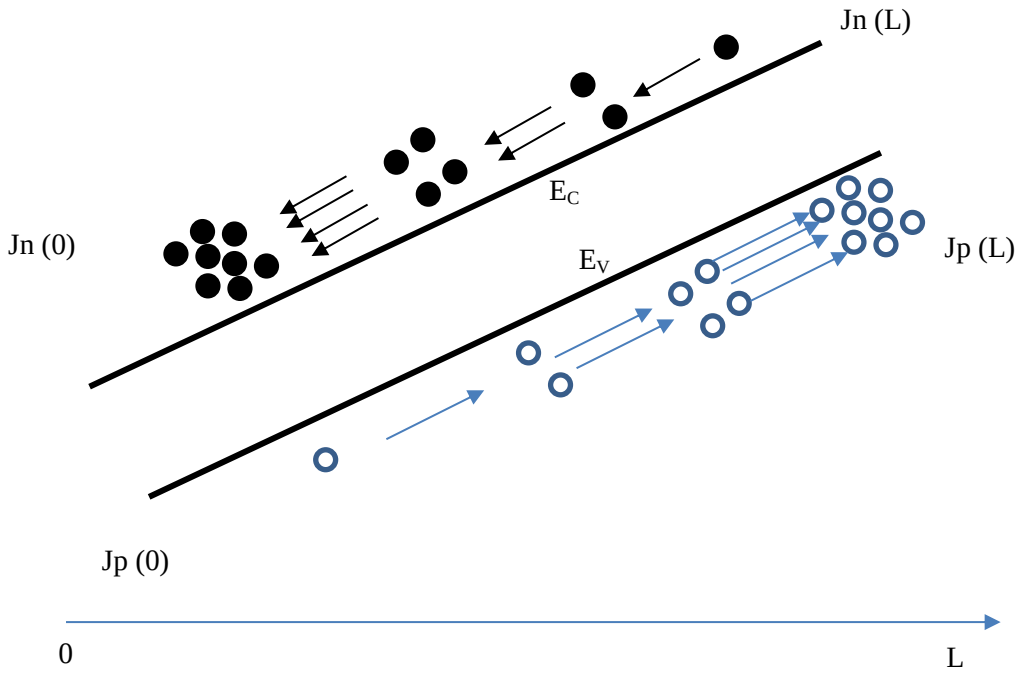

Figure 1-6 Avalanche multiplication with impact ionization, within a high-field region of length L[4]

1.1.2.4 Phototransistor

A phototransistor is a bipolar junction transistor. Like a standard transistor, it can amplify photocurrent by its built-in photodiode. The structure of a phototransistor is usually similar to a common transistor, the major difference is that phototransistors usually have a small emitter and a large base and collector, compared to a common transistor. A phototransistor works under a reversed biased collector-base bias. However, unlike a regular transistor, there is no base-emitter bias, the phototransistor generates the base current with incident light.

As shown in **Figure 1-7**, when light shines on a phototransistor, carriers generated in the base float into the collector, while carriers generated in collector float to the base. As charges accumulate in the base, there is a forward bias that appears between the emitter and the base, making charges float from emitter to base. However, only a small portion of charges neutralise in the base, most of them inject into the collector, and result in the gain.

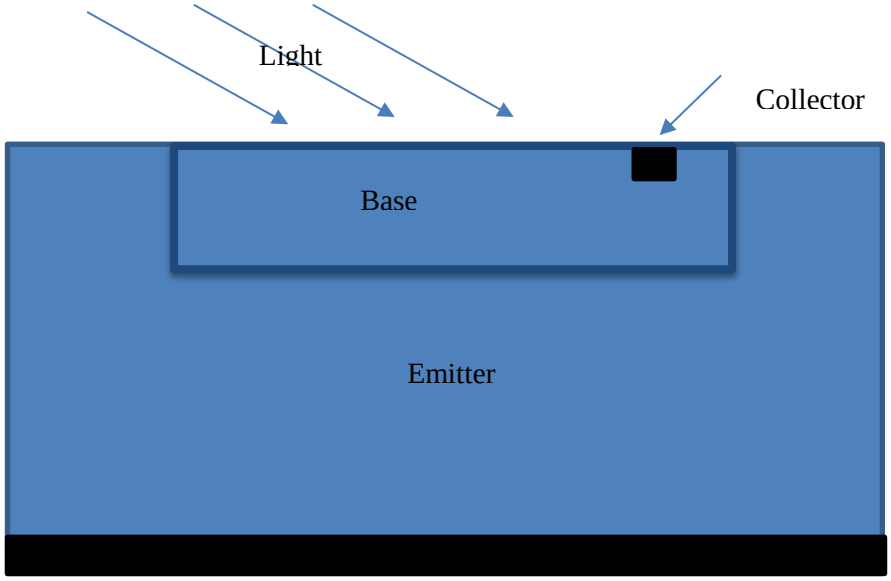

Figure 1-7 Example of a phototransistor

We can see from the mechanism that, the higher the emitter-base potential, the more charges inject from emitter to collector, which lead to a higher gain. The reason of a large base is that the base is the light-absorbing area.

1.1.2.5 Quantum well and quantum dot infrared photodetector

Unlike the photodetectors that we introduced previously, which work by band to band photon absorption, the photon absorption of a quantum well/dot photodetector occurs within the conduction band or valence band.

A quantum well is a potential well with discrete energy values. A photon excites an electron from the ground states in the quantum well to the first bound state, for which the excitation energy is lower than the barrier energy. Then, the electron tunnels out of the quantum well as photocurrent. **Figure 1-8** shows the basic scheme of the mechanism:

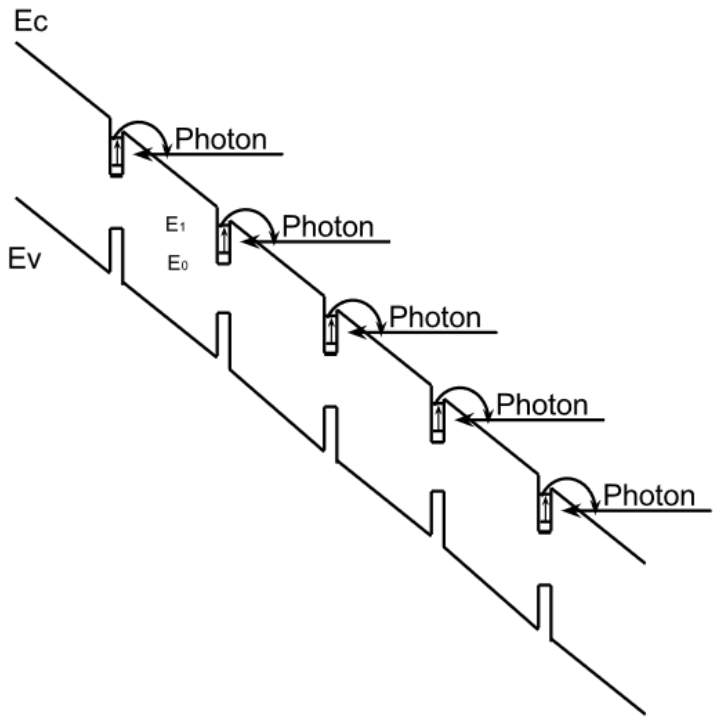

Figure 1-8 Energy band scheme of quantum well infrared photodetector[4]

As the energy needed to excite an electron from the ground state to the first bound state is lower than the barrier, and the consequent electron tunneling out is easy, quantum well photodetectors can have higher absorption, broader wavelength response, lower dark current and higher detection sensitivity.[4]

A quantum-dot infrared photodetector is similar to a quantum-well infrared photodetector. The only difference is that a quantum-dot, instead of quantum well, is used as the quantum potential well. There are some advantages compared to quantum-well

photodetectors: Because quantum-dots are 0-dimensional, there is no need for a set angle of incident light, for quantum-well photodetectors. Furthermore, people can tune the working wavelength easily by tuning the size of the quantum-dots.

1.1.3 Organic small molecule and polymer photodetector

1.1.3.1 Definition of organic photodetector

Organic materials, including organic small molecules, oligomers and polymers, are used as semiconductive material instead of inorganic material, such as Si and GaAs in an organic photodetector.

1.1.3.2 Organic semiconductor materials

According to Hückel's model, conjugated π-electron systems, which are defined by alternating single and double bonds in the molecular structures, are the key parameter and origin of conduction of all kinds of organic semiconductor materials. The scheme of energy level of a π-conjugated molecule is shown below:

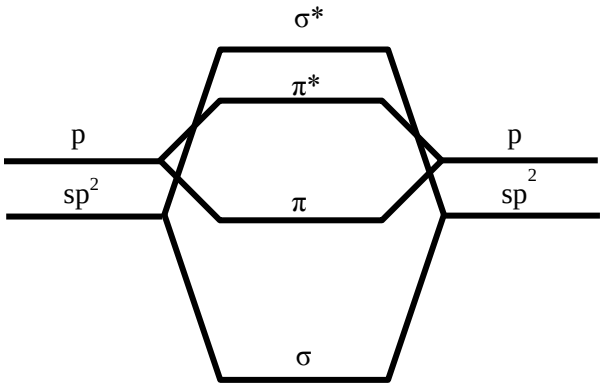

Figure 1-9 Schematic diagram of organic molecule energy level

In a π-conjugated molecule, the carbon atom is sp^2 hybridized, with three sp^2 orbitals per atom and one leftover unhybridized pz orbital. The weaker interactions of the parallel pz orbitals form weaker π bond and π* antibond molecular orbital (MO) energy levels, making the π-π* transition the smallest electron excitation in the molecule. Therefore, the π bonding MO and π* bonding MO are the highest occupied molecular orbital (HOMO) and lowest unoccupied molecular orbital (LUMO) of the organic semiconductor.

With a larger conjugated area, the π electrons are more delocalized, and the charges can move more freely within the π conjugated area. A red shift of absorption spectrum is also a result of larger conjugated area because of the smaller HOMO-LUMO transition energy. This is one of the major benefits of organic semiconductor material, as people can easily tune the HOMO and LUMO energy level by changing or modifying the organic material.

1.1.3.3 Small organic molecules and oligomers as semiconductive materials

1.1.3.3.1 Porphyrins and phthalocyanines

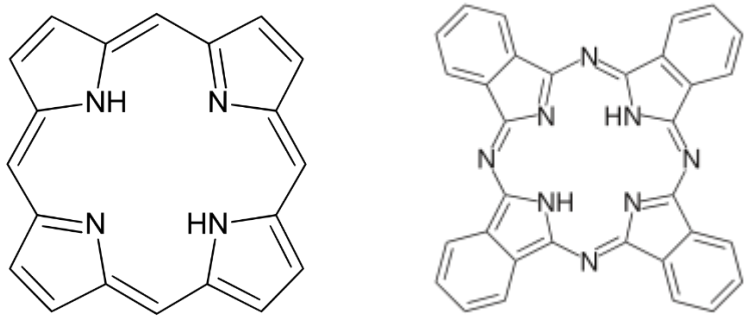

Figure 1-10 Porphyrin and phthalocyanine

Phthalocyanines and porphyrins are aromatic macrocycles with large π-conjugated systems. There are at least 26 π-electrons for porphyrins and 42 π-electrons for

phthalocyanines. As a popular semiconductor material, good chemical and thermal stability, photoactivity and high charge mobility are found in these materials. [5]

A major benefit of phthalocyanines and porphyrins is that their molecular structure can be easily modified, like adding functional groups, adding more π-conjugated atoms, etc. to modify their optical and electrical property, and they, therefore, can meet different requirements of devices.[6]

Photodetectors based on phtalocyanines and porphyrins can have a very fast response. For example, a single-layered heterostructure (SLH) and multi-layered heterostructure (MLH) organic photodetectors, using copper phthalocyanine (CuPc) and N,N0-bis(2,5-di-tert-butylphenyl)3,4,9,10-perylene dicarboximide (BPPC), are reported by Morimune et al. and show a cutoff frequency of more than 20MHz [7]. A cutoff frequency of more than 1MHz is reached by titanyl phthalocyanine (TiOPc) and fluorinated zinc phthalocyanine (F16ZnPc) based photodetectors.[5]

1.1.3.3.2 Acene-based derivatives

The acenes or polyacenes are a class of organic compounds that are made up of linearly fused benzene rings. Because of their coplanar π -conjugated conformation and highly ordered domain from their good crystalline formation, acene-based derivatives are promising materials for photo-semiconductor.

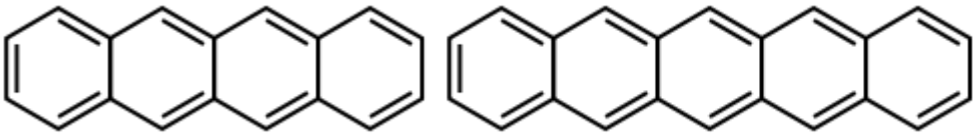

Figure 1-11 Tetracene (left) and Pentacene (right)

One of the most researched acenes for photodetector, pentacene-based thin-film transistors (TFTs), are known for their device performance characteristics that almost surpass amorphous Si-based TFTs on mobility[8]. Yakuphanoglua and Farooqb[9] reported an ultraviolet and white light photo transistors using pentacene as the active material; Choi et al. have reported a tetracene based transistor that has higher photo-to-dark current ratio compared to pentacene based transistors, despite its low mobility[8].

1.1.3.3.3 Oligothiophene

Oligothiophene and polythiophene are among the most popular organic photo-semiconductors because of their excellent optical and electric properties and good stability. The good crystallinity of thiophene based conjugated system is the reason of its good charge mobility and large domain area.[10]

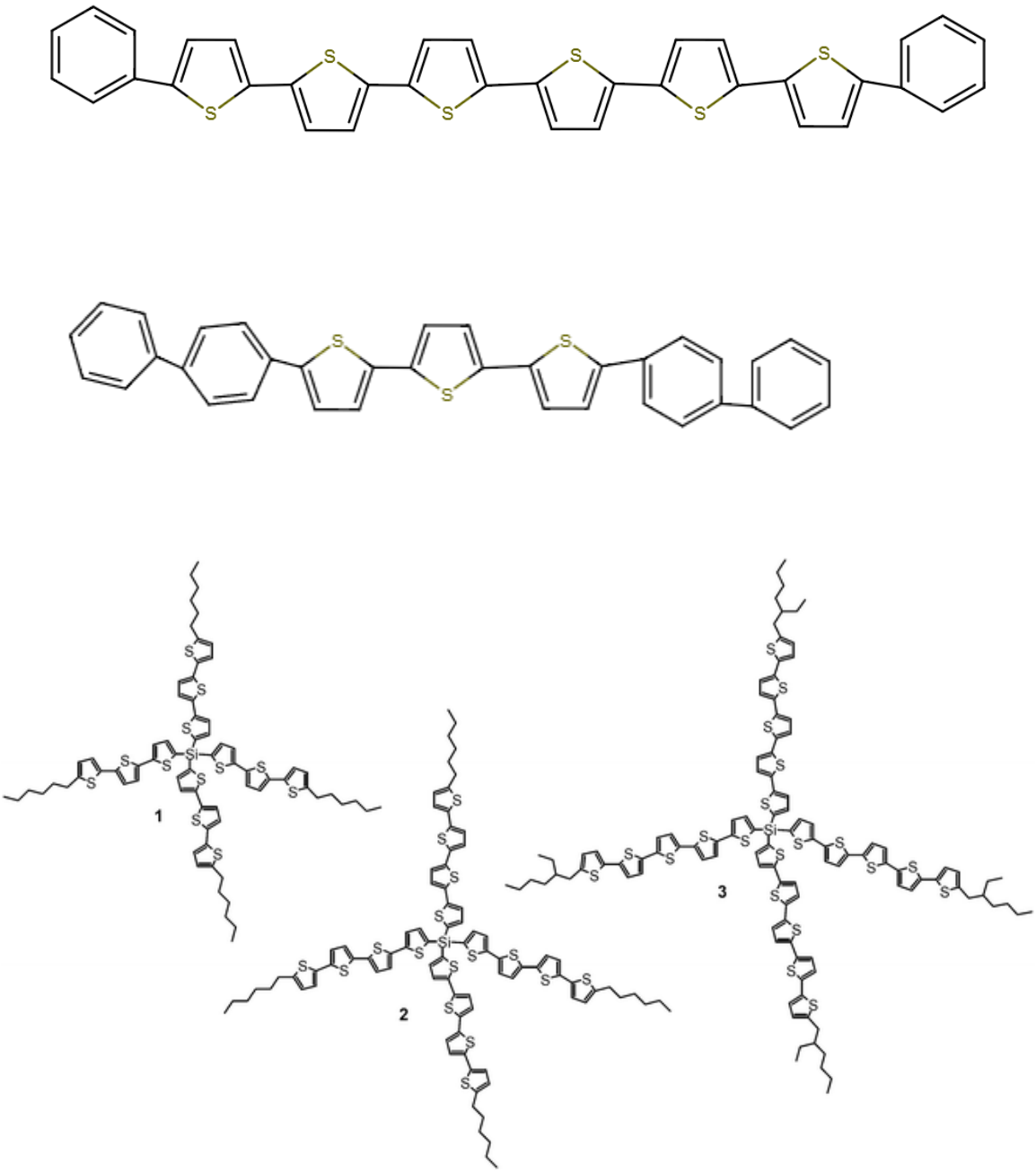

Figure 1-12 B6T (upper), BP3T (middle) and 3 tetrakis(oligothienyl)silanes (lower)[11]

A quaterthiophenesilane: Phenyl-C71-butyric acid methyl ester ([70]PCBM) (**2** in **Figure 1-4**) and a quinquethiophenesilane : [70]PCBM (**3** in **Figure 1-4**) photodetectors have been reported. 1–2 MHz frequency response is reached with zero bias voltage, which is

approximately one order of magnitude higher than for the reference devices based on a conventional Poly(3-hexylthiophene-2,5-diyl) (P3HT)/ Phenyl-C61-butyric acid methyl ester (PCBM) system. [11] Another interesting example of the utilization of oligothiophene in the field of photodetectors is that, P6T and BP3T (**Figure 1-4**) are used as a light-absorbing and exciton-blocking system. In this system, P6T blocks blue light, and BP3T blocks the excitation energy transfer from P6T to CuPc, which is the active material of the photodetector.[12]

1.1.3.3.4 Donor–acceptor small molecule materials

Donor-acceptor small molecule materials are a kind of small organic molecule that has a donor-acceptor system. A π-conjugated backbone connects the donor part and acceptor part. By modifying the donor and acceptor parts and the π-conjugated backbone, the absorbance band of the system can be tuned. This is a promising way to fabricate a broader band photodetector or a selected wavelength sensitive photodetector.

Diketopyrrolopyrrole (DPP) is a highly absorbing chromophoric acceptor. In 2008, a DPP-Thiophene oligomer system was introduced by Nguyen et al., as the active material in the solar cell. Its optical absorption extends to 720 nm in solution and to 820 nm in the film. [13] In 2012, Gang Qian reported a photodetector based on a similar DPP-Thiophene system. The major benefit of this photodetector is that the detectability is extended to near infrared, and a potential of band-gap tuning. [14] [15]

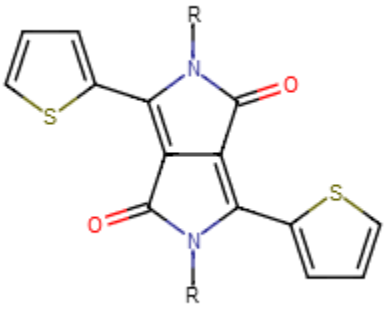

Figure 1-13 An example of DPP-thiophene system

Dicyanovinyl (DCV) is another acceptor molecule used as the end groups in donor systems to form conjugated A–D–A systems. DCV-thiophene system (dicyanovinyl-substituted terthiophene derivative, DCV3T) was used originally for organic solar cell in 2007 by Uhrich et al.,[16] then a green-sensitive organic photodetectors consisting of a bulk heterojunction blend of N,N-dimethylquinacridone and DCV-terthiophene was introduced by Leem et al. at 2013. The response wavelength almost covers the whole visible light spectrum, making it a good all colour organic photodetector[17]

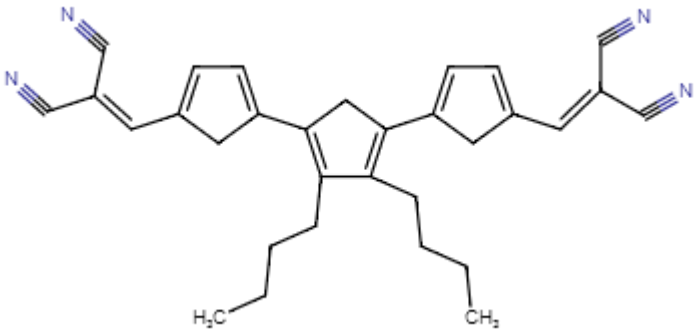

Figure 1-14 DCV3T

1.1.3.3.5 Perylene diimide and fullerene acceptors

Unlike various organic donor materials, there are not many choices for organic acceptors. Perylene and fullerene derivatives are two major kinds of n-type conjugated semiconductors due to their low LUMO energy level, good stability, good solubility and good crystalline by solution process. [18] [19]

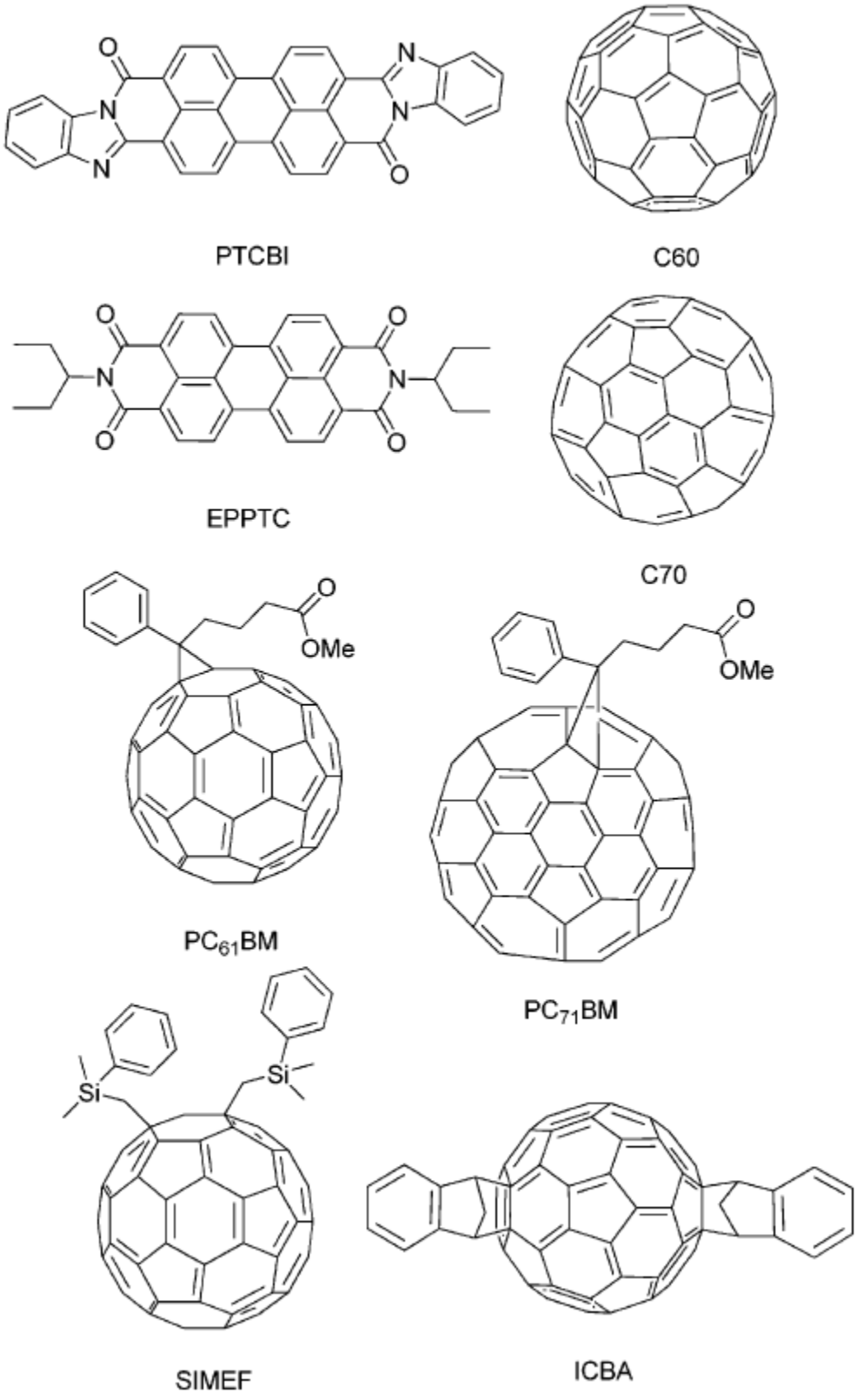

Figure 1-15 Structures of commonly used acceptors [6]

1.1.3.4 Polymer as photoconductor material

1.1.3.4.1 Polyphenylenevinylenes

Polyphenylenevinylenes (PPV) are well known as conjugated conductive polymers. PPV based electronic devices are widely used. A soluble PPV, poly[2-methoxy-5-(20-ethylhexyloxy)-1,4-phenylene vinylene] (MEH-PPV) was firstly used in photodetector in 1994 by G. Yu et al., a sensitive UV-visible photodetector made with MEH-PPV and C_{60} was introduced.[20] In 2005, the response band of an MEH-PPV photodetector was extended to infrared using PbS quantum dots. [21] Poly[2-methoxy-5-(3,7-dimethyloctyloxy)-1,4-phenylene vinylene] (MDMO-PPV) is another similar polymer, which was used for photodetector at 1999 by Brabec, C.J. et al..[22]

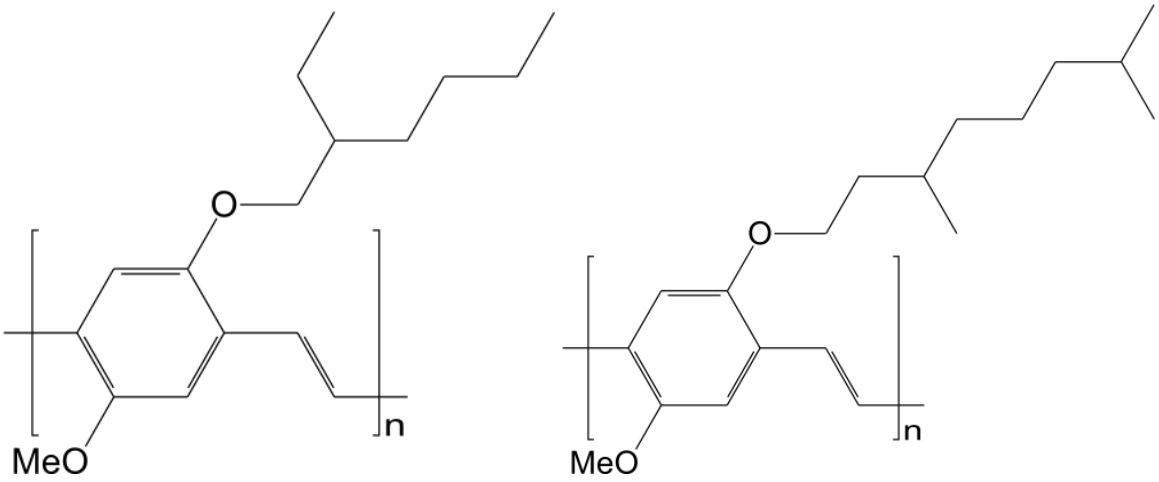

Figure 1-16 MEH-PPV (left) and MDMO-PPV (right)

1.1.3.4.2 Polythiophenes

Polythiophene is a kind of very important and popular conjugated polymer for organic electronic devices, poly(3-hexylthiophene) (P3HT) is one of the most investigated and used polythiophenes. In 2002, Schilinskya et al. reported the first P3HT based bulk

heterojunction photovoltaic cell as well as its utilization as a photodetector.[23] After that, many optimizations were introduced to improve the performance. Recently, nanotechnology is also introduced to boost P3HT based photodetectors. [24]

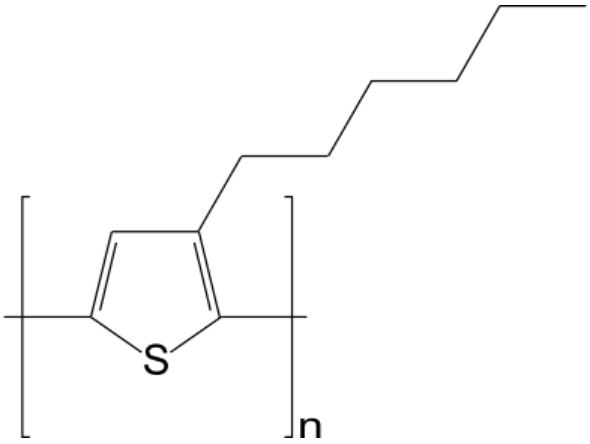

Figure 1-17 Poly(3-hexylthiophene-2,5-diyl) (P3HT)

1.1.3.4.3 Third generation polymers

Compared to the first generation organic semiconductor, polyacetylene, and second generation organic semiconductor, polythiophenes, the third generation semiconducting polymers have more complex molecular structures with more atoms in the repeat unit.[25]

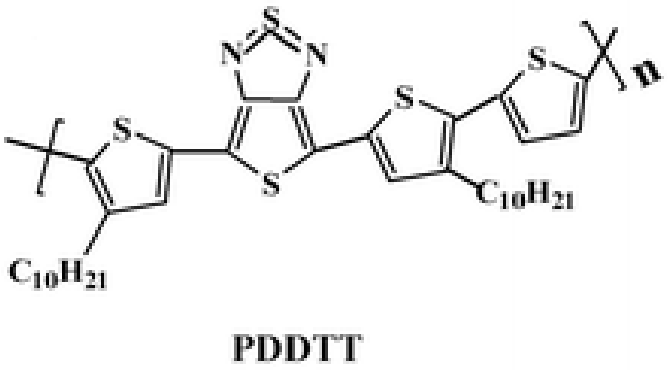

Figure 1-18 PDDTT

PDDTT (**Figure 1-18**) is one of the important examples of the third generation semiconducting polymers. A PDDTT:$PC_{60}BM$ based photodetector reported by Gong et al. exhibits an amazing response spectrum from 300nm to 1450 nm, with ditectivity greater than 10^{12} cm $Hz^{1/2}$ W^{-1} and a linear dynamic range larger than 100 dB, making it even better than any inorganic photodetector.[26]

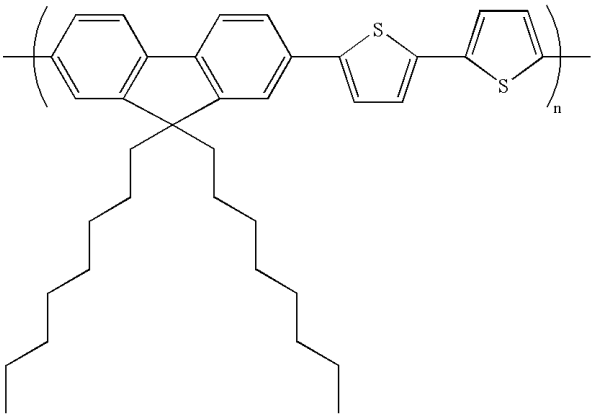

Figure 1-19 Poly[(9,9-dioctylfluorenyl-2,7-diyl)-co-bithiophene] (F8T2)

Poly[(9,9-dioctylfluorenyl-2,7-diyl)-co-bithiophene] (F8T2) is another third generation co-polymer. The F8T2:PCBM photodetector shows good performance in the dark and under detection. A cutoff frequency of 50MHz is reached under reverse bias voltage of 10V, showing the potential to be a good high speed photodetector.

1.1.3.4.4 Advantage and limitation of organic photodetector

The advantages of organic photodetectors include good affordability, flexibility, being able to cast or print on a large area with low cost. The potential of tuning the characters,

such as response spectrum, colour, or even transparency is also very attractive. However, most organic photodetectors are still considered as low performance compared to inorganic (Si, GaAs, InP, etc.) photodetectors.

1.2 Essential characteristics of photodetector

1.2.1 Relationship between photodetector and solar cell

Organic solar cell and organic photodiode photodetector are essentially the same: they are photodiodes. In both the photodetectors and solar cells, the carriers are generated out of light absorption: Incident photons excite electrons from lower energy level to a higher energy level; thus electron-hole pairs are generated. The carriers result in a photocurrent, holes move toward the anode, and electrons toward the cathode.

When the photodiode is used in photovoltaic mode (solar cell), the photocurrent flowing out of the device is restricted, and a voltage builds up. Usually, no bias will be added to the device. When the photodiode is used in a photodetector mode, a reversed bias (cathode driven positive) is usually added. The current of the photodetector is measured and is proportional to the light intensity. The reason a reverse bias is needed is that it increases the depletion width of the p-n junction, which increases the frequency response of the device by decreasing its capacitance.

1.2.2 Important characteristics of photodetector

Unlike solar cells, which focus almost only on the energy conversion efficiency, the performance of a photodetector relies on many characteristics. Quantum efficiency, response speed, noise, response spectrum and linearity are some of the most important characteristics of a photodetector.

1.2.2.1 Quantum efficiency

Quantum efficiency is defined as absorbed incident photon to converted electron ratio. [27] As the absorbed incident photon is hard to measure, "external quantum efficiency" is defined as shined photon to converted electron ratio.

The external quantum efficiency depends on three factors: how many photons are irradiate onto the semiconductor; how many photons are absorbed and converted to carriers and how many carriers reach the outer circuit before they recombine. Quantum efficiency is no doubt important, because it's a key factor of the sensitivity of a photodetector.

1.2.2.2 Response speed

The time delay of the incident light to an electrical signal is the response speed of a photodetector. It is measured by sending light pulses to the photodetector, and measuring how fast the photodetector can respond to these signals.

There are two factors that affect the response speed. First is the time that carriers travel through the active layer and reach the electrode; second is the RC time constant of the device, where C is the capacitance of the device junction, and R is the equivalent parallel resistance that includes the parasitic resistance.[1] Response speed is the key for the frequency bandwidth of a photodetector.

1.2.2.3 Noise

Like other electronic devices, photodetectors suffer from electronic noise. Noise is defined as a random fluctuation in an electrical signal, either current or voltage. There

are mainly three kinds of noise in a photodetector: shot noise, dark current and thermal noise.

In a photodetector, shot noise is associated with the particular nature of photons. For this reason, the number of photons is uncertain, but exhibits detectable statistical fluctuations, which is the source of shot noise. The shot noise cannot be avoided because of its theory, but it's usually not a big issue unless the light intensity to be detected is very low.

Dark current is the current signal that the photodetector exhibits in the dark. "Reverse bias leakage current" is another name for it. The dark current is due to the thermal generated electron-hole pair, which are swept by the voltage bias. The dark current is strongly depending on operation temperature so lower temperature can reduce the dark current.

The thermal noise is a result of thermal agitation of carriers. It is also known as Johnson–Nyquist noise. The power of thermal noise is given by:

Equation 1-1

$$\overline{v}_n^2 = 4k_B TR$$

Where $\overline{v}_n^2$ stand for voltage variance (mean square) per Hertz of bandwidth, k_B is the Boltzmann's constant in joules per Kelvin, T is the resistor's absolute temperature in Kelvins, and R is the resistance of the resistor.

1.2.2.4 Response spectrum

Response spectrum is the wavelength range that a photodetector can response to. As a photodetector will respond only to photons with energy higher than its band gap energy, the band gap energy is, therefore, the cutoff energy of the photodetector.

Inorganic photodiodes, like Si photodiodes, have a certain cutoff energy of 1100 nm. On the other hand, the cut off energy of an organic photodiode can be modified by changing the semiconductor material. This gives an advantage for organic photodetectors as infrared photodetectors.

1.2.2.5 Other characteristics of a photodetector

Stability under the operation condition is very important for a commercialized photodetector. Fidelity, which defined by the reproducibility for the waveform of the incident light of a photodetector, is very important for some utilizations. The linearity of a photodetector's output to light intensity is also a concern. The range of the linear operation wavelength of a photodetector is called the dynamic range.

1.3 Chirality and chiral transfer

1.3.1 An introduction to chirality

Long before the existence of the word "chiral", plane polarized light was first discovered by Malus (1809), a French physicist. Later, in 1911, another French scientist Biot discovered that a quartz plate can rotate the plane of the polarized light. Furthermore, he found that some quartz plates can turn the plane left while others turn it right.

In 1848, the genius Louis Pasteur successfully manually spectated 2 different types of the crystals of the sodium ammonium salts of (+)- and (-)-tartaric acid, using a tweezers and lens, which are formed from slow evaporated liquid solution of wine caskets. Pasteur discovered that, when he dissolved these two types of crystals, one solution rotates the polarized light to the right while the other solution rotated to the left.[28]

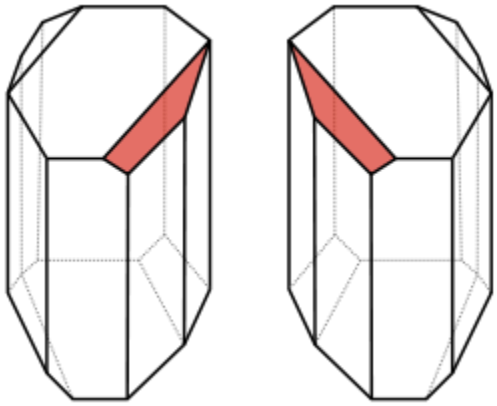

Figure 1-20 The two types of the crystals of the sodium ammonium salts. (Imagine from Wikipedia)

The word “chiral” first came out in 1884 using by Thomson, representing “handed” (from Greek “cheir”, means hand.). In 1960s, Mislow and Cahn, Ingold and Prelog strictly defined “chiral” as having no plane, centre, on alternating axis symmetry, plus at most one axis of rotation.

1.3.2 Chiroptic

1.3.2.1 Optical Activity

Chiroptical activity is a phenomenon when polarized light interacts with a chiral substance, which can be different between the two enantiomers of a chiral compound. Optical rotatory dispersion (ORD), circular dichroism (CD) and circular polarization of emission (CPE) are some of the aspects of chiroptical activities.

Before explaining how the chiral compounds interact with polarized light, a brief introduction to polarized light is stated here. Light is an electromagnetic radiation which is a representation of time-dependent electric and magnetic fields. In ordinary light, or isotropic light, the light randomly polarized. When the oscillations are removed or filtered, except one direction left, the light is called plane polarized, or linear polarized. When it comes to circular polarization, like linear polarized light, there is only one direction of the oscillation left, but the direction is changed as the light propagates. (**Figure 1-21**) A linear polarized light can be considered as a combination of equivalent of opposite circular polarized light of the same intensity.

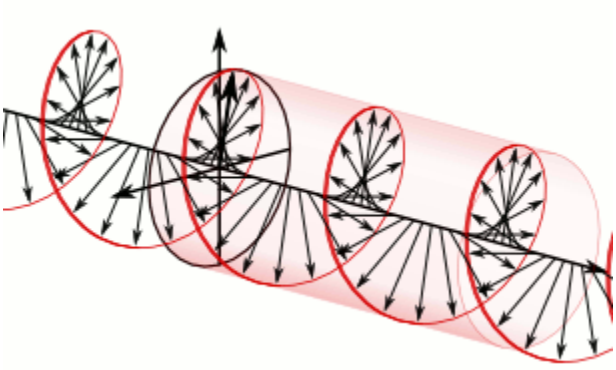

Figure 1-21 The electric field vectors of a traveling circularly polarized electromagnetic wave [29]

As a characteristic of the enantiomer, when linear polarized light pass through a chiral compound enantiomer, one-handed circular polarized light of the linear polarized light is more favoured so the velocity of, say right circular polarized light, is slower than the left circular polarized light. As we know that the refractive index n equals c_0/v in a particular medium where v is the velocity of light in the medium and c_0 is the vacuum light velocity, the n_L will be greater than n_R. As a result, when viewed towards the light source, the outgoing linear polarized light will be clockwise rotated by an angle [α]. When $n_L \neq n_R$, the medium is called to be circular birefringent and having optical activity.

1.3.2.2 Optical Rotatory Dispersion

The measurement of the optical rotation of a sample, as a function of wavelength, is called optical rotatory dispersion (ORD).

Figure 1-22 is an example of ORD curve. The cross point of the ORD curve is very close to the maximal absorbance of the sample, which also means that, at that wavelength, the sample is optical null. Also, a maxima, a minimum and an inflection point are exhibited in the curve. This anomaly of the curve is called Cotton effect. [30] When the curve increases as the wavelength decreases, and then decreases, the curve is called positive; when the curve decreases as wavelength decreases, it's called negative.

ORD reflects information about the configuration of the chromophore and the stereogenic that perturb it. [31]

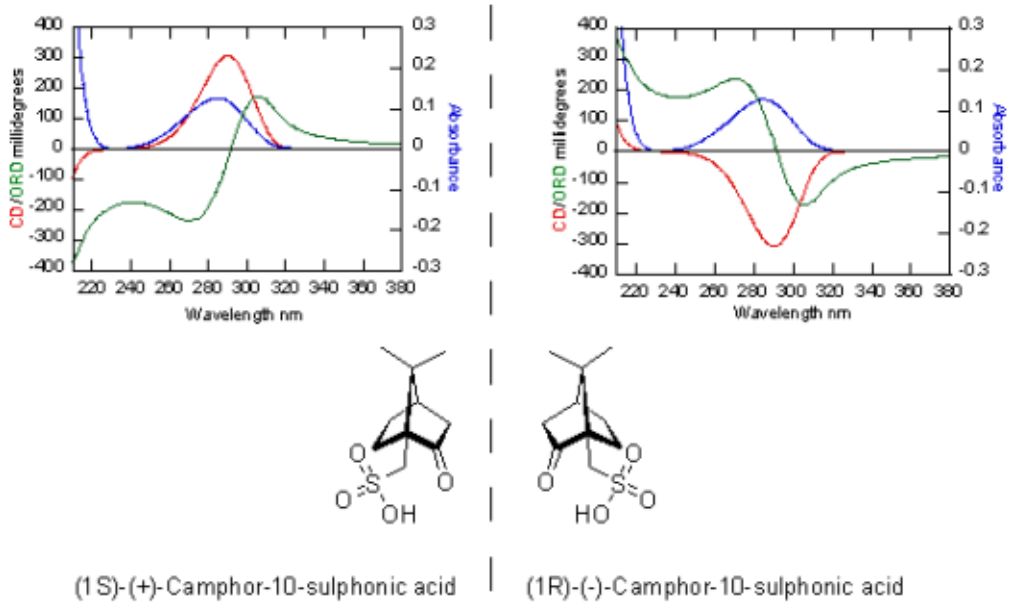

Figure 1-22 CD, ORD and Absorbance spectra of R and S forms of camphor sulphonic acid[32]

1.3.2.3 Circular Dichroism

Circular dichroism (CD) is another chiroptic phenomenon discovered later. It's a chiroptic phenomenon that is observed in the chiral materials non-transparent region of their absorbance spectrum. The different absorption of left- and right-handed polarized light of a chiral material comes from the electronic transition of the chiral chromophore. CD reflects the anisotropic absorption of circular polarized light of a chiral sample which is a Cotton effect too.

The sign of a Cotton effect of CD is defined similar to ORD (see 1.3.2.2), and the corresponding CD of an ORD has the same sign as the ORD (positive or negative).

Corresponding ORD and CD in the same wavelength range reflect the same chiral chromophore. [31]

1.3.2.4 Chirality transfer

Achiral compounds can show Cotton effect in their ORD and CD when chirality is induced by other chiral substances. This phenomenon is called chirality transfer. Chirality transfer was first discovered in 1959, showing that the achiral dye compound-polypeptides complex exhibiting optical activity, at the absorbance region of the dye.[33] In 1966, chiral solvent induced chirality to achiral molecule was discovered by Bosnich, et al. [34]

The chiral transfer is generated by some interaction between the chiral compound and achiral compound. The interaction can be hydrogen bond, solvation effect, covalent bond or supermolecular interaction. A chiral conformation will be usually created by the interaction.

The chirality transfer of polymer is an interesting research object since Khatri, et al. discovered the optical activity of polyisocyanates devoid of chiral center. The chirality is due to the helical conformation that was induced by chiral solvent.[35] The poly(n-hexyl isocyanate) is a polymer devoid of chiral centre. In the presence of (R)-2-chlorobutane, which is a kind of chiral solvent, the achiral poly(n-hexyl isocyanate) shows CD activity at 250 nm, which is transparent to the chiral solvent. This phenomenon indicates that the achiral poly(n-hexyl isocyanate) obtains chirality by chirality transfer.

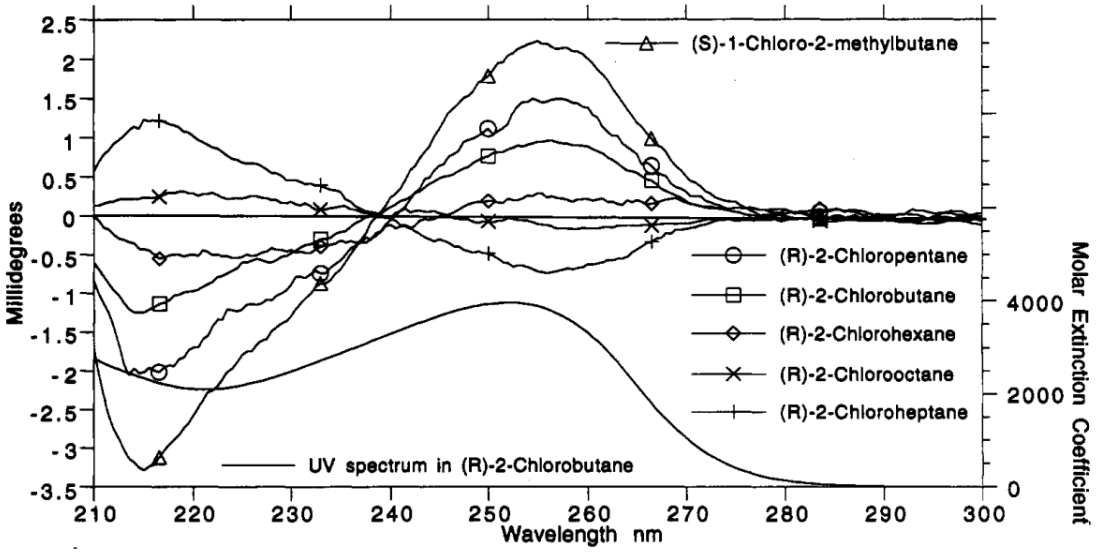

Figure 1-23 Circular dichroism spectra of poly(n-hexyl isocyanate) dissolved in optically active solvents at 20 ˚C. Ultraviolet spectrum (-) shown only [35]

The chiral transfer from chiral solvent to achiral polymer is a promising way to fabricate optically active organic photoelectronic devices because this method avoids expensive and complex asymmetric synthesis. Moreover, the well-studied photo semiconductor polymer can be used directly to ensure the successful fabrication of the device, and avoid unnecessary optimizations.

1.3.3 Current method to detect circular polarized light

1.3.3.1 Circular polarized light detecting in nature

Long before humans discovered circular polarized light (CPL), animals were able to detect CPL and utilize CPL for their advantage. Though CPL is not common in Nature, scientists found that some kind of scarab beetle reflects only left-handed polarized light.[36] The mantis shrimp, which is an extremely colourful yet aggressive creature, also has very powerful eyes that can detect CPL. On the top of the eye of mantis shrimp, there is a

biological quarter-wave plate; under it, there are two orthogonal rhabdom layers that can detect the property of linear polarized light. In this way, the mantis shrimp can detect all four linear and two circular polarization components, giving itself a full description of polarization.[37]

1.3.3.2 ORD spectroscopy

ORD spectroscopy can be used to examine optical activity of samples by detecting the optical rotation. The basic scheme is shown below:

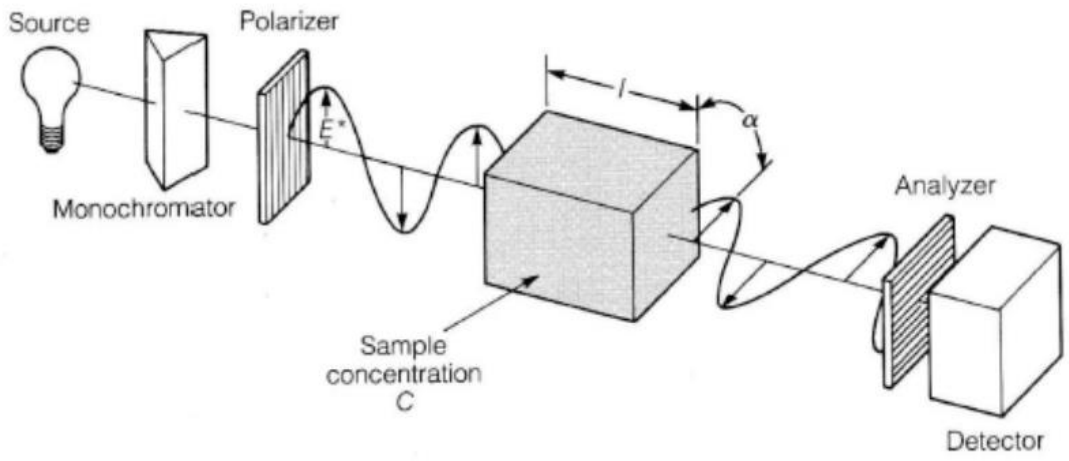

Figure 1-24 ORD spectroscopy scheme [38]

The linear polarized monochromatic light enters the sample, and the direction of the linear polarized light is rotated by a certain angle α, which is detected by a polarizer acting as an analyzer. The ORD spectroscopy works with non-absorbing samples or non-absorbing at the detecting wavelength samples.

1.3.3.3 CD spectroscopy

Circular dichroism (CD) spectroscopy is a spectroscopic technique where the CD of the sample is measured over a range of wavelengths. A CD spectroscopy measures the absorbance difference of left-handed CPL and right-handed CPL of the sample at a given wavelength. In a CD spectrometer, a photo-elastic modulator (PEM) is used instead of a quarter-wave plate, to generate CPL. A PEM contains a piezoelectric element cemented to fused silica, and the silica can be driven to be birefringent and oscillating at a set frequency, turning the PEM into a dynamic quarter wave plate that produces left-handed and right-handed CPL.

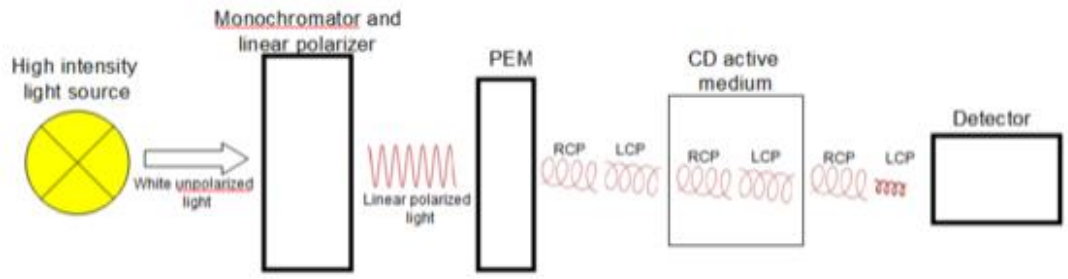

Figure 1-25 scheme of modern CD spectrometer (ChemWiki)

The detector is locked-in to the frequency of the PEM, so that the differential CPL absorbance at given wavelength, also known as CD, can then be calculated.

Chapter 2

Project Objectives

2.1 Organic photodetector for circular polarized light

The project is aiming at fabricating a simple, light weight, flexible and potentially low cost photodetector that can detect and identify circular polarized light. Organic material is used as the photo-semiconductor of the photodetector to achieve a lightweight and flexibility attribute; a single layer heterojunction structure is adopted to keep the device simple and reliable.

The basic theory of the organic photodetector for circular polarized light is based on the circular dichroism property of the photo-semiconductor. The absorbance values of the left handed and right handed circular polarized light of the material are slightly unequal, resulting in the unequal output voltage or current value, therefore, the left handed and right handed circular polarized light can be identified.

The organic photodetector for circular polarized light (or CPL sensitive photodetector) can be used as a special way of communication. Circular polarized light can be modulated to carry information, not only by frequency or intensity, but also by polarization property. As circular polarized light is very rare in nature, the photodetector can also work as a selective sensor to detect specially designed objects.

Chapter 3

Experimental

3.1 Photodetector using optically active polythiophene with chiral side chains

3.1.1 Material

3.1.1.1 Polythiophene with chiral side chains

As mentioned in 1.1.3.4.2, Polythiophenes are a kind of very good organic optical electronic material, which are very well studied as the active material in an organic photodetector. When a chiral group is substituted on the 3 position of thiophene, the polythiophene usually shows optical activity, making it a potential active material of CPL sensitive photodetector.

Lemaire et al. introduced the first polythiophene with chiral side chains in 1988. The polythiophene (**Figure 3-1**) was studied to stereoselectively recognize chiral anions. Later in 1991, polythiophene with a free amino-acid side-chain was reported with circular dichroism activity. [39]

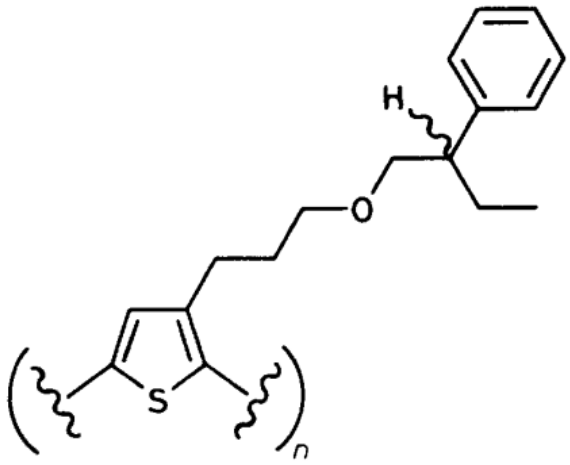

Figure 3-1 Polythiophene with chiral side chains (Lemaire et al.)

In 1996, a polythiophene with an alkyl side-chain was reported by Bidan et al.,(**Figure 3-2**) showing significant CD in solution and solid state. [40] The good crystalline property and optical activity make it a promising electro optical material for a chiral photodetector.

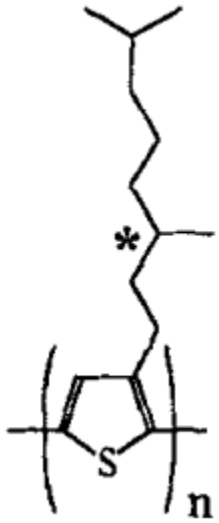

Figure 3-2 Poly3-(R-3',7'-dimethyloctyl)thiophene [40]

The polythiophene with a chiral alkyl side-chain— poly3-(R-3',7'-dimethyloctyl)thiophene (chiral PT, or cPT will be used as names for this compound), which obtained from Dr. Guillerez, is the active material of the photodetector, used as received.

3.1.1.2 [6,6]-Phenyl C61 butyric acid methyl ester (PCBM)

Reported in 1995 [41], PCMB is a soluble form of fullerenes blended with conjugated polymers with nanoparticles such as C60 that has been found to be a good electron acceptor in organic photonics.

The 99% purity PCBM used in the project is received from SES research, is shown below:

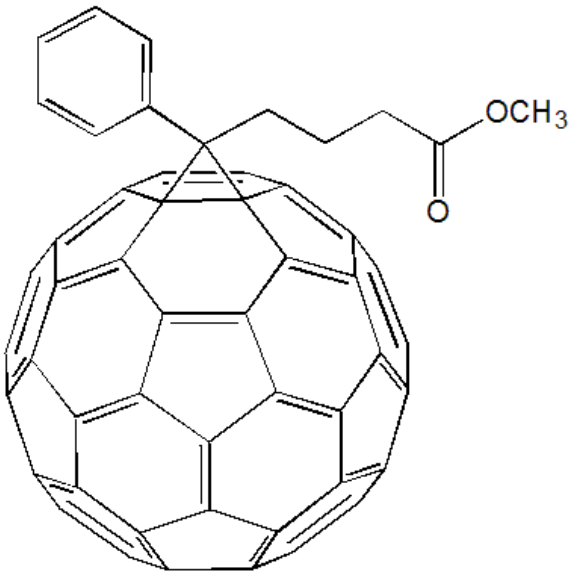

Figure 3-3 PCBM

3.1.1.3 Indium Tin Oxide （ITO） transparent conductive coated glass

Indium Tin Oxide (ITO) coated glass is used as transparent conductive substrate. The 35mm × 25mm glass slides are received from luminescence technology. The following is the manufacturing details provided by the manufacturer: The ITO is deposited onto polished soda lime float glass in two standard smooth thicknesses giving 9~15 ohms per square and 4~6 ohms per square. Then SiO_2 barrier coating is deposited between the ITO and glass.

3.1.1.4 Solvents

Chloroform, certified ACS, from Fisher Scientific.

3.1.2 Instruments

Laurell Technologies WS-400-6NPP Spin Coater is used for solution processed device fabrication. VWR 1410 Vacuum Oven is used for pre-heating of substrate and annealing. Kurt J. Lesker Organic Thin Film Deposition & Metallization System is used for the metal electrode deposition. Keithley 4200-SCS Semiconductor Characterization System is used for electronic characteristics. Jasco J-815 CD Spectroscope is used for CD and UV-Vis measurement of the photodetectors.

Fabrication experiment procedure

3.1.2.1 Device design

The basic structure of the CPL sensitive photodetector is a heterojunction organic photodiode. The substrate is a glass slide; ITO is pre-coated as transparent conductive layer. The electron donor and acceptor chiral polythiophene and PCBM are mixed in solution, and then cast on the ITO layer as the heterojunction active layer. Last, silver is evaporated onto the active layer as the metal electrode.

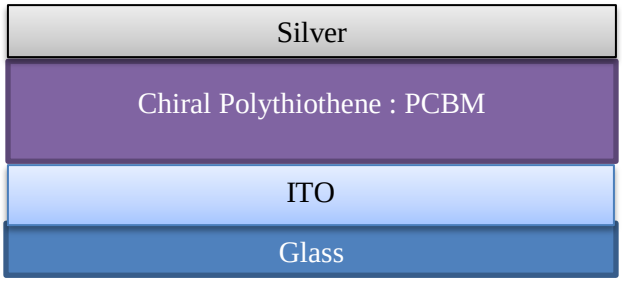

Figure 3-4 Scheme of the photodetector structure

3.1.2.2 ITO patterning

The ITO pre-coated glass slide needs to be patterned to make the photodiode. The original size is 20mm × 25mm. The patterning is done by covering a certain area of ITO by tape, covering it with powdered zinc metal, and then immersing the slide into 1 mol/L HCl solution for 10 minutes. As ITO is a metal oxide, the area not covered with tape is etched by acid. Subsequently, the slide is washed thoroughly with water, and the covering tape is removed. Then the slide is washed by acetone for 3 times and immersed into toluene, ultrasonic for 10 minutes. 10 minutes of ultrasonication rinse by acetone and distilled water are then performed, and the slide is blown to dry with nitrogen.

The pattern scheme is shown below:

Figure 3-5 Pattern scheme of ITO glass slide. The blue part is covered by tape so that the ITO layer remains, the white part is uncovered glass.

3.1.2.3 Active layer

Chiral PT and Phenyl-C61-butyric acid methyl ester (PCBM) are used as electron donor and electron acceptor.

20 mg cPT and 20 mg PCBM are dissolved in 1ml chloroform and stirred overnight. A dark purple coloured solution is formed. The solution is casted onto the patterned ITO slide using spin-coating process: The spin-coater is programed to 1000 rpm, 1000 rpm acceleration, timing for 60 seconds. The solution is dropped onto the ITO slide to form a liquid film, and spin-coating afterwards. A uniform, transparent purple film is formed over of the slide.

3.1.2.4 Deposition of silver electrode

The slide from the last step is placed under vacuum for 10 minutes to evaporate the solvent, then physical vapour deposition is used under higher vacuum (<1^10-7 mbar). The deposition rate is 1.5 Å per second, the thickness of silver is 100 nm. The deposition area is shown below: (**Figure 3-6**)

The active area of the device is the overlap area of ITO and silver. The small active area contributes to a smaller capacitance, and, therefore a faster response. It is also easier to fabric a uniform active layer when the active area is small.

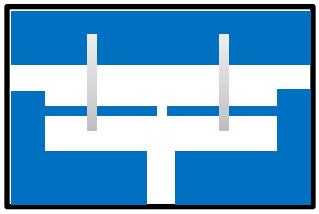

Figure 3-6 Silver electrode deposition scheme

3.2 Photodetector using limonene induced chiral F8T2

3.2.1 Material

Poly[(9,9-dioctylfluorenyl-2,7-diyl)-co-bithiophene] (F8T2) is a popular conjugated polymer that was well studied as the active material for phototransistors, photodetectors and polymer solar cells. (**Figure 3-6**) The F8T2 is purchased from Luminescence Technology Corp., molecular weight is 20000~60000 and it is used as received.

Limonene, taking its name from lemon, is a kind of cyclic terpene. Limonene can be found in citrus fruits rind, like lemon, in a considerable amount.

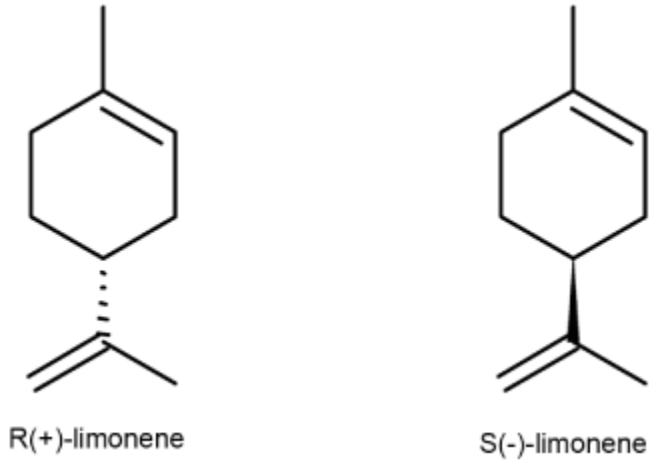

Figure 3-7 R (+) -limonene and S (-) –limonene

Limonene is a chiral molecule. (**Figure 3-8**) The R (+) –limonene is naturally found in citrus fruits, while the S (-) –limonene is synthetic. The racemic limonene is called dipentene. Limonene is wildly used as fragrant in cosmetic products, cleanser, and medicine. It's also becoming more and more popular as biodegradable solvent.

The R (+) –limonene, S (-) –limonene and dipentene were purchased from Alfa Aesar. Both enantiomers are in 97% purity.

3.2.2 Instrumental

See 3.1.2 instrumental

3.2.3 Fabrication experiment procedure

The device design of limonene induced F8T2 photodetector is quite similar to that described at 3.1.3.1. The major difference is the preparation of the active layer:

3.2.3.1 Active layer

Similar to chiral polythiophene the active layer, an F8T2: PCBM blend, weight ratio 1:1, is used as the active material for the photodetector. However, because F8T2 and PCBM are not soluble in limonene at room temperature, a process called “hot spin-coating” is performed to fabricate uniform limonene induced active layer.

10.0 mg F8T2 and 10.0 mg PCBM are weighed and put into a 50 ml round bottom flask, then 1.0 ml of limonene (R-, S- or racemic) is added into the flask. The flask is connected with a Liebig condenser in oil bath and heated to 150 ˚C. (**Figure 3-8**)

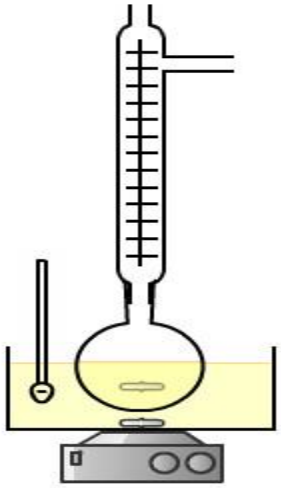

Figure 3-8 Apparatus setup

When the temperature reached 150 ˚C, the mixture turned to a homogeneous dark brown solution. The patterned ITO glass slides are pre-heated to 120 ˚C in oven, quickly transferred to the spinning substrate of the spin-coater. Then a pre-heated to 150 ˚C short

Pasteur pipette is used to quickly transfer the hot F8T2: PCBM solution to the ITO patterned slide, and spin-coated at 1000 rpm for 60 seconds. A yellow to orange, fairly uniform film is formed.

After placing the sample in vacuum for 10 minutes to remove any solvent (limonene) residue, the slide is deposited with silver using the same procedure at 3.1.3.4.

3.3 Photodetector using limonene induced chiral P3HT

3.3.1 Material

The P3HT was purchased from Rieke Metals, Inc. The molecular weight (Mw) is approximately 50-70K and 91-94% regioregular via NMR. It is used as received.

3.3.2 Instrumental

See 3.1.2 Instrumental

3.3.3 Fabrication experimental procedure

The device design of limonene induced P3HT photodetector is similar to that described at 3.1.3.1.

3.3.3.1 Active layer

20.0 mg P3HT and 20.0 mg PCBM are weighed into a 10 ml vial. 1.0 ml R-(S-) limonene is added to the vial, and stirring using magnetic stir bar under 90 ˚C, until the mixture becomes a homogeneous solution-gel.

The patterned ITO slides are pre-heated to 90˚C, then perform the "hot spin-coating" in 3.2.3.1 to cast the P3HT limonene sol-gel. The device is then placed in vacuum to remove any limonene and deposited silver as described at 3.1.3.4.

3.4 Electrical characteristics measurement

Electrical characteristics of the photodetectors are measured by a Keithley 4200-SCS Semiconductor Characterization System. Current is measured under a swept voltage bias, from -30V to 30V for F8T2 devices and from -5V to 5V for P3HT devices. All the devices are measured under dark first, and then measured under a solar simulator light. The light intensity is approximately 100 mW/cm^2.

3.5 CPL response test of the photodetector

3.5.1 Test principle

In the following experiments the CPL sensitive photodetector is the photodetector giving a differential output current for left-handed CPL and right-handed CPL. Because the output current difference can be very small compared to overall output and noise, a lock-in amplifier is used to amplify the output current signal.

3.5.2 Laser setup

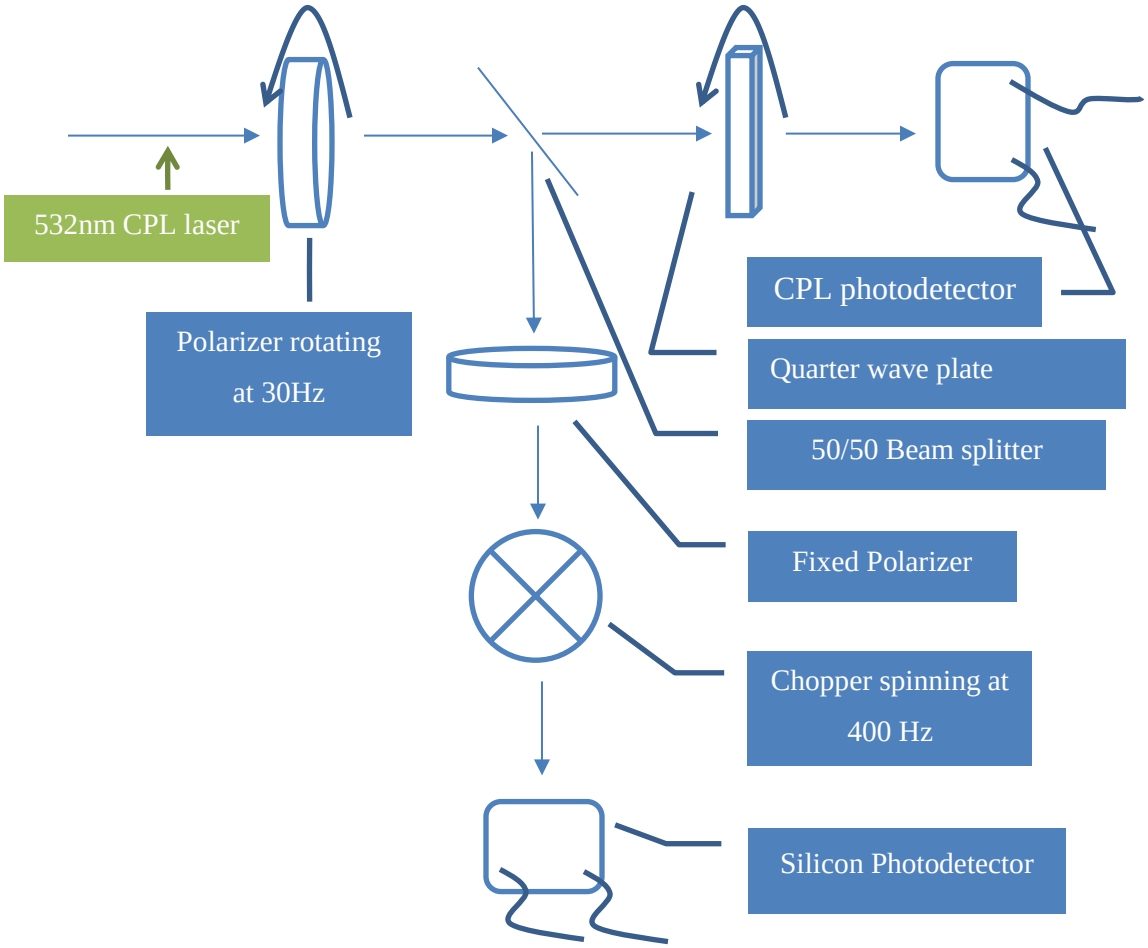

Figure 3-9 Laser setup

The laser source is circular polarized light (CPL) at 532 nm. It is generated from a coherent Verdi diode-pumped laser, followed by a quarter-wave plate. The wattage of the laser is 0.05w.

The outgoing CPL then passes a rotating polarizer, which drives the CPL to linear polarized light that its polarization direction is periodically changing.

After the beam splitter, the first beam passes through a quarter-wave plate. The outgoing light, which is now CPL periodically changing its polarization direction, goes into the CPL sensitive photodetector.

The other beam first passes a fixed polarizer, then the outgoing light, which is now flashing dark and bright at the same frequency as the rotation polarizer, passes a chopper to reach the silicon photodetector. The chopper and the silicon photodetector are synchronized by a lock-in amplifier to amplify the reference signal of the silicon photodetector.

3.5.3 Circuit setup

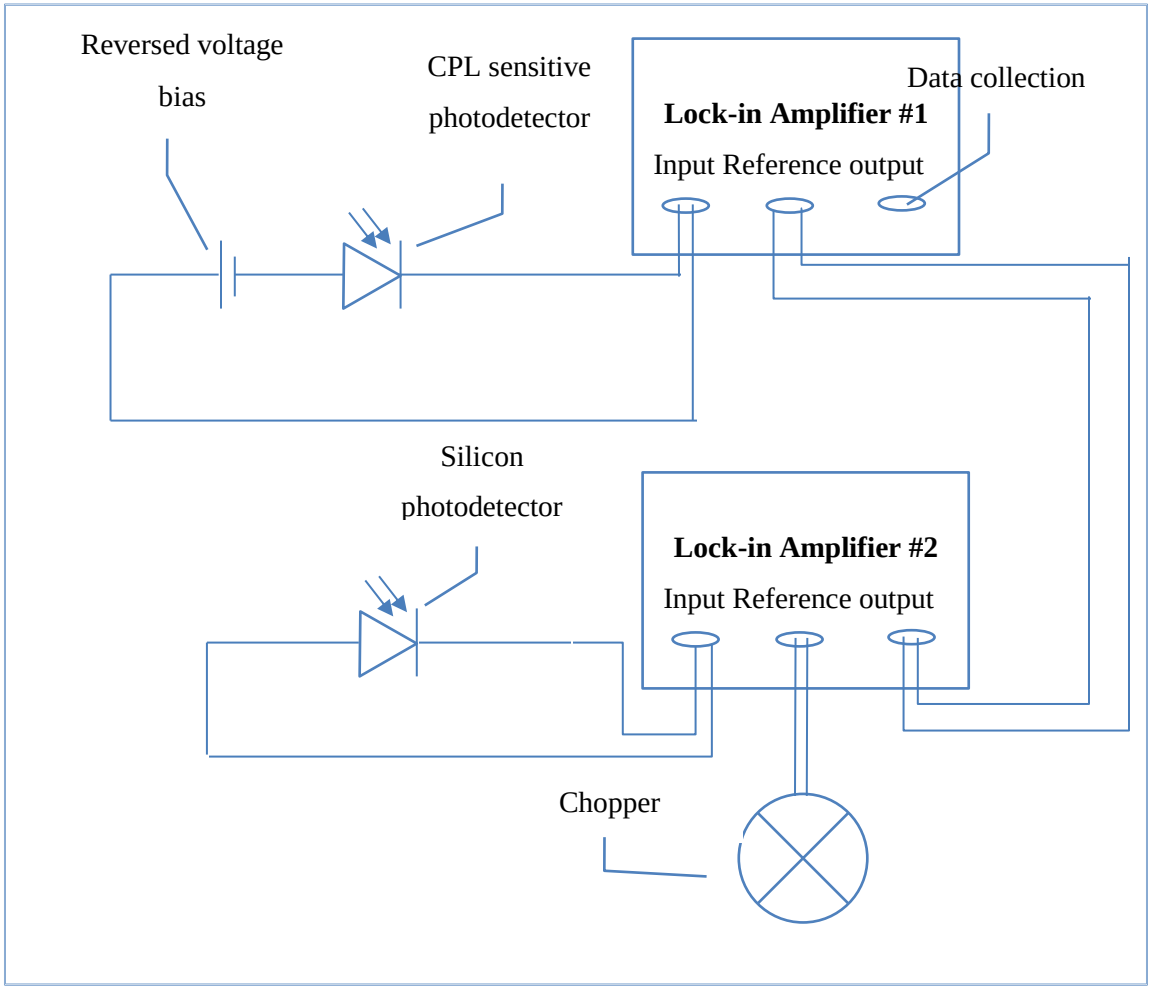

Figure 3-10 Circuit setup

A reversed voltage is added to the CPL sensitive photodetector, then the current is input into the lock-in amplifier #1. The output voltage signal of the silicon photodetector is input into the lock-in amplifier #2, while the frequency of the chopper is the reference signal. The output signal of the lock-in amplifier #2, which is the amplified silicon photodetector signal, is input to the reference channel of the lock-in amplifier #1. The output channel is connected to a PC for data collection.

3.5.4 Light polarization calculation

Assuming the light source is left-handed polarized, and the quarter wave plate has its fast axis horizontal, and assumes the fixed polarizer has the same direction as the start position of the rotating polarizer. Now we use Jones calculation to see the intensity and polarization of the light that shine to the CPL sensitive photodetector and the silicon photodetector.

The Jones vector of light source:

Equation 3-1

$$\frac{\sqrt{2}}{2}\begin{pmatrix}1\\+i\end{pmatrix}$$

The Jones matrix of the rotating polarizer with axis at angle θ:

Equation 3-2

$$\begin{pmatrix}\cos^2\theta & \sin\theta\cos\theta\\ \sin\theta\cos\theta & \sin^2\theta\end{pmatrix}$$

The Jones matrix of the quarter wave plate, with the fast axis at angle φ:

Equation 3-3

$$\begin{pmatrix}\cos^2\varphi + \mathrm{i}\sin^2\varphi & (1-\mathrm{i})\sin\theta\cos\theta\\ (1-\mathrm{i})\sin\theta\cos\theta & \sin^2\varphi + \mathrm{i}\cos^2\varphi\end{pmatrix}$$

The light that shine to the CPL sensitive photodetector:

Equation 3-4

$$\begin{pmatrix} \cos^2\varphi + \mathrm{i}\sin^2\varphi & (1-\mathrm{i})\sin\theta\cos\theta \\ (1-\mathrm{i})\sin\theta\cos\theta & \sin^2\varphi + \mathrm{i}\cos^2\varphi \end{pmatrix} \cdot \begin{pmatrix} \cos^2\theta & \sin\theta\cos\theta \\ \sin\theta\cos\theta & \sin^2\theta \end{pmatrix} \cdot \frac{\sqrt{2}}{2} \cdot \begin{pmatrix} 1 \\ +i \end{pmatrix}$$

Incident light on the silicon photodetector:

Equation 3-5

$$\begin{pmatrix} \cos^2\theta & \sin\theta\cos\theta \\ \sin\theta\cos\theta & \sin^2\theta \end{pmatrix} \cdot \begin{pmatrix} 1 & 0 \\ 0 & 0 \end{pmatrix} \cdot \frac{\sqrt{2}}{2} \cdot \begin{pmatrix} 1 \\ +i \end{pmatrix}$$

$$= \frac{\sqrt{2}}{2} \cdot \begin{pmatrix} \cos^2\theta + \mathrm{i}\sin\theta\cos\theta \\ 0 \end{pmatrix}$$

Firstly, we fix the quarter wave plate (QWP) to $\varphi = 0$:

$$When\ \theta = 0, Equation\ 3-4 = \begin{pmatrix} 1 \\ 0 \end{pmatrix}, vector\ length$$

$$= 1, \text{the light is horizontally linear polarized.}$$

$$When\ \theta = \frac{\pi}{4}, Equation\ 3-4 = \frac{\sqrt{2}}{2} \cdot \begin{pmatrix} \frac{1}{2} - \frac{1}{2}i \\ \frac{1}{2} + \frac{1}{2}i \end{pmatrix}, vector\ length$$

$$= 1, the\ light\ is\ left-handed\ polarized.$$

Similarly:

$$When\ \theta = 0, Equation\ 3-5 = \begin{pmatrix}1\\0\end{pmatrix}, vector\ length$$

$$= 1, the\ light\ is\ horizontally\ linear\ polarized.$$

$$When\ \theta = \frac{\pi}{4}, Equation\ 3-5 = \frac{\sqrt{2}}{2}\cdot\begin{pmatrix}\frac{1}{2}-\frac{1}{2}i\\0\end{pmatrix} vector\ length = \frac{1}{\sqrt{2}},$$

$$the\ light\ is\ linear\ polarized.$$

We can calculate the result when the rotating polarizer rotates from 0 to 2π for $\varphi = 0$:

Table 3-1

θ =	Jones vector of equation 3-4 (set $\varphi = 0$)	Polarization of Jones vector of equation 3-4	Jones vector of equation 3-5	Vector length of equation 3-4	Vector length of equation 3-5	
0	$\begin{pmatrix}1\\0\end{pmatrix}$	Linear	$\begin{pmatrix}1\\0\end{pmatrix}$	1	1	
π/4	$\begin{pmatrix}\frac{1}{2}-\frac{1}{2}i\\\frac{1}{2}+\frac{1}{2}i\end{pmatrix}$	Left-handed	$\begin{pmatrix}\frac{1}{2}-\frac{1}{2}i\\0\end{pmatrix}$	1	$\frac{1}{\sqrt{2}}$	
π/2	$\begin{pmatrix}0\\1\end{pmatrix}$	linear	$\begin{pmatrix}0\\0\end{pmatrix}$	1	0	
3π/4	$\begin{pmatrix}\frac{1}{2}+\frac{1}{2}i\\\frac{1}{2}-\frac{1}{2}i\end{pmatrix}$	Right-handed	$\begin{pmatrix}\frac{1}{2}+\frac{1}{2}i\\0\end{pmatrix}$	1	$\frac{1}{\sqrt{2}}$	
π	$\begin{pmatrix}1\\0\end{pmatrix}$	Linear	$\begin{pmatrix}1\\0\end{pmatrix}$	1	1	

5π/4	$\begin{pmatrix} \frac{1}{2}-\frac{1}{2}i \\ \frac{1}{2}+\frac{1}{2}i \end{pmatrix}$	Left-handed	$\begin{pmatrix} \frac{1}{2}-\frac{1}{2}i \\ 0 \end{pmatrix}$	1	$\frac{1}{\sqrt{2}}$	
3π/2	$\begin{pmatrix} 0 \\ 1 \end{pmatrix}$	linear	$\begin{pmatrix} 0 \\ 0 \end{pmatrix}$	1	0	
7π/4	$\begin{pmatrix} \frac{1}{2}+\frac{1}{2}i \\ \frac{1}{2}-\frac{1}{2}i \end{pmatrix}$	Right-handed	$\begin{pmatrix} \frac{1}{2}+\frac{1}{2}i \\ 0 \end{pmatrix}$	1	$\frac{1}{\sqrt{2}}$	
2 π	$\begin{pmatrix} 1 \\ 0 \end{pmatrix}$	Linear	$\begin{pmatrix} 1 \\ 0 \end{pmatrix}$	1	1	

Generally the sum of the squares of the absolute values of the two components of vectors calculated by **equation 3-4**, which equals the light intensity irradiate to the CPL sensitive photodetector is shown below:

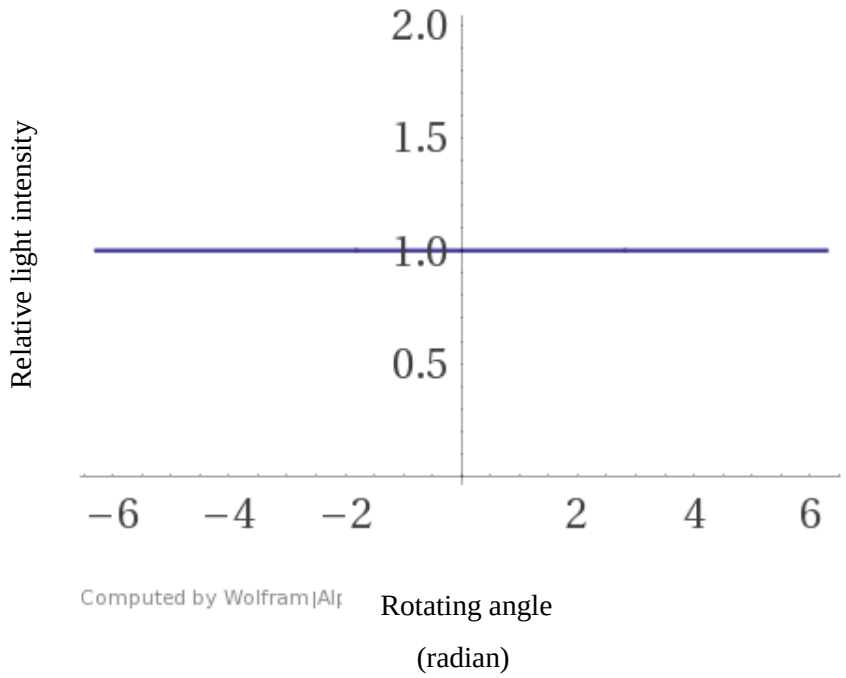

Figure 3-11 Relative light intensity calculated using equation 3-4 (Constant 1)

And the sum of the squares of the absolute values of the two components of vectors calculated by **equation 3-5**, which equal to the light intensity irradiate to the silicon photodetector is shown below:

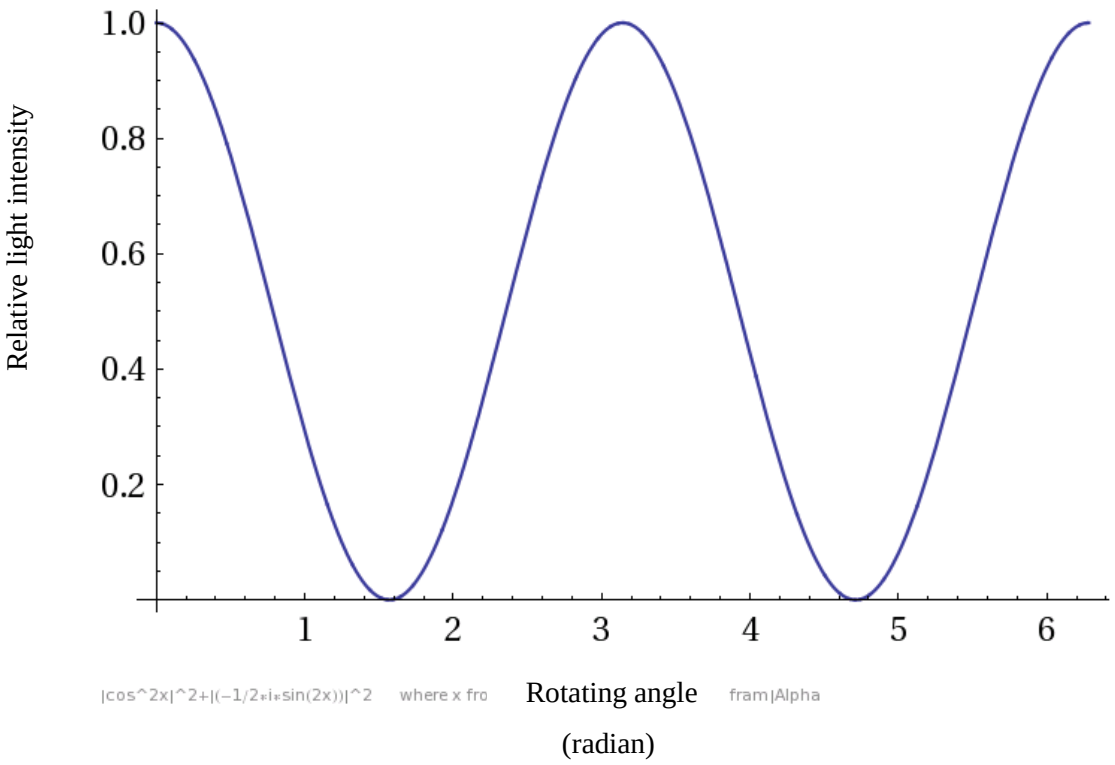

Figure 3-12 Relative light intensity calculated using equation 3-5

3.5.5 Data collection

In the laser setup, the axis angle of the quarter wave plate can be changed. By changing it, the right-handed and left-handed CPL can be obtained at different phase of the reference signal. For instance, if the quarter wave plate axis angle is horizontal, the left-handed CPL will appear at the maxima $+\pi/4$ of the reference signal; if the quarter wave plate is placed at horizontal $-\pi/4$, the left-handed CPL will appear at the reference maxima.

The output signals from the lock-in amplifier #1 (voltage or current) are recorded while the quarter wave plate rotates from 0 degree (fast axis vertical) to 360 degrees, with an EasySync^{TM} USB oscilloscope and export as comma-separated values (CSV) data.

3.5.6 Test setup conclusion

In conclusion, the light intensity shined to the CPL sensitive photodetector doesn't change with time, but the light polarization changes from left-handed CPL to right-handed CPL at a period of π (considering the rotation of the polarizer). The light intensity shined at the silicon photodetector oscillates from its maxima to minima at a period of π (considering the rotation of the polarizer), which is the same period as the polarization change of the incident light to the CPL sensitive photodetector. Thus, we can use the silicon photodetector output as the reference signal of the lock-in amplifier, to amplify the signal corresponding to the circular polarization.

Chapter 4

Results and Discussion

Figure 4-1 to **Figure 4-3** show the CD and UV-Vis spectra of the 3 kinds of CD active polymers.

The absorbance spectrum of limonene induced P3HT shows a red-shift compared to good solvent casted P3HT film, but matches the spectrum of annealed P3HT. This indicates that the "hot spin-coating" process results in a similar crystallinity of P3HT as annealing.[42]

4.1 CD and UV-Vis spectra of the devices

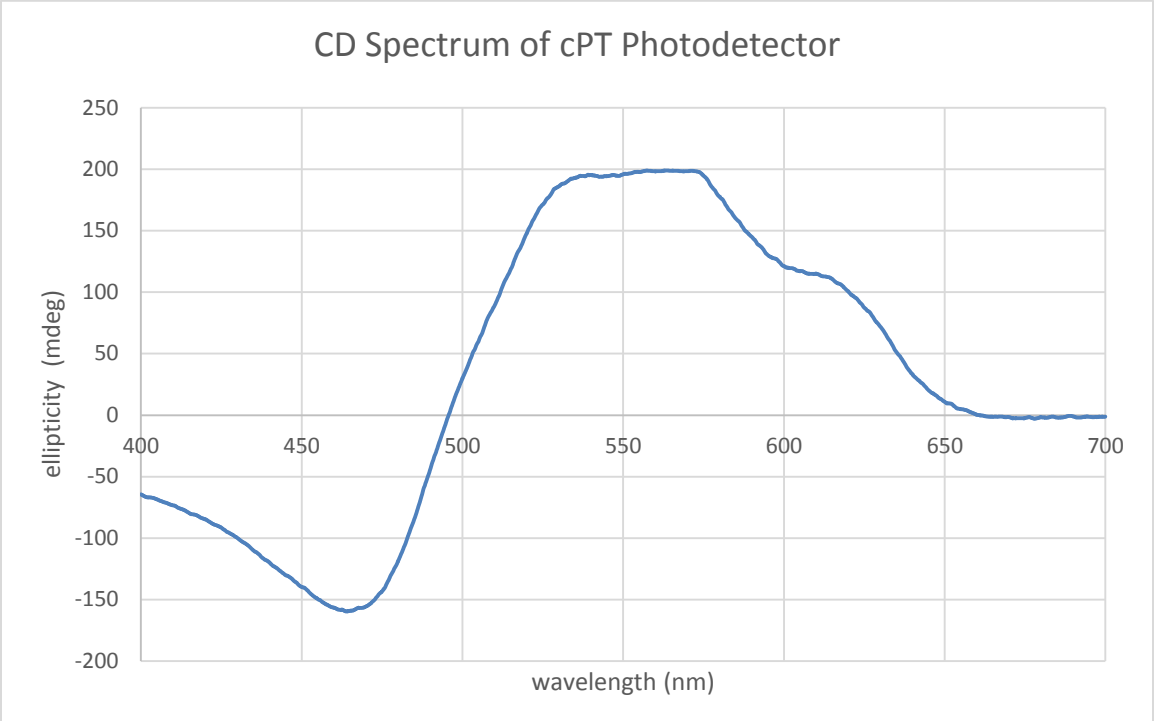

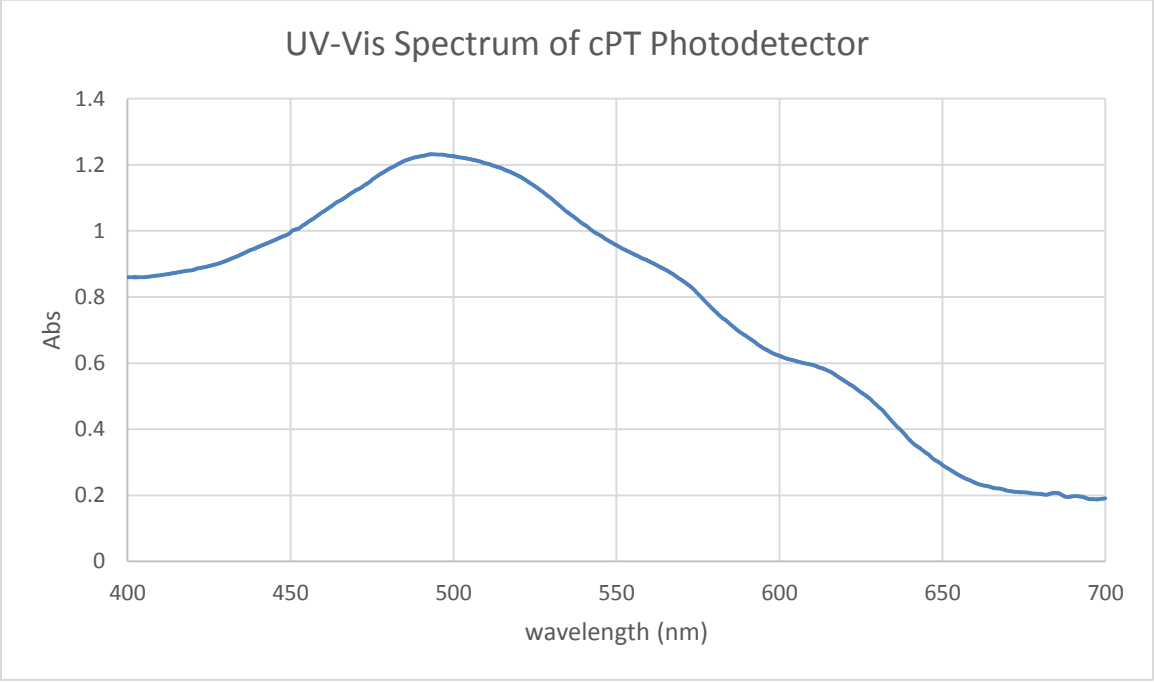

Figure 4-1 CD and Uv-Vis spectra of Polythiophene with chiral side chain (chiral PT,cPT) Photodetector

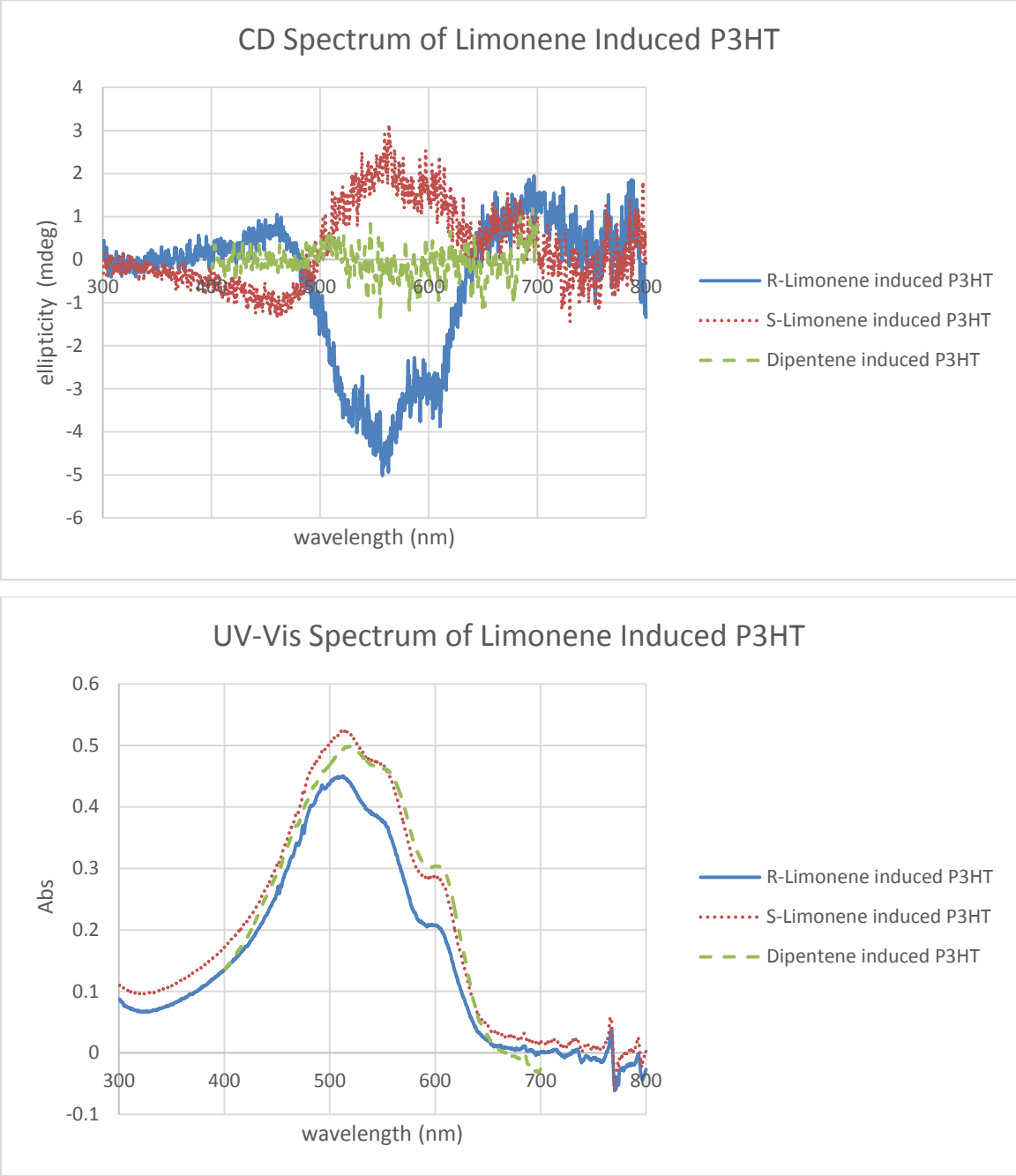

Figure 4-2 CD and Uv-Vis spectra of Limonene induced P3HT:PCBM Photodetectors

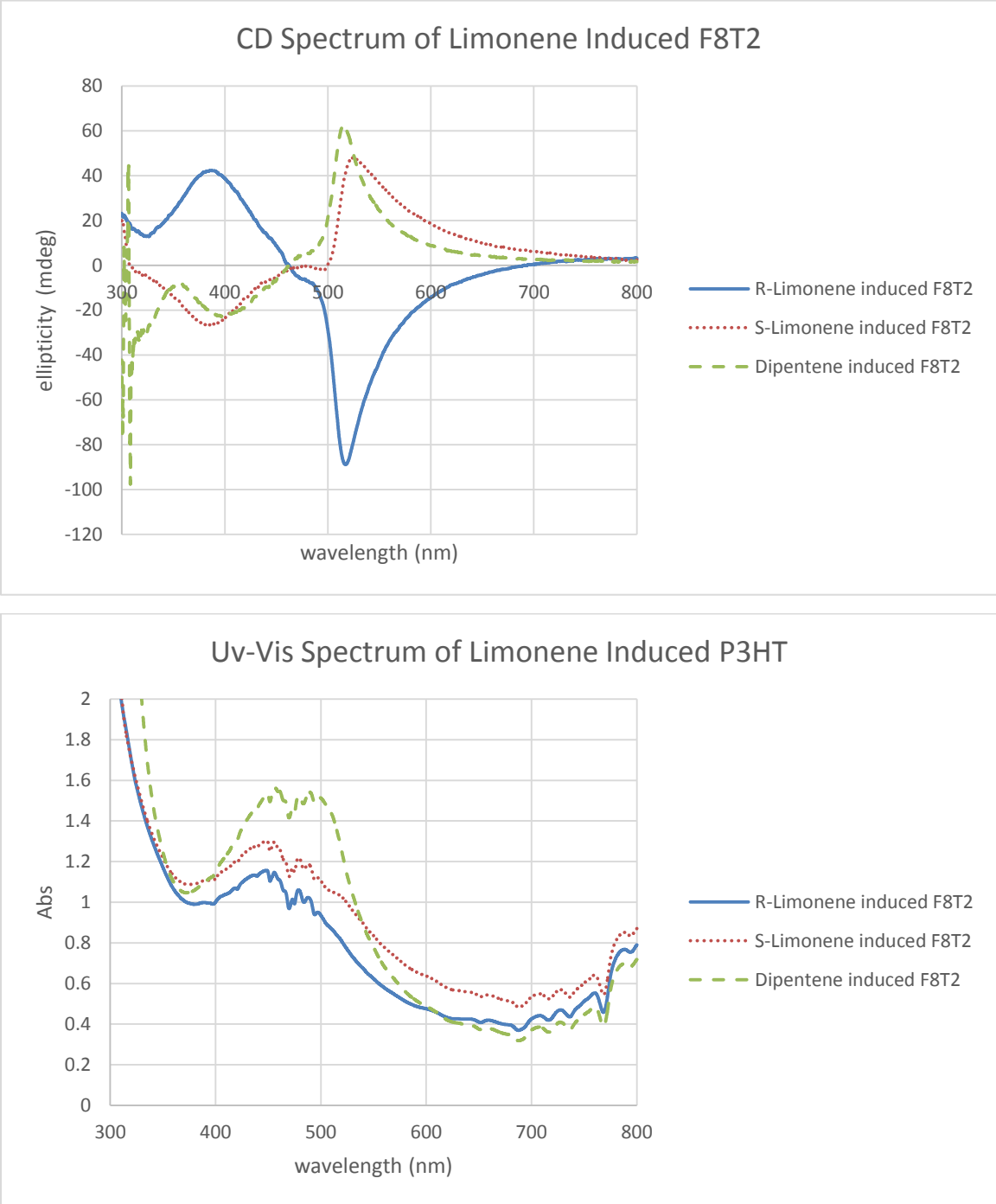

Figure 4-3 CD and Uv-Vis spectra of Limonene induced F8T2:PCBM Photodetectors

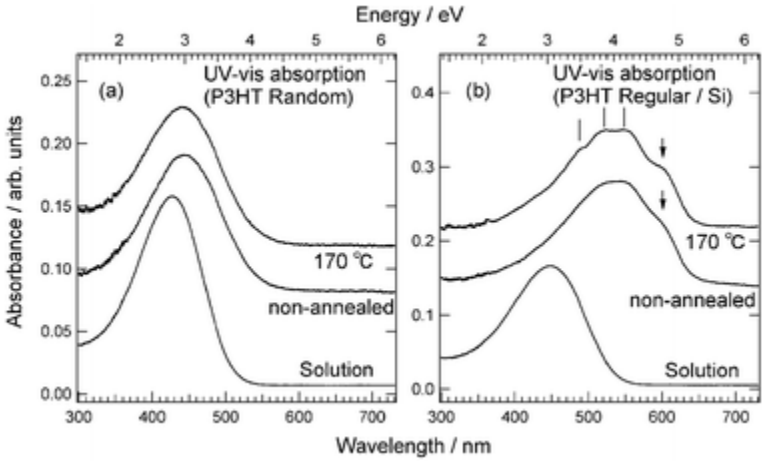

Figure 4-4 UV-vis absorption spectra of P3HT with/without annealing [42]

In order to normalize the CD of each device, Kuhn's g-factor [43], which is the ratio of a sample's CD and absorbance signals, is used:

Equation 4-1

$$g_{CD} = \frac{A_l - A_r}{A}$$

A_l is the absorbance of left-handed circular polarized light and A_r is the absorbance of right-handed circular polarized light, A is the absorbance of unpolarised light.

The CD is measured as ellipticity (θ) in mdeg (1/1000 degree), and it can be easily transformed as ΔA by the equation:

Equation 4-2

$$\theta\ (\text{mdeg}) = 1000 \cdot \ln 10 \cdot \frac{360}{8\pi} \cdot \Delta A$$

Equation 4-3

$$g_{CD} = \frac{\Delta A}{A}$$

Table 4-1 CD data of limonene induced polymers

	Wavelength at Peak CD	Peak CD	Absorbance at peak CD	gcd
cPT	563.7	1.99E+02	0.889	6.79E-03
R-limonene induced P3HT	557.3	-5.02E+00	0.352	-4.32E-04
S-limonene induced P3HT	563.3	3.10E+00	0.419	2.25E-04
Dipentene induced P3HT	555.4	-1.40E+00	0.458	-9.25E-05
R-limonene induced F8T2	517.1	-8.89E+01	0.827	-3.26E-03
S-limonene induced F8T2	524.6	4.81E+01	0.998	1.46E-03
Dipentene induced F8T2	515	6.26E+01	1.357	1.40E-03

Chiral PT devices show significant Cotton effect at its absorbance band. The CD spectrum shape and g_{cd} are relatively repeatable using the fabrication method described at 3.1.3.

Limonene induced P3HT devices show weak yet obvious Cotton effect. The CD and UV-Vis spectra of S-limonene induced P3HT and the cPT device are very similar, suggesting that they may share the same mechanism to generate CD activity.

Limonene induced F8T2 devices have much stronger Cotton effect, with a g_{cd} higher than 1E-03, which is close to the g_{cd} of polythiophene with covalent connected chiral centre.

As the fabrication procedures of the limonene induced polymer devices are complex and inaccurate due to lack of temperature control and fast crystallization, the characteristics of products are inconstant. The g_{cd} values and spectrum shape can be very different from one batch to another, one spot of the film to another. An R-limonene induced F8T2 is recorded CD signal of 645 mdeg and g_{cd} of 1.36E-02, which is about twice as high as of cPT device. However, the sample is not repeatable. (See Appendix)

Moreover, the polarization of spectrum can be reversed when the same limonene induced device at different spot are measured. This can be a result of non-uniform film, and small domains that are crystallized differently. The strong CD signal of the racemic limonene induced F8T2 can be explained by the small domain, too.

4.2 Surface morphology of active layers

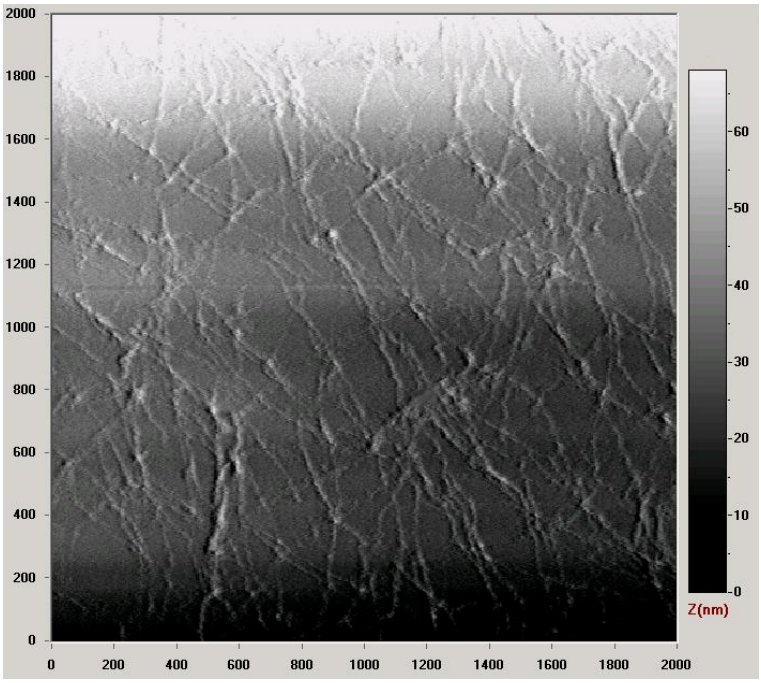

Figure 4-5 AFM image of R-limonene induced P3HT

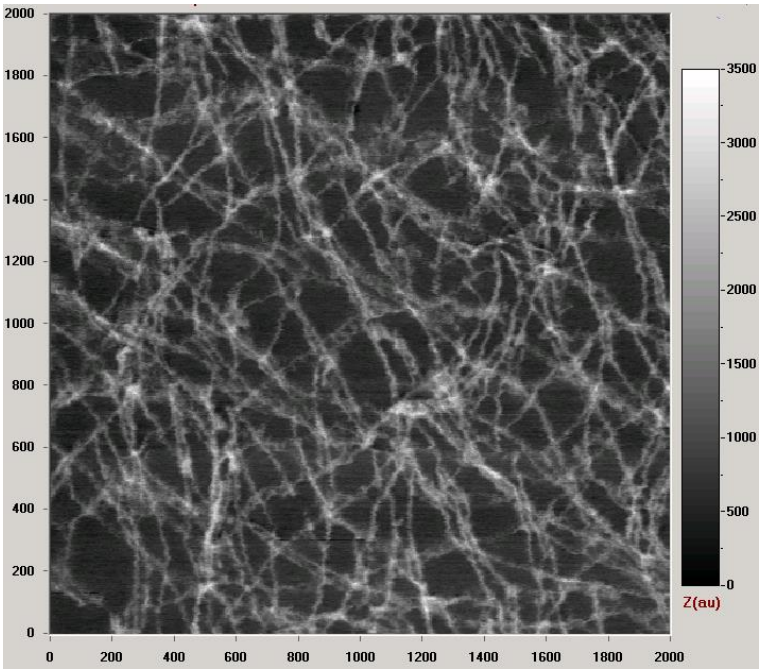

Figure 4-6 AFM phase image of R-limonene induced P3HT

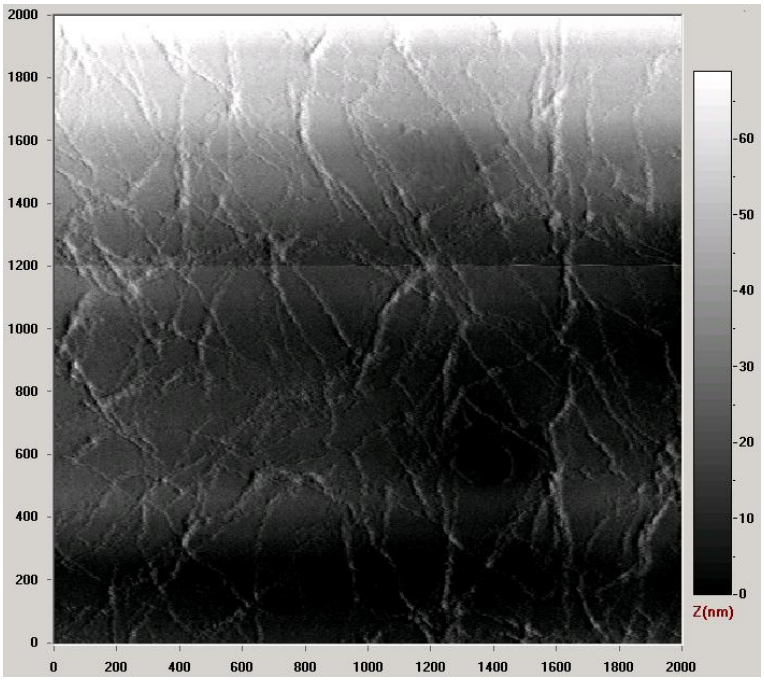

Figure 4-7 AFM image of S-limonene induced P3HT

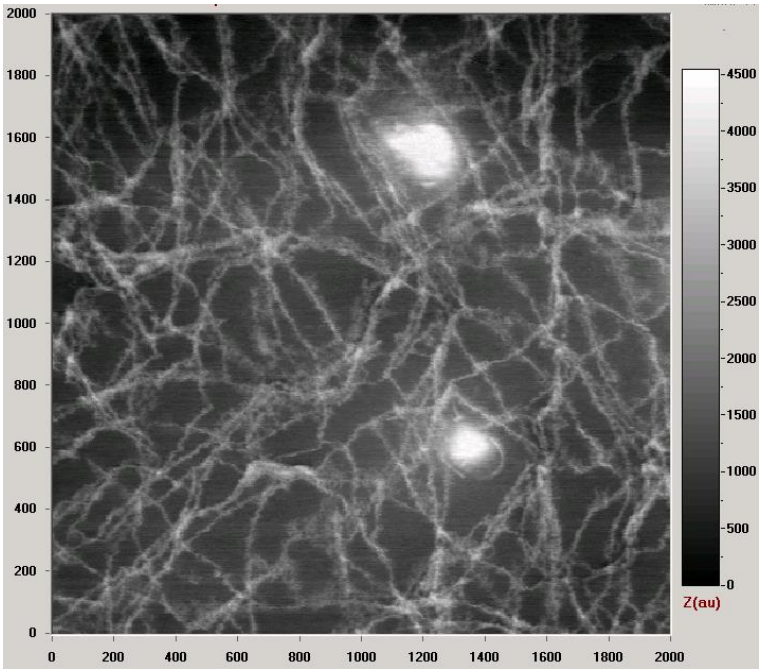

Figure 4-8 AFM image of S-limonene phase induced P3HT

Nano rods can be clearly seen from limonene induced P3HT, supports that “hot spin-coating” process forms similar crystallinity of P3HT as annealed P3HT film.

4.3 Electrical characteristics of the photodetectors

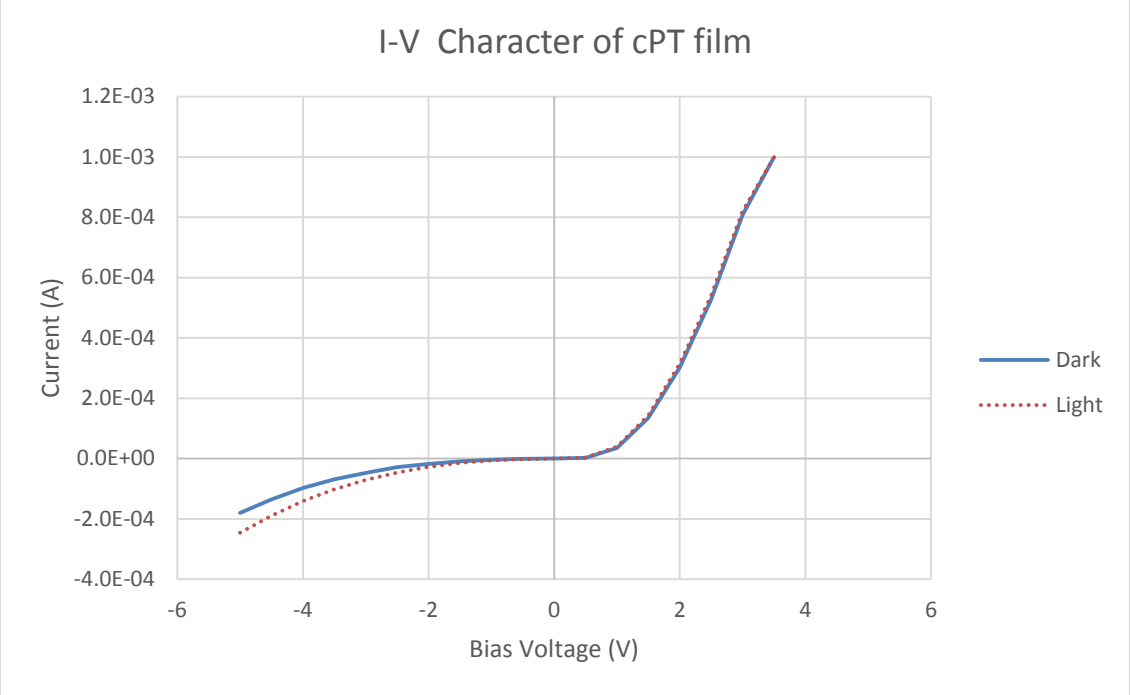

Figure 4-9 I-V Character of cPT

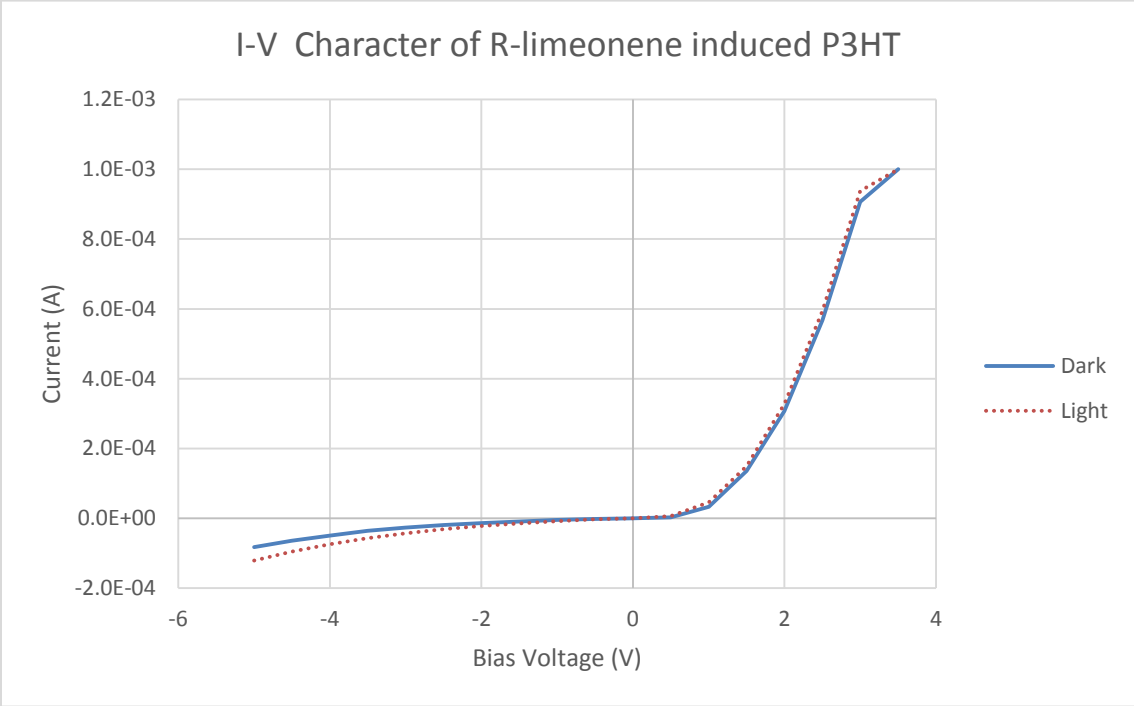

Figure 4-10 I-V Character of R-limonene induced P3HT

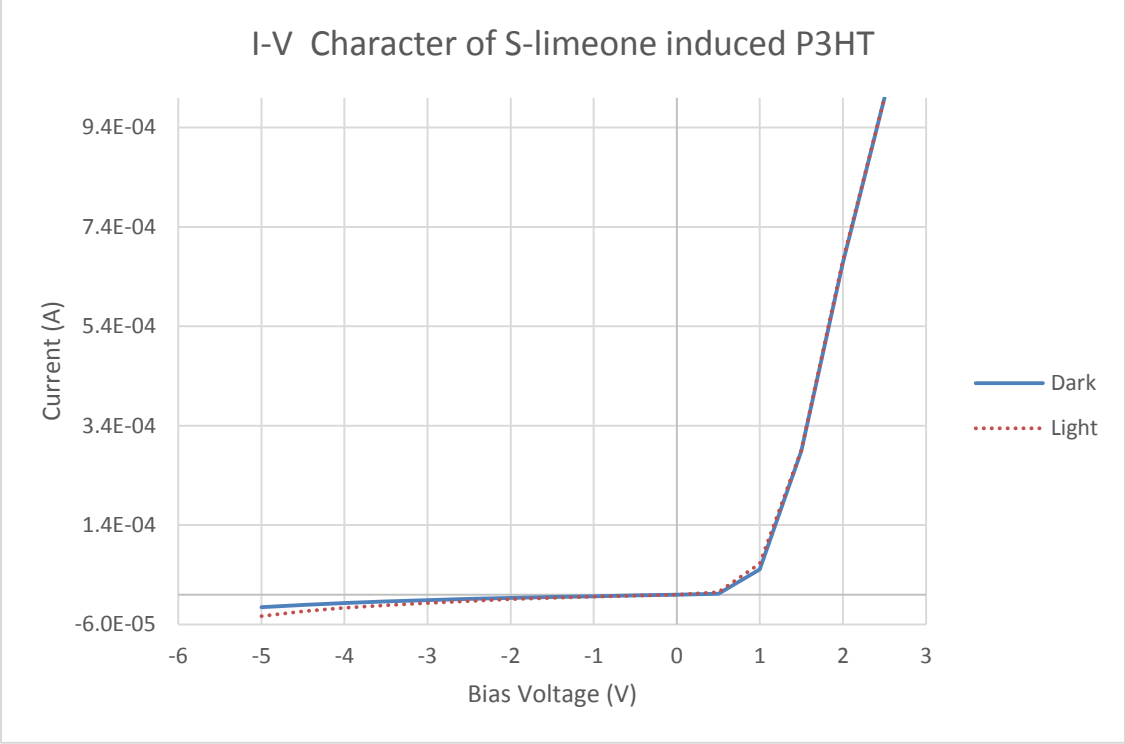

Figure 4-11 I-V Character of S-lime one induced P3HT

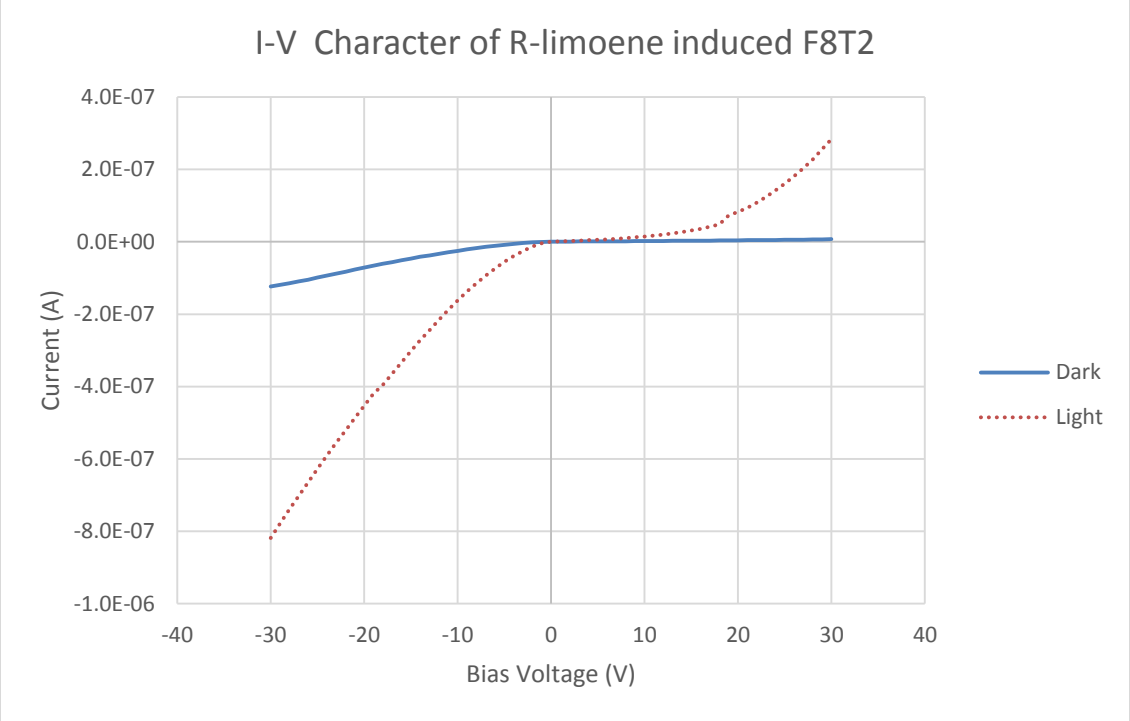

Figure 4-12 I-V Character of R-limonene induced F8T2

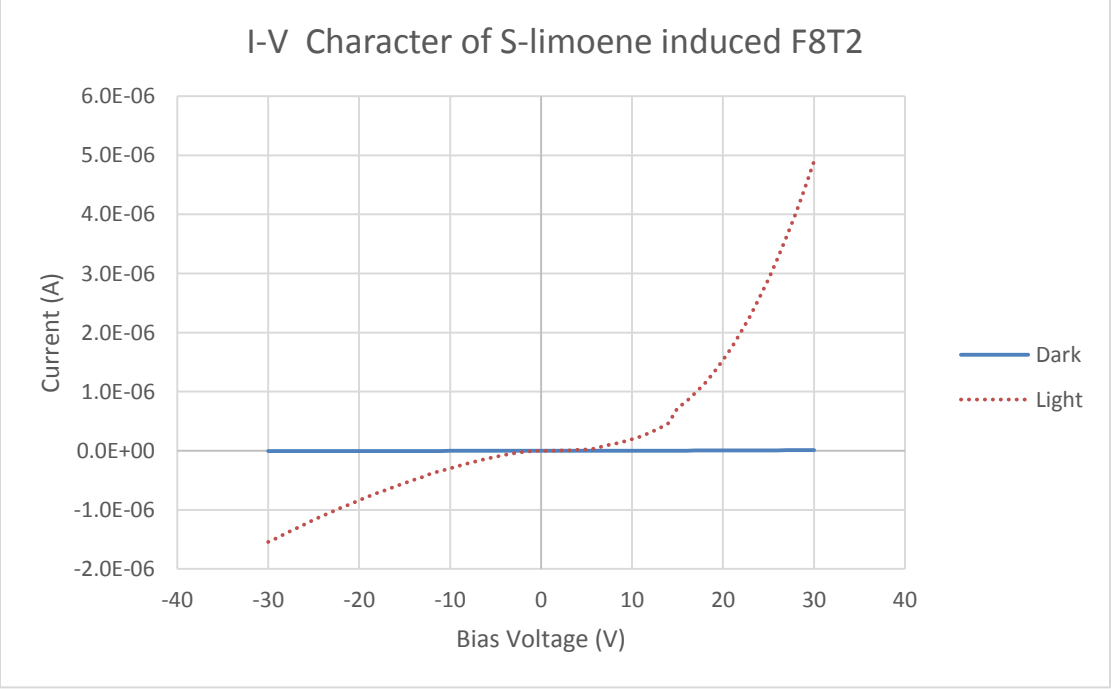

Figure 4-13 I-V Character of S-limonene induced F8T2

Structurally, all the tested devices are photodiodes. All of these photodiodes generate negative current when irradiated by light. When apply negative voltage bias to it, the reverse current increases. These electrical characteristics make them good photodetectors. The optimal work condition can be also determined by the measurement data.

4.4 Study of devices' circular polarized light response

Firstly, because the light intensity that was shined onto the quarter-wave plate varied periodically due to imperfect purity circular polarized light. The intensity change can be considered as a sine wave, which has the same frequency of the reference signal.

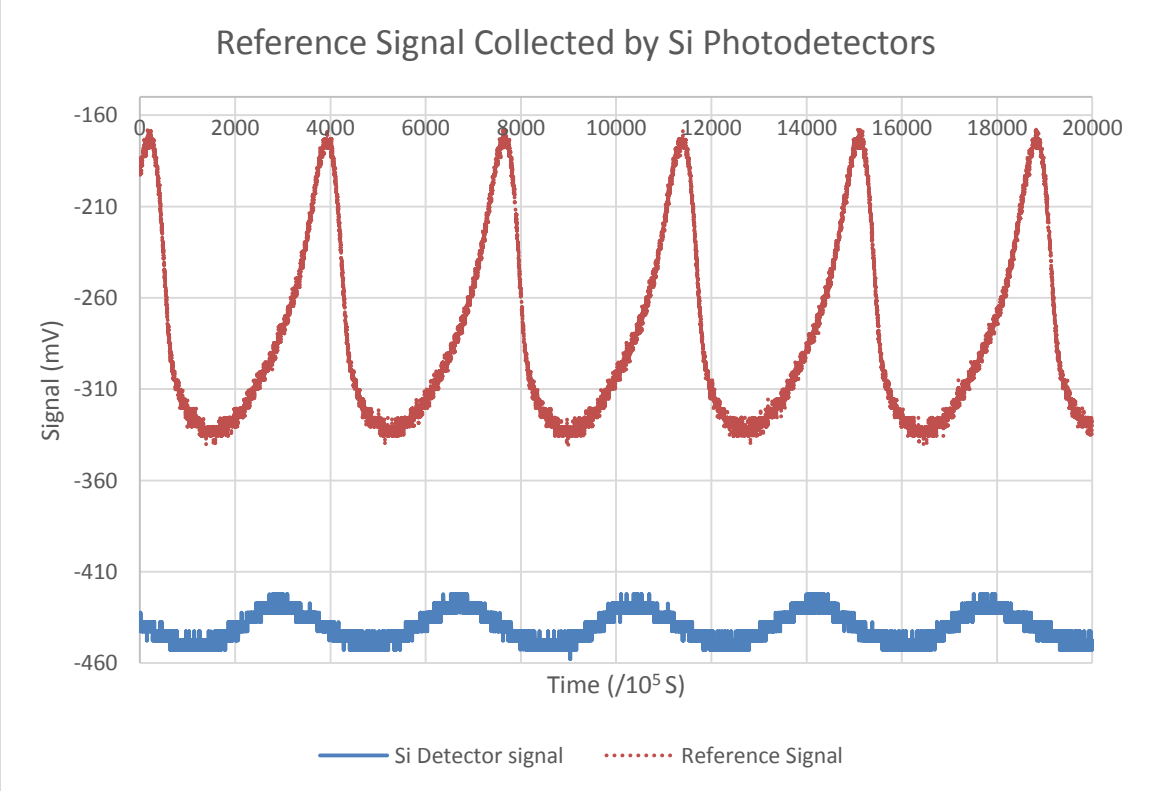

Figure 4-14 Reference Signal Collected by Si Photodetectors

Figure 4-14 shows the light intensity signal collected by silicon photodetector. Blue data points are collected by the Si photodetector that replaced the organic photodetector; the red data points are collected by the reference Si photodetector. All data are collected directly without lock-in amplifiers. (See **Figure 3-11**).

We can see from **Figure 4-14** that, as proposed above, both beams oscillate at the same frequency of 30 Hz, which is the frequency of the Rotating Polarizer (**Figure 3-11**). The phase shift is 85˚, the phase shift comes from the relative position of the fixed polarizer and the position of the quarter-wave plate.

Meanwhile, when the laser passed through the quarter-wave plate, left-handed and right-handed CPL are periodically generated with the same frequency of the reference signal. Furthermore, the phase can be changed by rotating the quarter-wave plate. Thus, assuming the polymer photodetector is more sensitive to left-handed CPL than right-handed-CPL, when the left-handed CPL overlaps the intensity peak of the incoming laser, the photodetector output is increased. When the right-handed CPL overlaps the intensity, peak, the output signal will be decreased. Therefore, we can study the photodetector's sensitivity to the different polarization light, by studying the output signal to quarter-wave plate rotation graph. A reference test (**Figure 4-15**) is performed by a Si photodetector, which is known to be inert to CPL. The irregular while relatively flat graph shows that the transparency of the quarter-wave plate is relatively uniform over the circle. And the data allows determination of the noise on the measurements.

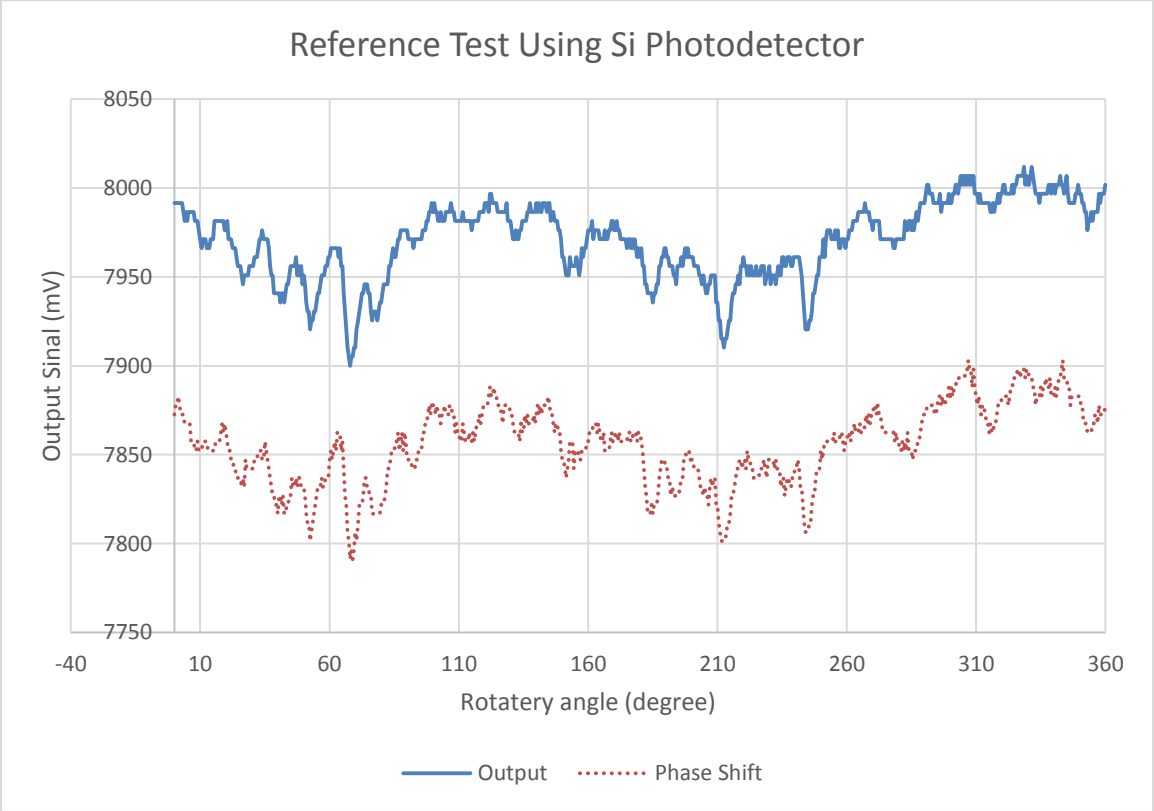

Figure 4-15 Reference Test Using Si Photodetector

4.4.1 Photodetector using cPT

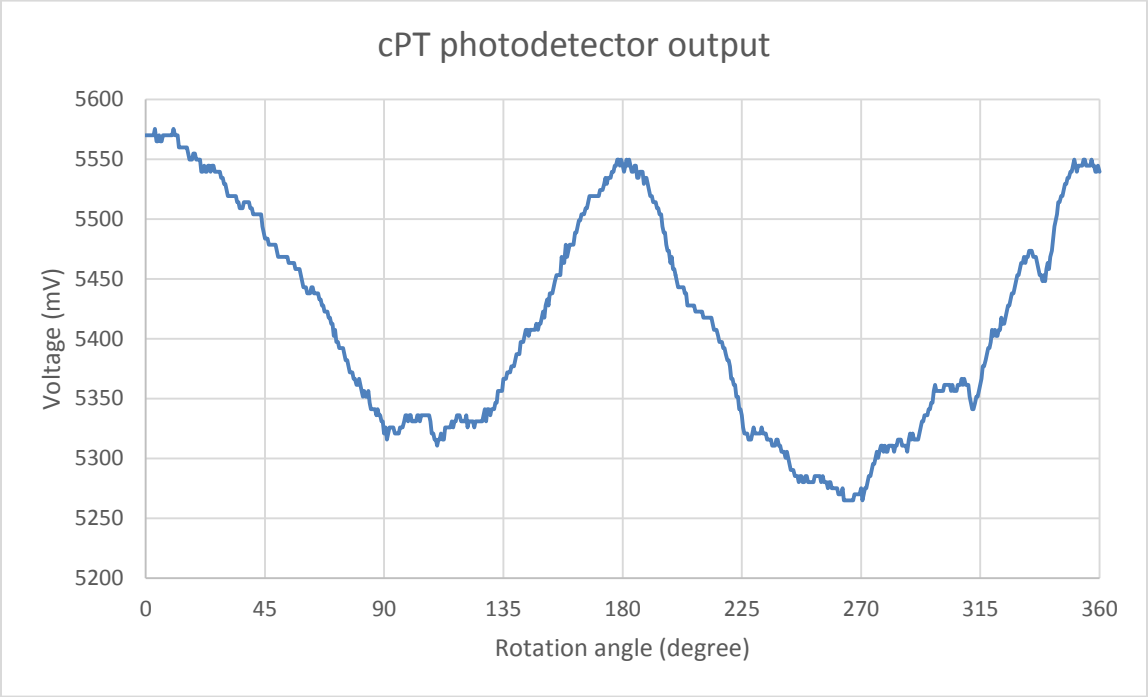

Figure 4-16 cPT photodetector output

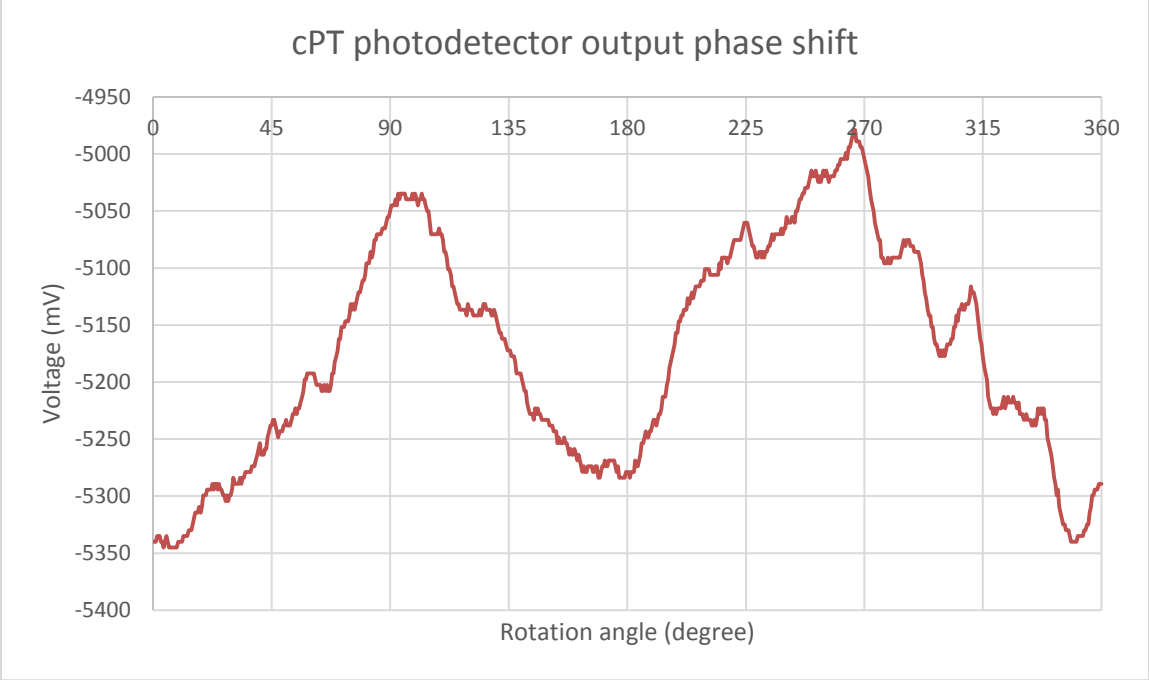

Figure 4-17 cPT photodetector output phase shift compare to the reference signal

From **Figure 4-16** we can see that the device has the maximal output when the quarter-wave plate has its fast axis vertical and has a repeat period of π. According to Table 3-1, the same polarization of CPL appears at a repeat period of π. So it is highly likely that cPT photodetector output a maximal signal when one polarization CPL irradiate to it and output a minimal signal when the other polarization CPL irradiate to it.

The photodetector's sensitivity to CPL can be defined as:

Equation 4-4

$$a_{sensitivity} = \frac{2(V_{max} - V_{\min})}{(V_{max} + V_{\min})}$$

$$a_{sensitivity} = \frac{2(5.6\text{E}3 - 5.3\text{E}3)}{(5.6\text{E}3 + 5.3\text{E}3)} \times 100\% = 6\%$$

V_{max} and V_{min} are maximal and minimal output signals in voltage that are collected from the lock-in amplifier #1.

Interestingly, the g_{CD} = 6.79E-03 is much lower than the $a_{sensitivity}$ value of 6%, suggesting that the CPL response may not all come from the device's absorbance difference to left-handed CPL and right-handed CPL.

4.4.2 Photodetectors with limonene induced polymers

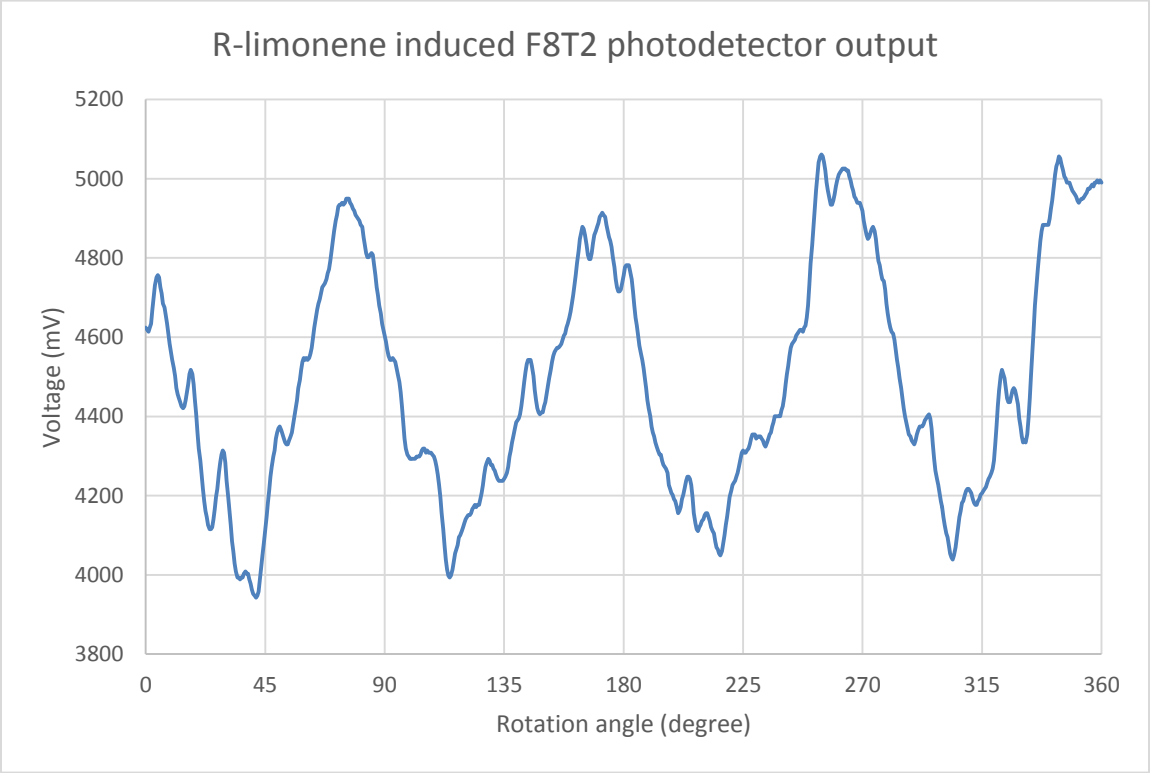

Figure 4-18 R-limonene induced F8T2 photodetector output

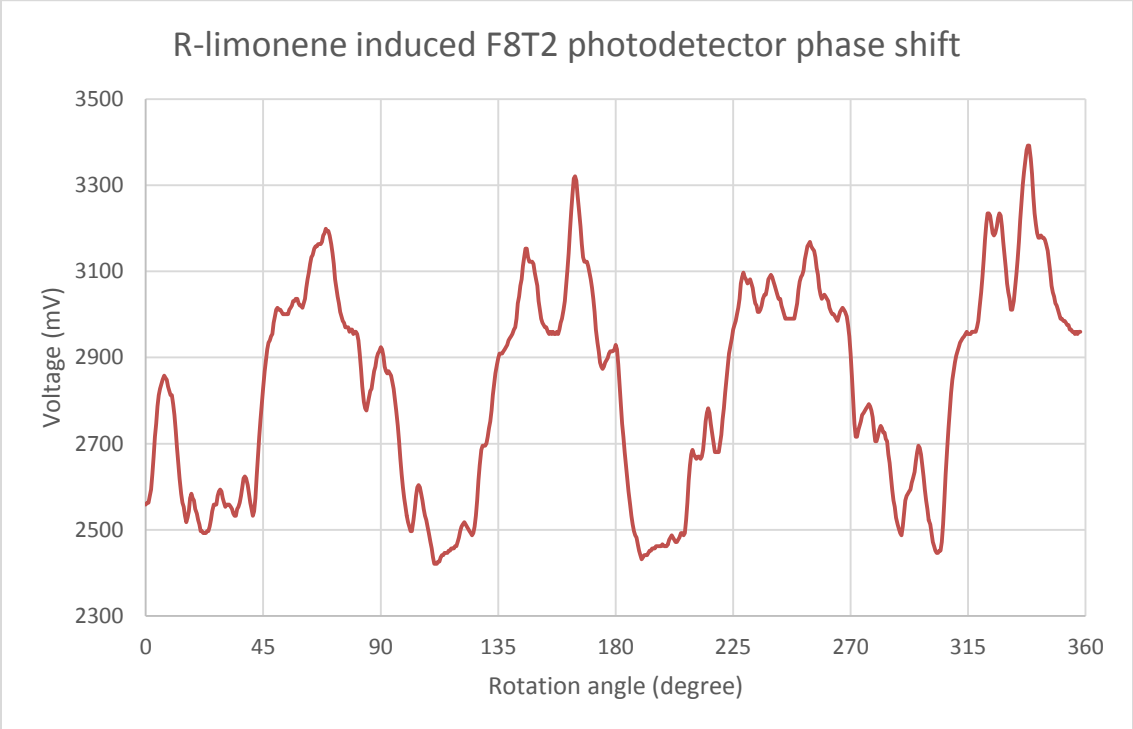

Figure 4-19 R-limonene induced F8T2 photodetector phase shift compare to the reference signal

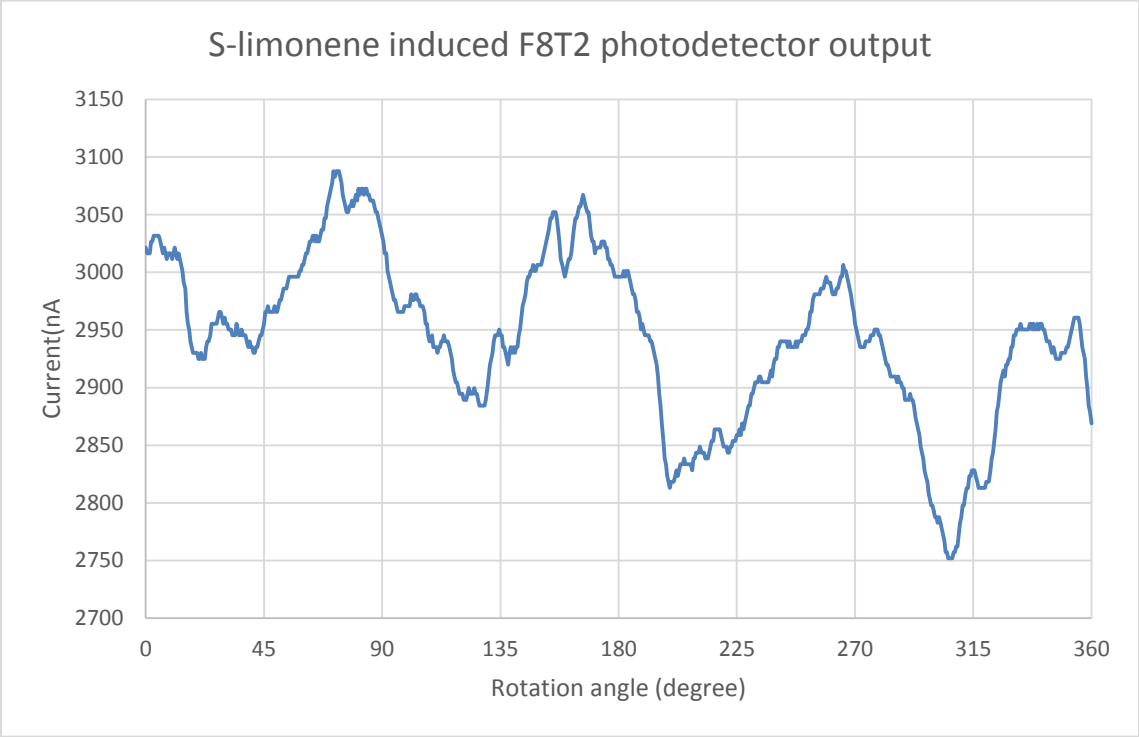

Figure 4-20 S-limonene induced F8T2 photodetector output

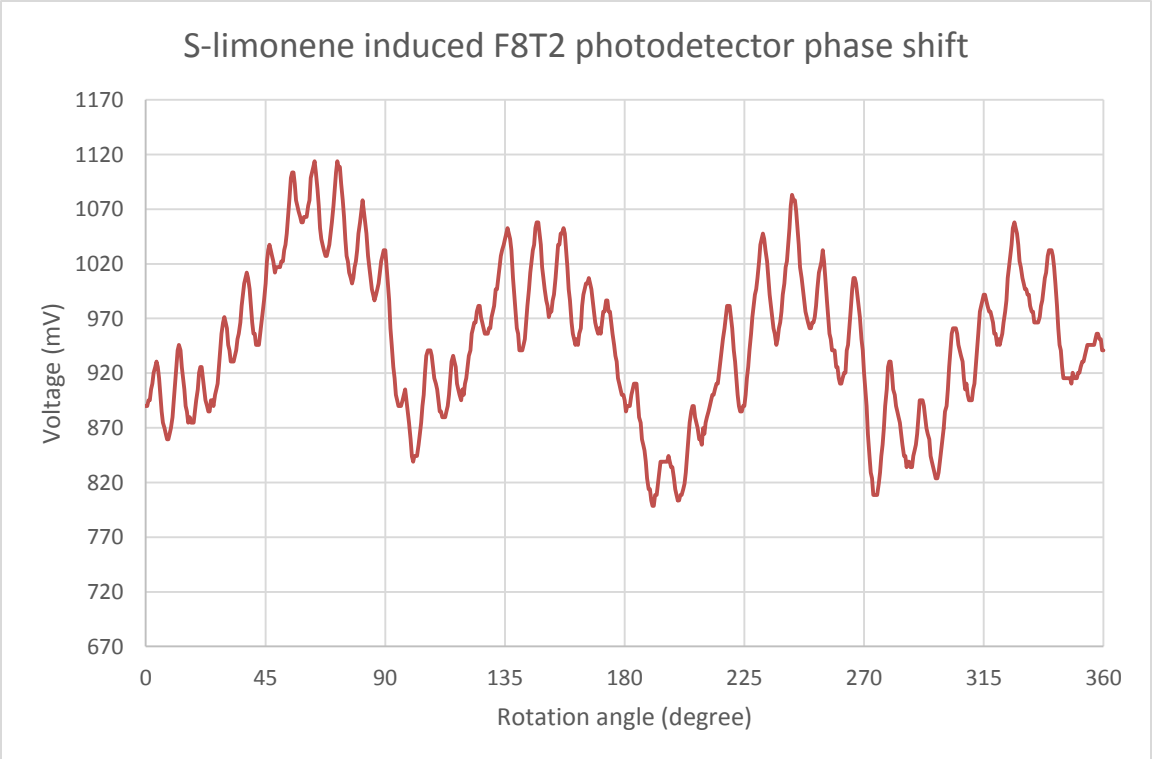

Figure 4-21 S-limonene induced F8T2 photodetector phase shift compare to the reference signal

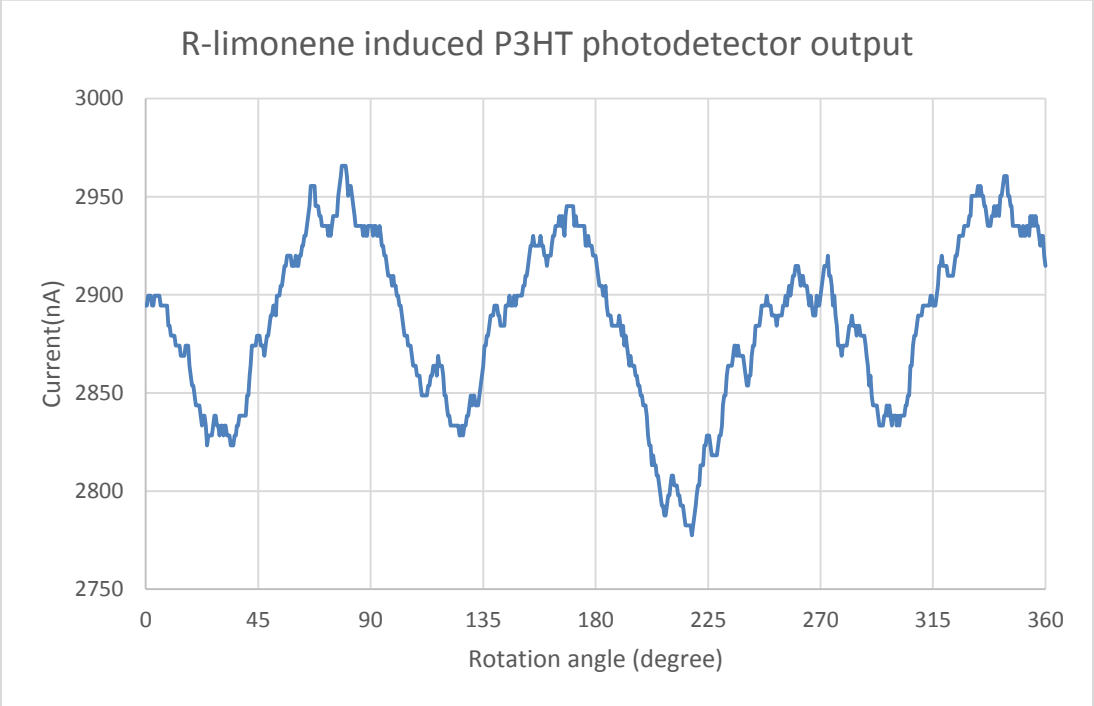

Figure 4-22 R-limonene induced P3HT photodetector output

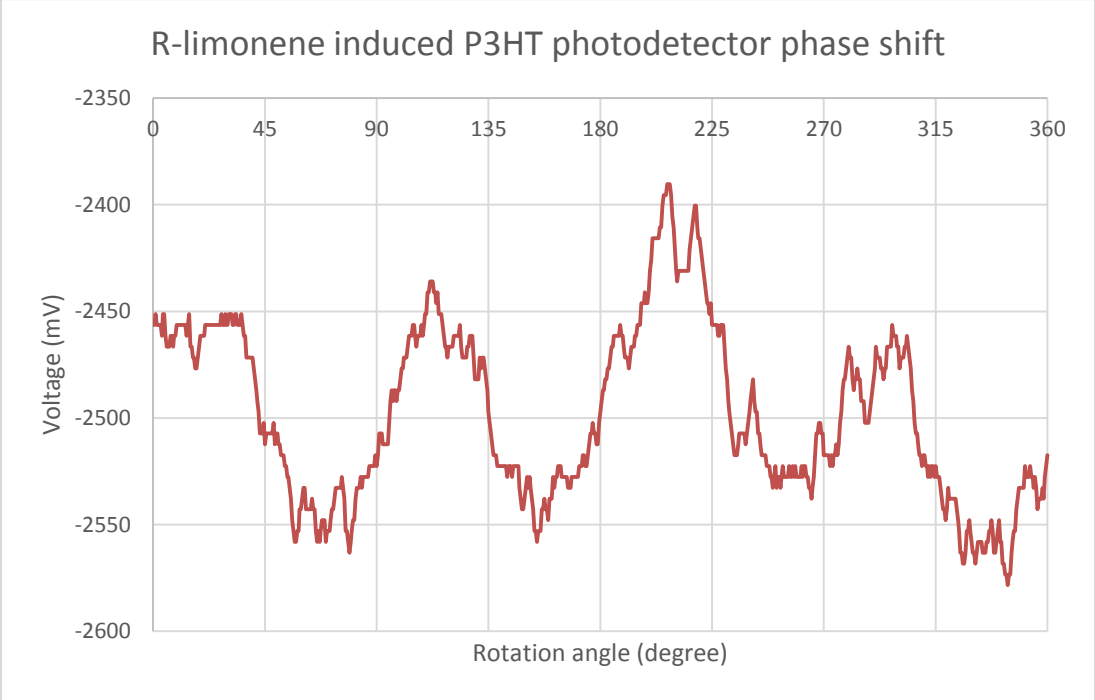

Figure 4-23 R-limonene induced P3HT photodetector phase shift compare to the reference signal

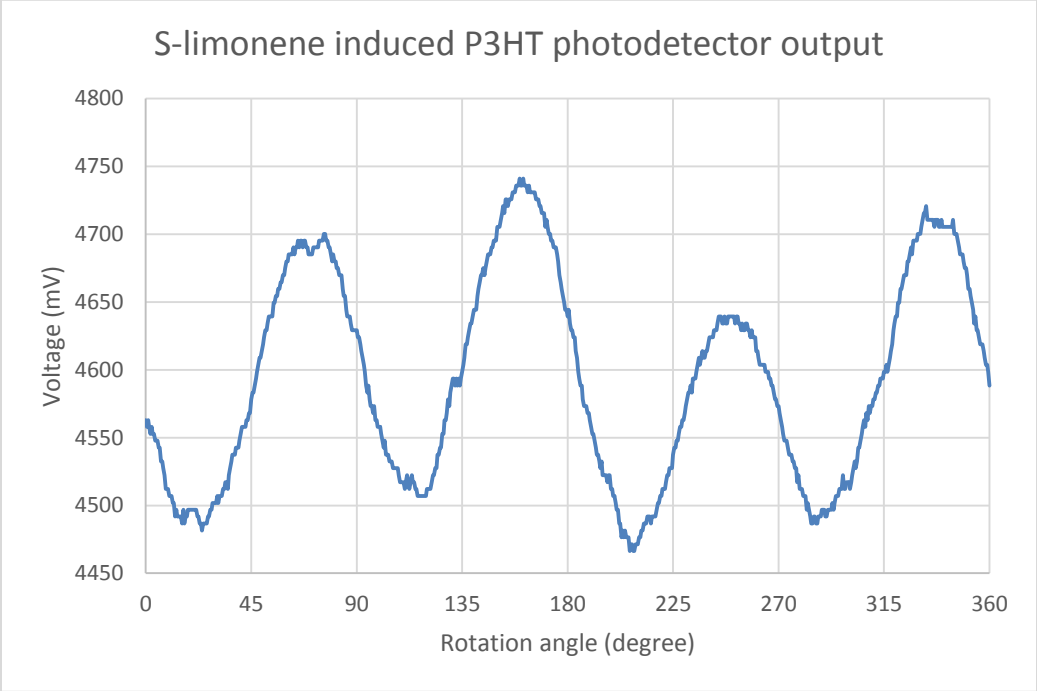

Figure 4-24 S-limonene induced P3HT photodetector output

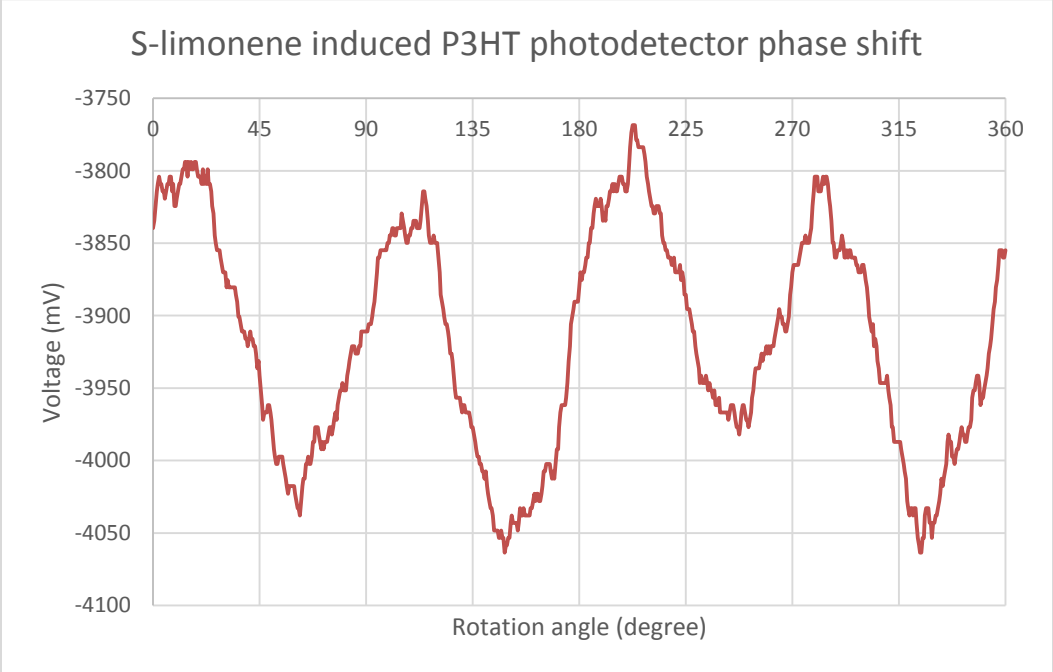

Figure 4-25 S-limonene induced P3HT photodetector phase shift compare to the reference signal

Table 4-2 Polarization sensitivity of photodetectors (The output voltage signals are relative values that generated by the lock-in amplifier #1.)

	Maxima output (mv, ±1%)	Minima output (mv, ±1%)	$a_{sensitivity}$ (±1%)
cPT	5.6E3	5.3E3	6%
R-limonene induced F8T2	5.1E3	3.9E3	27%
S-limonene induced F8T2	3.1E3	2.8E3	10%
R-limonene induced P3HT	3.0E3	2.8E3	7%
S-limonene induced P3HT	4.7E3	4.5E3	4%

All the limonene induced polymer photodetectors reach their maxima when the quarter-wave plate rotates every π/2. Furthermore, there is no significant difference for the output diagram of R- or S- limonene induced polymer. The sensitivity of limonene induced F8T2 is higher than 10%, and sensitivity of limonene induced P3HT is about 4%, close to that of cPT.

The oscillation at period π/2 for the limonene induced polymer photodetectors can be a result of the birefringence of limonene induced polymers. The polymer films absorb more energy when the light is circular polarized, while they absorb less energy when it is linear polarized. This lead to a higher response to either left-handed or right-handed polarized light than linear polarized light.

4.5 Suggested mechanism

From a previous study on X-ray diffraction of P3HT and F8T2, both polymers form π-π stacking in their microcrystalline structure.[42, 44]

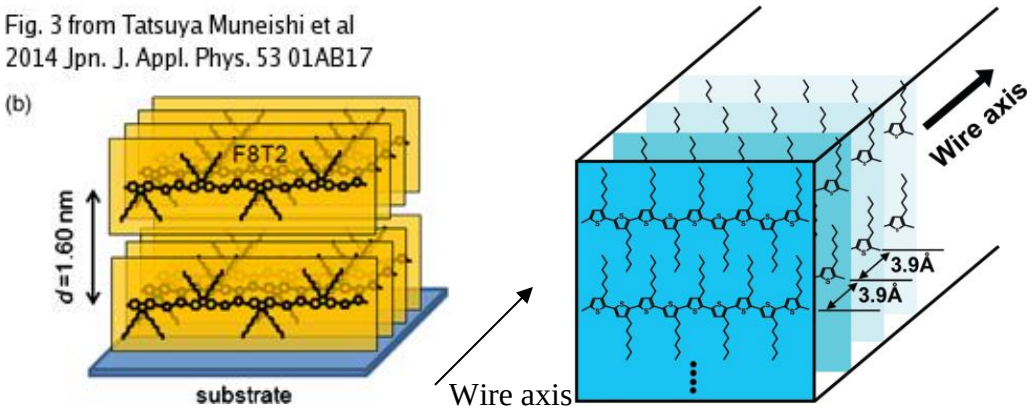

Figure 4-26 Schematic structure of F8T2 and P3HT crystalline structure [42, 44]

We discussed at 4.1 that, "hot spin-coated" F8T2 and P3HT have similar UV-Vis spectra to annealed films, suggesting that their crystalline structure are the same as **Figure 4-14**. Kawagoe et al. suggested a model structure of limonene induced F8T2 particles, which are formed by good-bad solvent method. **Figure 4-15** shows the limonene molecules induce the forming of helically ordered F8T2 π–π stacks. [45]

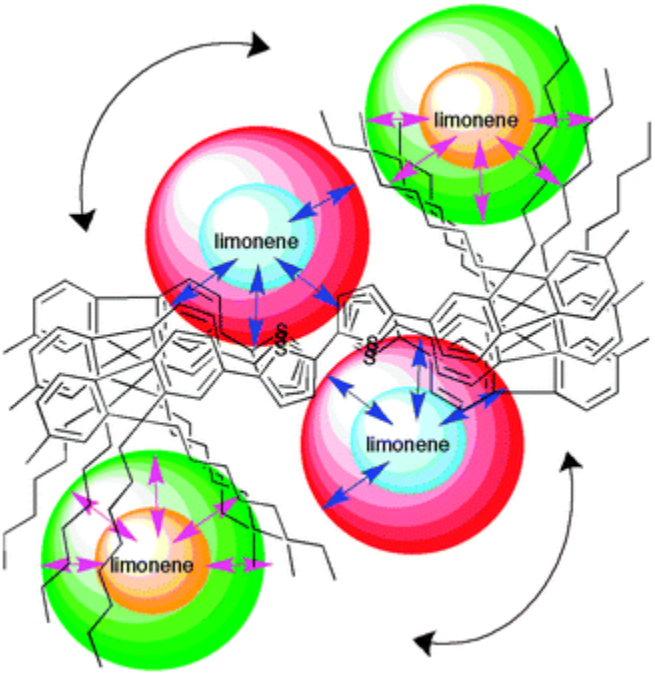

Figure 4-27 A proposed model structure of helically ordered F8T2 π–π stacks with limonene molecules. [45]

With the similar crystalline structure, P3HT may follow the same mechanism to gain helical structure:

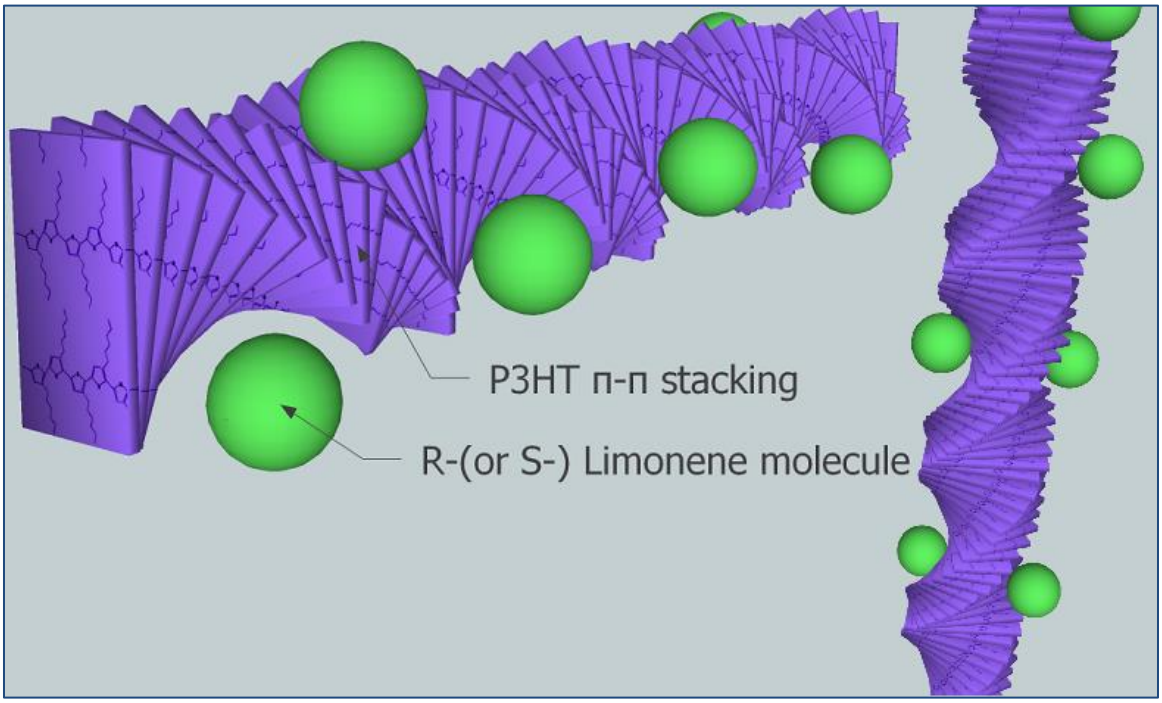

Figure 4-28 Proposed model structure of helically ordered P3HT π–π stacks with limonene molecules.

The π–π stacks of F8T2 or P3HT are induced to helix, and keep their helical orders after limonene is removed by vacuum evaporation.

Chiral substituted polythiophenes are believed to gain their chirality from inter-chain helical conformation, as well. It is very likely that, a splitting of the excited state of a chiral substituted polythiophene in two exciton levels when the polymer is in an aggregated phase. This splitting, which is not detected in absorption or emission spectroscopy, gives strong support for an inter-chain origin of the optical activity.[46]

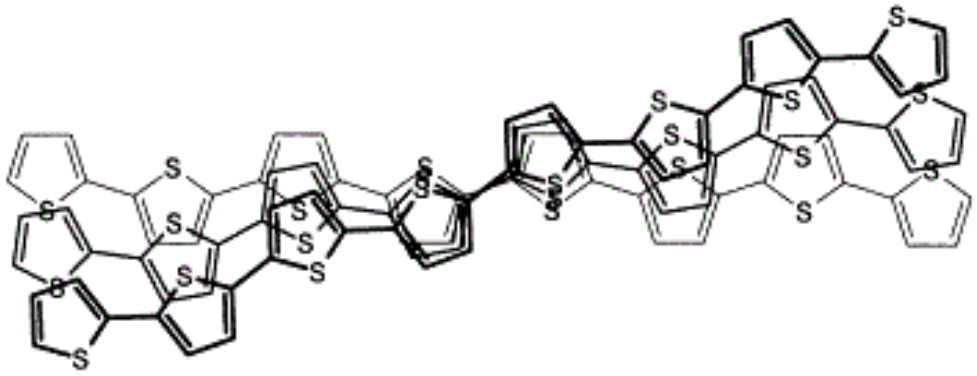

Figure 4-29 Helical packing of predominantly planar chains [46]

In Chapter 4.4.1, we see that the CPL response of the photodetector is significantly stronger than the CPL absorbance difference. A possible explanation is proposed here: In the bulk heterojunction photodetectors, the photoelectric effect is usually stronger when the polymer is in a higher crystallinity. Owing to the mechanism of the induction of the optical activity, higher crystallinity domains would have a stronger CD. Thus, as the CD of the photodetectors is measured all over the slide, the CD data delivers a lower estimate of the CD in the higher crystallinity regions that contribute more efficiently to the photoelectric effect.

Chapter 5

Conclusions and Future Work

5.1 Conclusions

The polymer photodetector fabricated using polythiophene with chiral alkyl side chains is proven to be able to identify left- and right-handed CPL. However, the distinction sensitivity of the photodetector is measured to be higher than the inequality of left- and right-handed CPL absorbance, indicating a mechanism of CPL sensitivity other than CPL absorbance inequality. As a solution-casting thin film electronic device, it can be promising for low-cost and miniaturized circular polarized light detection.

CPL distinction is not observed in polymer photodetectors that are made from chiral limonene induced achiral polymers. Instead, these photodetectors can identify incident light between linear polarized light and CPL. This phenomenon is suggested due to the birefringence of the polymer film.

A model is suggested to explain the chirality generation of the polythiophene with chiral alkyl side chains and limonene induced achiral polymers. The similar shape of the CD spectra of limonene induced P3HT and cPT suggests that they may share the same mechanism of chirality generation.

5.2 Future works

Though the products of "hot spin-coating" process are very unrepeatable due to the unrepeatable process condition, optimization of limonene induced polymers is one of the future directions of this project. Isolated examples already show very strong Cotton effect in chiral induced polymer's CD spectra (see appendix), showing promising potential of high CPL sensitivity.

The suggested model of the polymer crystalline will be tested by X-ray diffraction and morphology study. The mechanism of CPL sensitivity of the polythiophene with chiral alkyl side chains will be studied in the future.

More polymer photoelectric devices can be fabricated from chiral polymers. For instance, polymer light-emitting diodes (LED) made from chiral polymers can be a cheap, simple and efficient solution of CPL source.

1. Deen, M. J., and Prasanta Kumar Basu, *Silicon Photonics: Fundamentals and Devices*. Wiley: 2012.

2. Leigh, W. B., *Devices for optoelectronics*. CRC Press: 1996.

3. Agrawal; P, G.; Agrawal, G., *Lightwave technology: components and devices*. Wiley-Interscience: 2004.

4. Ng; Kwok, K., *Complete guide to semiconductor devices*. IEEE press: 2002.

5. Kaneko, M.; Taneda, T.; Tsukagawa, T.; Kajii, H.; Ohmori, Y., Fast response of organic photodetectors utilizing multilayered metal-phthalocyanine thin films. *Japanese Journal of Applied Physics Part 1-Regular Papers Short Notes & Review Papers* **2003,** *42* (4B), 2523-2525.

6. Dong, H. L.; Zhu, H. F.; Meng, Q.; Gong, X.; Hu, W. P., Organic photoresponse materials and devices. *Chemical Society Reviews* **2012,** *41* (5), 1754-1808.

7. Morimune, T.; Kam, H.; Ohmori, Y., High-speed organic photodetectors using heterostructure with phthalocyanine and perylene derivative. *Japanese Journal of Applied Physics Part 1-Regular Papers Brief Communications & Review Papers* **2006,** *45* (1B), 546-549.

8. Choi, J. M.; Lee, J.; Hwang, D. K.; Kim, J. H.; Im, S.; Kim, E., Comparative study of the photoresponse from tetracene-based and pentacene-based thin-film transistors. *Applied Physics Letters* **2006,** *88* (4).

9. Yakuphanoglu, F.; Farooq, W. A., Flexible pentacene organic field-effect phototransistor. *Synthetic Metals* **2011,** *161* (5-6), 379-383.

10. Dimitrakopoulos, C. D.; Malenfant, P. R. L., Organic thin film transistors for large area electronics. *Advanced Materials* **2002,** *14* (2), 99-+.

11. Kleymyuk, E. A.; Troshin, P. A.; Khakina, E. A.; Luponosov, Y. N.; Moskvin, Y. L.; Peregudova, S. M.; Babenko, S. D.; Meyer-Friedrichsen, T.; Ponomarenko, S. A., 3D quater- and quinquethiophenesilanes as promising electron-donor materials for BHJ photovoltaic cells and photodetectors. *Energy & Environmental Science* **2010,** *3* (12), 1941-1948.

12. Higashi, Y.; Kim, K. S.; Jeon, H. G.; Ichikawa, M., Enhancing spectral contrast in organic red-light photodetectors based on a light-absorbing and exciton-blocking layered system. *Journal of Applied Physics* **2010,** *108* (3).

13. Tamayo, A. B.; Walker, B.; Nguyen, T. Q., A low band gap, solution processable oligothiophene with a diketopyrrolopyrrole core for use in organic solar cells. *Journal of Physical Chemistry C* **2008,** *112* (30), 11545-11551.

14. Qian, G.; Qi, J.; Davey, J. A.; Wright, J. S.; Wang, Z. Y., Family of Diazapentalene Chromophores and Narrow-Band-Gap Polymers: Synthesis, Halochromism, Halofluorism, and Visible-Near Infrared Photodetectivity. *Chemistry of Materials* **2012,** *24* (12), 2364-2372.

15. Qian, G.; Qi, J.; Wang, Z. Y., Synthesis and study of low-bandgap polymers containing the diazapentalene and diketopyrrolopyrrole chromophores for potential use in solar cells and near-infrared photodetectors. *Journal of Materials Chemistry* **2012,** *22* (25), 12867-12873.

16. Uhrich, C.; Schueppel, R.; Petrich, A.; Pfeiffer, M.; Leo, K.; Brier, E.; Kilickiran, P.; Baeuerle, P., Organic thin-film photovoltaic cells based on oligothiophenes with reduced bandgap. *Advanced Functional Materials* **2007,** *17* (15), 2991-2999.

17. Leem, D. S.; Lee, K. H.; Park, K. B.; Lim, S. J.; Kim, K. S.; Jin, Y. W.; Lee, S., Low dark current small molecule organic photodetectors with selective response to green light. *Applied Physics Letters* **2013,** *103* (4).

18. Wurthner, F.; Stolte, M., Naphthalene and perylene diimides for organic transistors. *Chemical Communications* **2011,** *47* (18), 5109-5115.

19. Varotto, A.; Treat, N. D.; Jo, J.; Shuttle, C. G.; Batara, N. A.; Brunetti, F. G.; Seo, J. H.; Chabinyc, M. L.; Hawker, C. J.; Heeger, A. J.; Wudl, F., 1,4-Fullerene Derivatives: Tuning the Properties of the Electron Transporting Layer in Bulk-Heterojunction Solar Cells. *Angewandte Chemie-International Edition* **2011,** *50* (22), 5166-5169.

20. Yu, G.; Pakbaz, K.; Heeger, A. J., SEMICONDUCTING POLYMER DIODES - LARGE-SIZE, LOW-COST PHOTODETECTORS WITH EXCELLENT VISIBLE-ULTRAVIOLET SENSITIVITY. *Applied Physics Letters* **1994,** *64* (25), 3422-3424.

21. McDonald, S. A.; Konstantatos, G.; Zhang, S. G.; Cyr, P. W.; Klem, E. J. D.; Levina, L.; Sargent, E. H., Solution-processed PbS quantum dot infrared photodetectors and photovoltaics. *Nature Materials* **2005,** *4* (2), 138-U14.

22. Brabec, C. J.; Padinger, F.; Sariciftci, N. S.; Hummelen, J. C., Photovoltaic properties of conjugated polymer/methanofullerene composites embedded in a polystyrene matrix. *Journal of Applied Physics* **1999,** *85* (9), 6866-6872.

23. Ramuz, Marc, et al. High sensitivity organic photodiodes with low dark currents and increased lifetimes. *Organic Electronics* **2008,** *9* (3), 369 - 376.

24. Xu, J. J.; Hu, J. C.; Liu, X. F.; Qiu, X. H.; Wei, Z. X., Stepwise Self-Assembly of P3HT/CdSe Hybrid Nanowires with Enhanced Photoconductivity. *Macromolecular Rapid Communications* **2009,** *30* (16), 1419-1423; Gowrishankar, V.; Scully, S. R.; Chan, A. T.; McGehee, M. D.; Wang, Q.; Branz, H. M., Exciton harvesting, charge transfer, and charge-carrier transport in amorphous-silicon nanopillar/polymer hybrid solar cells. *Journal of Applied Physics* **2008,** *103* (6); Beek, W. J. E.; Wienk, M. M.; Janssen, R. A. J., Hybrid solar cells from regioregular polythiophene and ZnO nanoparticles. *Advanced Functional Materials* **2006,** *16* (8), 1112-1116.

25. Heeger, A. J., Semiconducting polymers: the Third Generation. *Chemical Society Reviews* **2010,** *39* (7), 2354-2371.

26. Gong, X.; Tong, M. H.; Xia, Y. J.; Cai, W. Z.; Moon, J. S.; Cao, Y.; Yu, G.; Shieh, C. L.; Nilsson, B.; Heeger, A. J., High-Detectivity Polymer Photodetectors with Spectral Response from 300 nm to 1450 nm. *Science* **2009,** *325* (5948), 1665-1667.

27. Shaheen, S. E.; Brabec, C. J.; Sariciftci, N. S.; Padinger, F.; Fromherz, T.; Hummelen, J. C., 2.5% efficient organic plastic solar cells. *Applied Physics Letters* **2001,** *78* (6), 841-843.

28. Pasteur, L., *Recherches sur les relations qui peuvent exister entre la forme cristalline: la composition chimique et les sens de la polarisation rotatoire*. Bachelier: 1848.

29. http://en.wikipedia.org/wiki/Circular_polarization.

30. Cotton, A., Anomalous rotatory dispersion in absorbing bodies. *Compt Rend* **1895,** *120*, 1044-1046.

31. Czichos, H.; Saiato, T.; Smith, L. L. R., *Springer handbook of materials measurement methods*. Springer: 2006.

32. The origin of optical activity. http://www.photophysics.com/tutorials/circular-dichroism-cd-spectroscopy/2-chiral-molecules.

33. Blout, E.; Stryer, L., Anomalous optical rotatory dispersion of dye: polypeptide complexes. *Proceedings of the National Academy of Sciences of the United States of America* **1959,** *45* (11), 1591.

34. Bosnich, B.; Dwyer, F., Bis-1, 10-phenanthroline complexes of divalent ruthenium. *Australian Journal of Chemistry* **1966,** *19* (12), 2229-2233.

35. Green, M. M.; Khatri, C.; Peterson, N. C., A macromolecular conformational change driven by a minute chiral solvation energy. *Journal of the American Chemical Society* **1993,** *115* (11), 4941-4942.

36. Sharma, V.; Crne, M.; Park, J. O.; Srinivasarao, M., Structural origin of circularly polarized iridescence in jeweled beetles. *Science* **2009,** *325* (5939), 449-451.

37. Chiou, T.-H.; Kleinlogel, S.; Cronin, T.; Caldwell, R.; Loeffler, B.; Siddiqi, A.; Goldizen, A.; Marshall, J., Circular polarization vision in a stomatopod crustacean. *Current Biology* **2008,** *18* (6), 429-434.

38. Microbeam Nuevo accesorio para medidas de Dispersión óptica rotatoria (ORD) en cinéticas rápidas. http://microbeam.wordpress.com/2012/01/23/nuevo-accesorio-para-medidas-de-dispersion-optica-rotatoria-ord-en-cineticas-rapidas/.

39. Andersson, M.; Ekeblad, P. O.; Hjertberg, T.; Wennerstrom, O.; Inganas, O., POLYTHIOPHENE WITH A FREE AMINO-ACID SIDE-CHAIN. *Polymer Communications* **1991,** *32* (18), 546-548.

40. Bidan, G.; Guillerez, S.; Sorokin, V., Chirality in regioregular and soluble polythiophene: An internal probe of conformational changes induced by minute solvation variation. *Advanced Materials* **1996,** *8* (2), 157-&.

41. Yu, G.; Gao, J.; Hummelen, J.; Wudl, F.; Heeger, A., Polymer photovoltaic cells: enhanced efficiencies via a network of internal donor-acceptor heterojunctions. *Science-AAAS-Weekly Paper Edition* **1995,** *270* (5243), 1789-1790.

42. Kanai, K.; Miyazaki, T.; Suzuki, H.; Inaba, M.; Ouchi, Y.; Seki, K., Effect of annealing on the electronic structure of poly (3-hexylthiophene) thin film. *Physical Chemistry Chemical Physics* **2010,** *12* (1), 273-282.

43. Kuhn, W., The physical significance of optical rotatory power. *Transactions of the Faraday Society* **1930,** *26*, 0293-0307.

44. Muneishi, T.; Ishizumi, A.; Yanagi, H., Annealing effect on light-emitting FET characteristics of π-conjugated liquid crystalline polymer. *Japanese Journal of Applied Physics* **2014,** *53* (1S), 01AB17.

45. Kawagoe, Y.; Fujiki, M.; Nakano, Y., Limonene magic: noncovalent molecular chirality transfer leading to ambidextrous circularly polarised luminescent [small pi]-conjugated polymers. *New Journal of Chemistry* **2010,** *34* (4), 637-647.

46. Langeveld-Voss, B. M. W., R. A. J. Janssen, and E. W. Meijer, On the origin of optical activity in polythiophenes. *Journal of Molecular Structure* **2000,** *521* (1–3), 285 - 301.

Appendix

Supplementary Data

Limonene induced P3HT batch #1

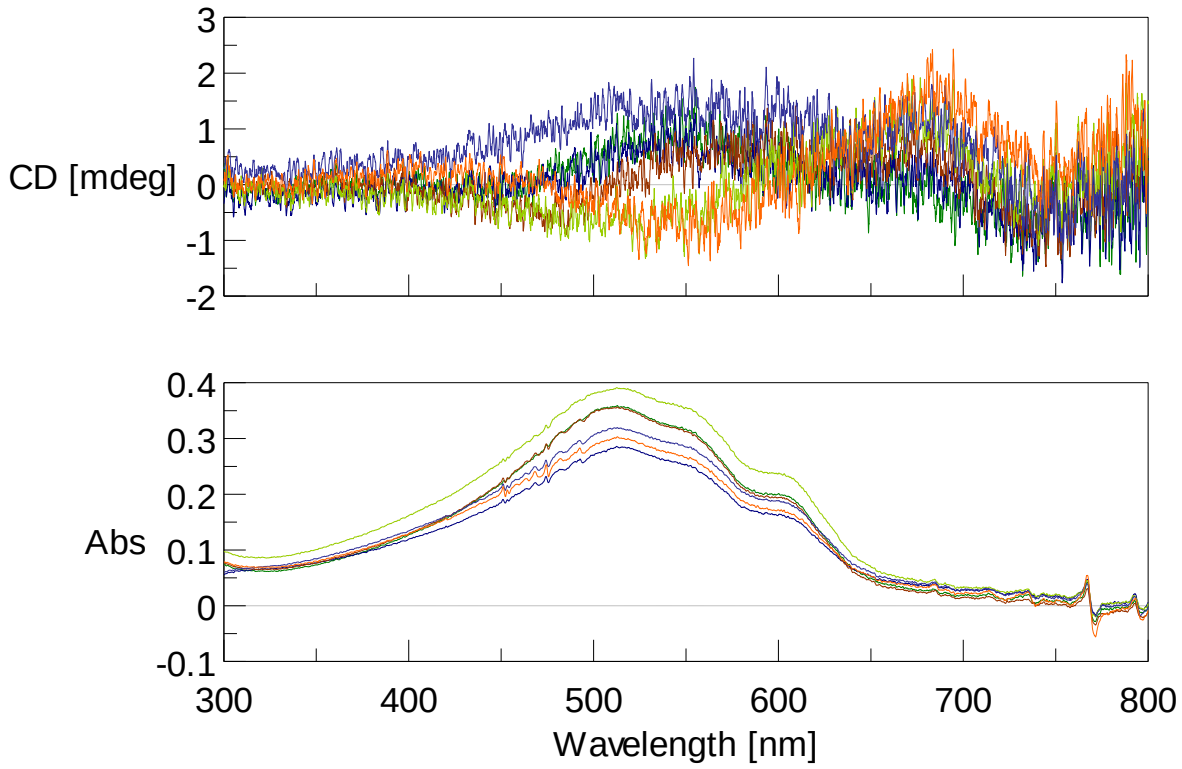

R-Limonene induced P3HT sample 1
R-Limonene induced P3HT sample 2
R-Limonene induced P3HT sample 3
S-Limonene induced P3HT sample 1
S-Limonene induced P3HT sample 2
S-Limonene induced P3HT sample 3

Limonene induced P3HT batch #2

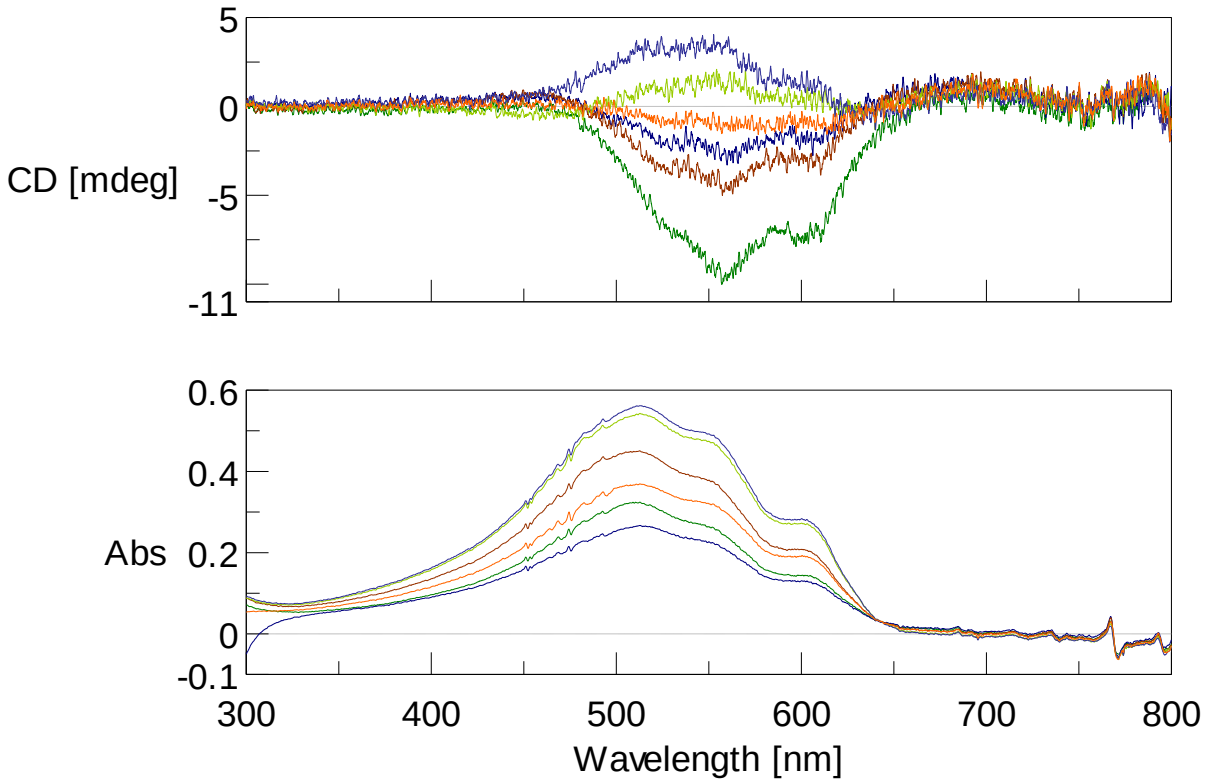

R-Limonene induced P3HT sample 1
R-Limonene induced P3HT sample 2
R-Limonene induced P3HT sample 3
S-Limonene induced P3HT sample 1
S-Limonene induced P3HT sample 2
S-Limonene induced P3HT sample 3

Limonene induced P3HT batch #3

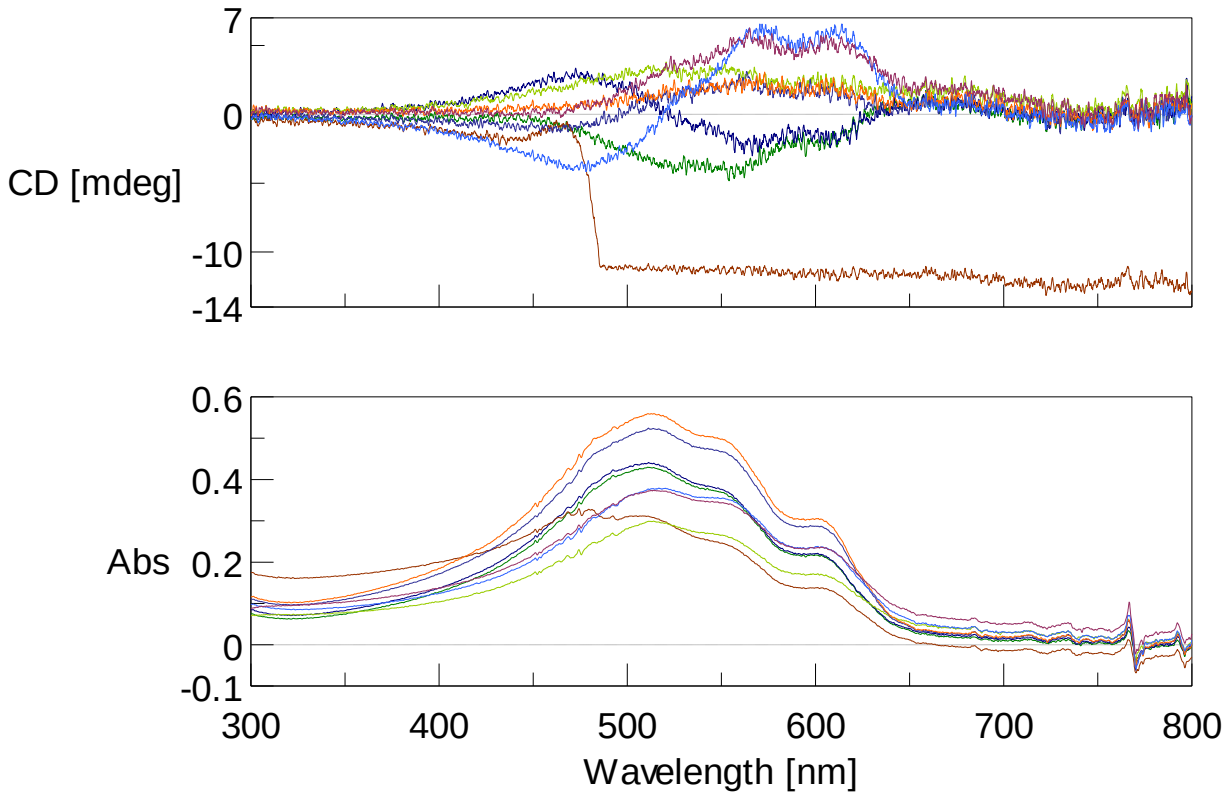

R-Limonene induced P3HT, measured vertically in middle

R-Limonene induced P3HT, measured horizontally in middle

R-Limonene induced P3HT, measured vertically on side

R-Limonene induced P3HT, measured horizontally on side

S-Limonene induced P3HT, measured vertically in middle

S-Limonene induced P3HT, measured horizontally in middle

S-Limonene induced P3HT, measured vertically on side

S-Limonene induced P3HT, measured horizontally on side

Limonene induced P3HT batch #4

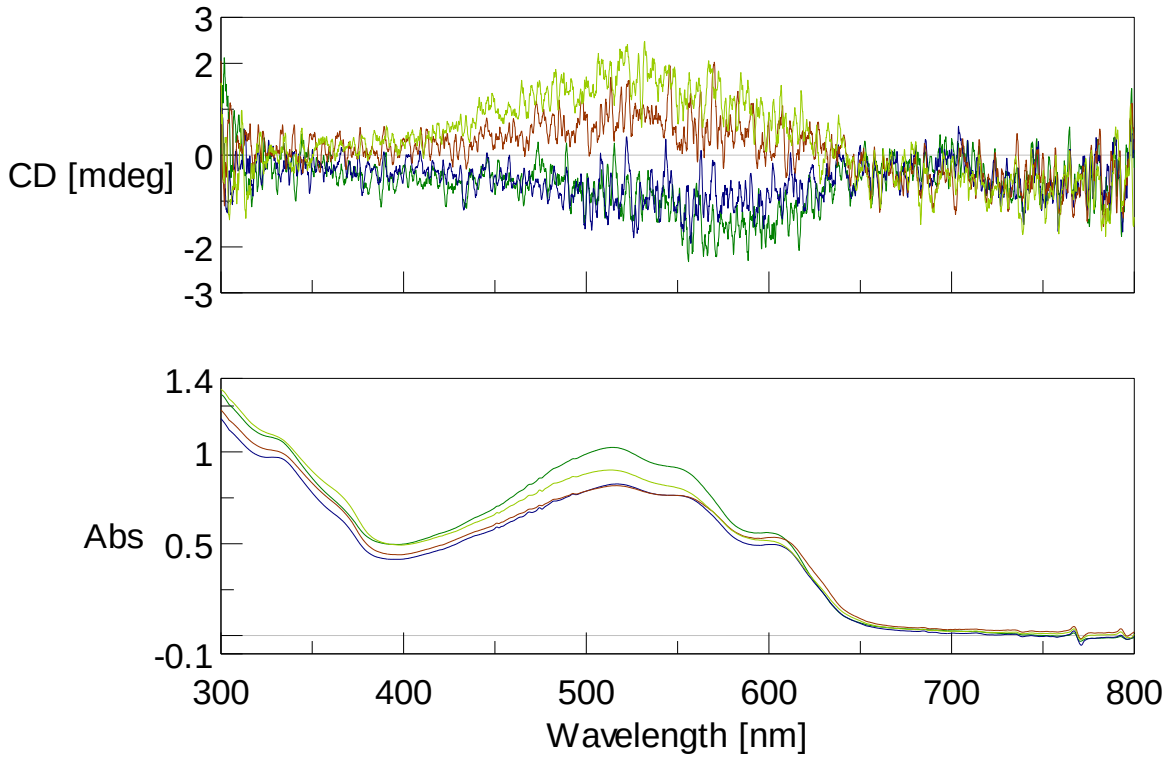

R-Limonene induced P3HT sample 1

R-Limonene induced P3HT sample 2

S-Limonene induced P3HT sample 1

S-Limonene induced P3HT sample 2

Limonene induced F8T2 batch #1

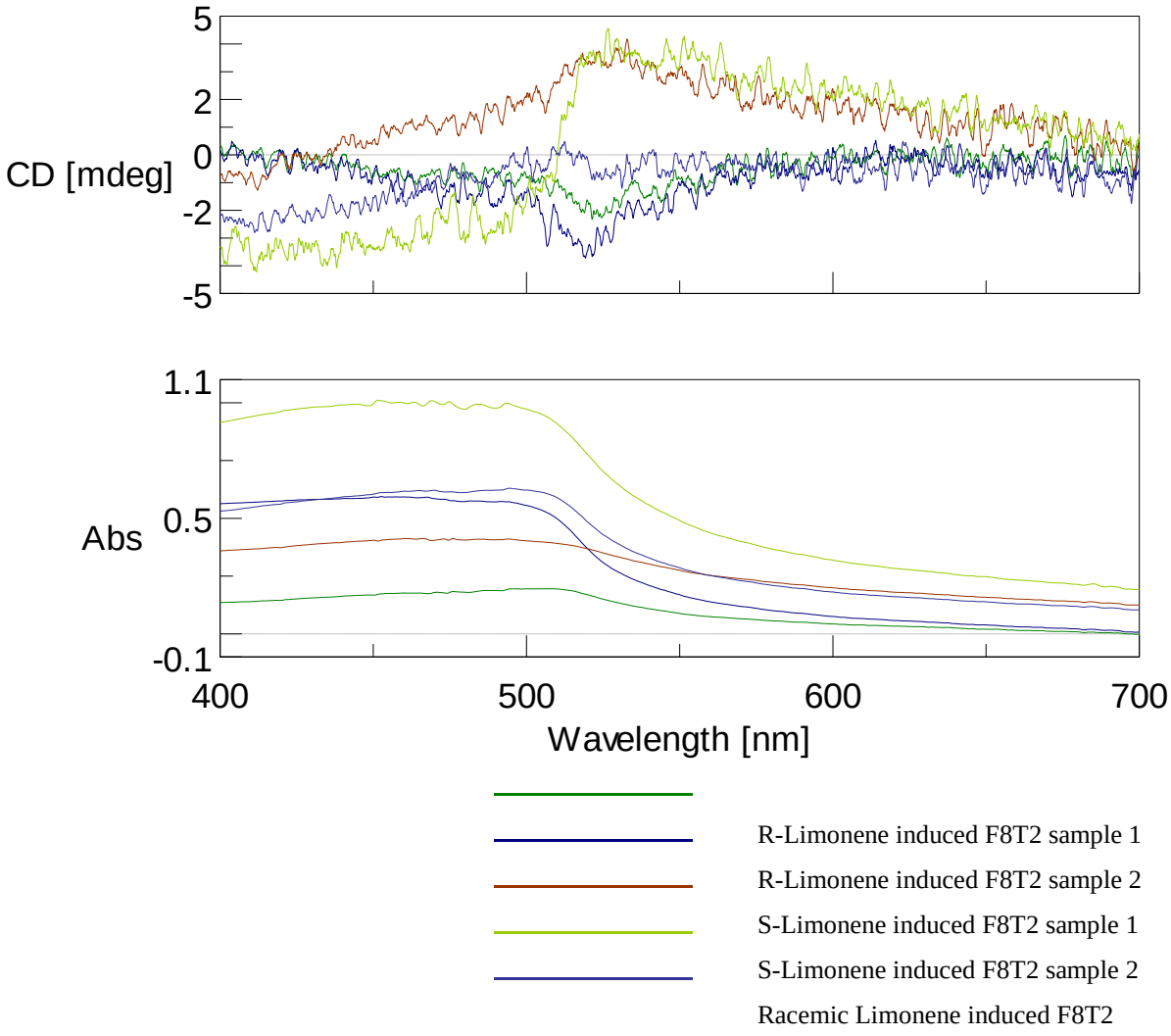

Limonene induced F8T2 batch #2

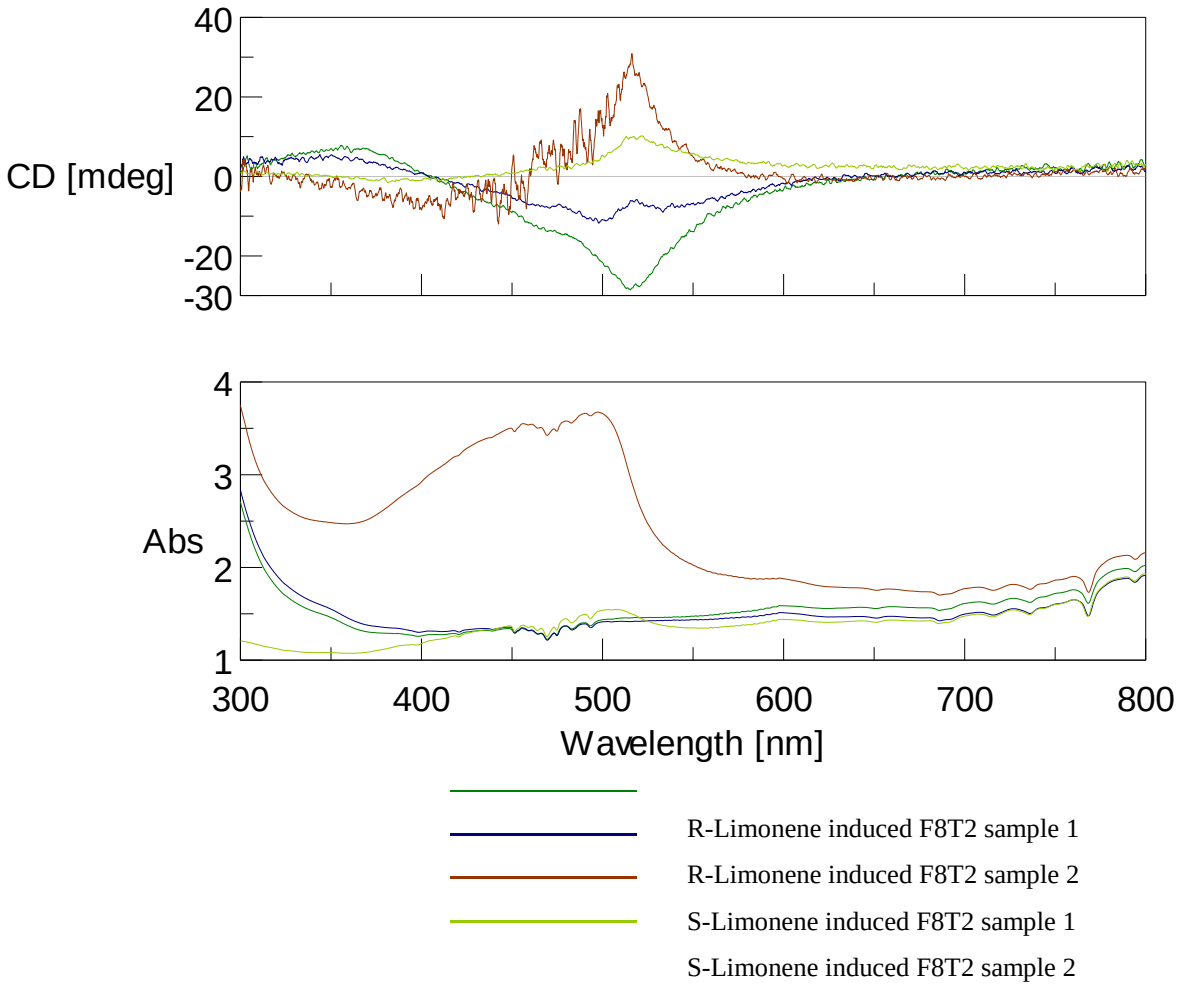

Limonene induced F8T2 batch #3

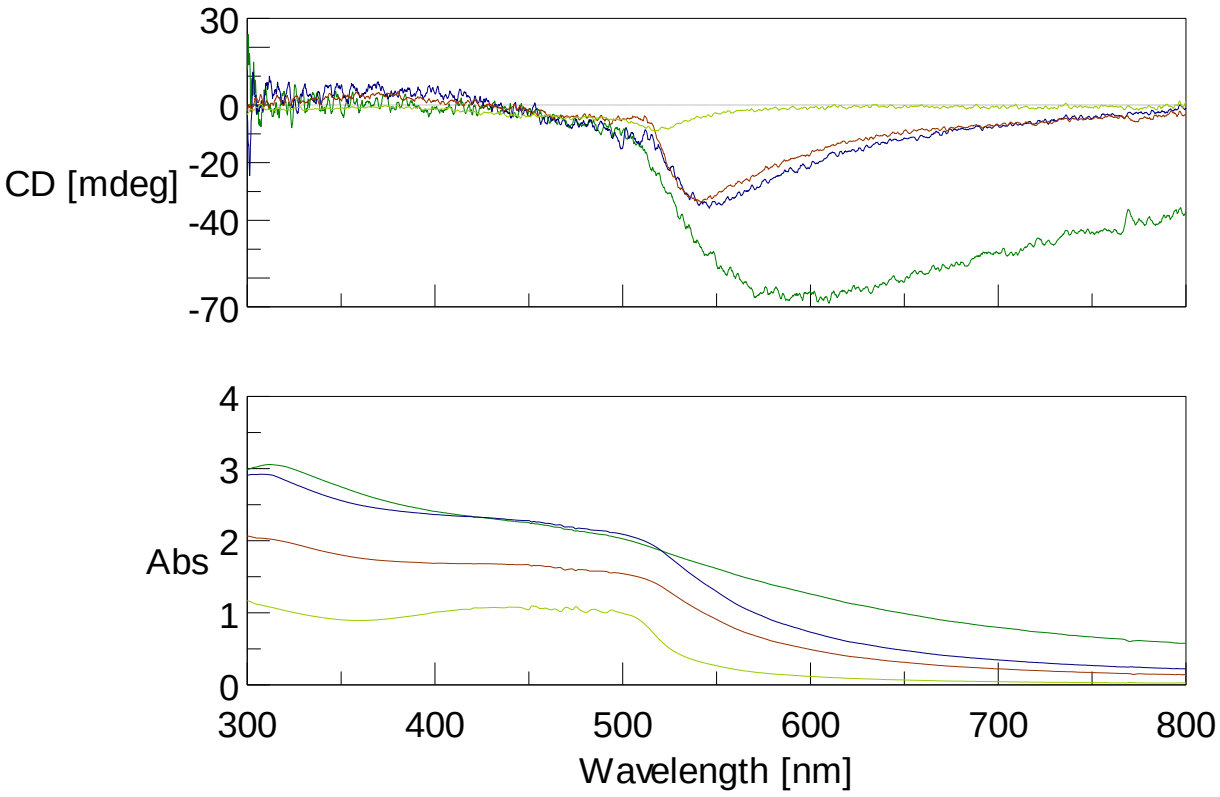

R-Limonene induced F8T2 sample 1

R-Limonene induced F8T2 sample 2

R-Limonene induced F8T2 sample 3

R-Limonene induced F8T2 sample 4

Limonene induced F8T2 sample #4

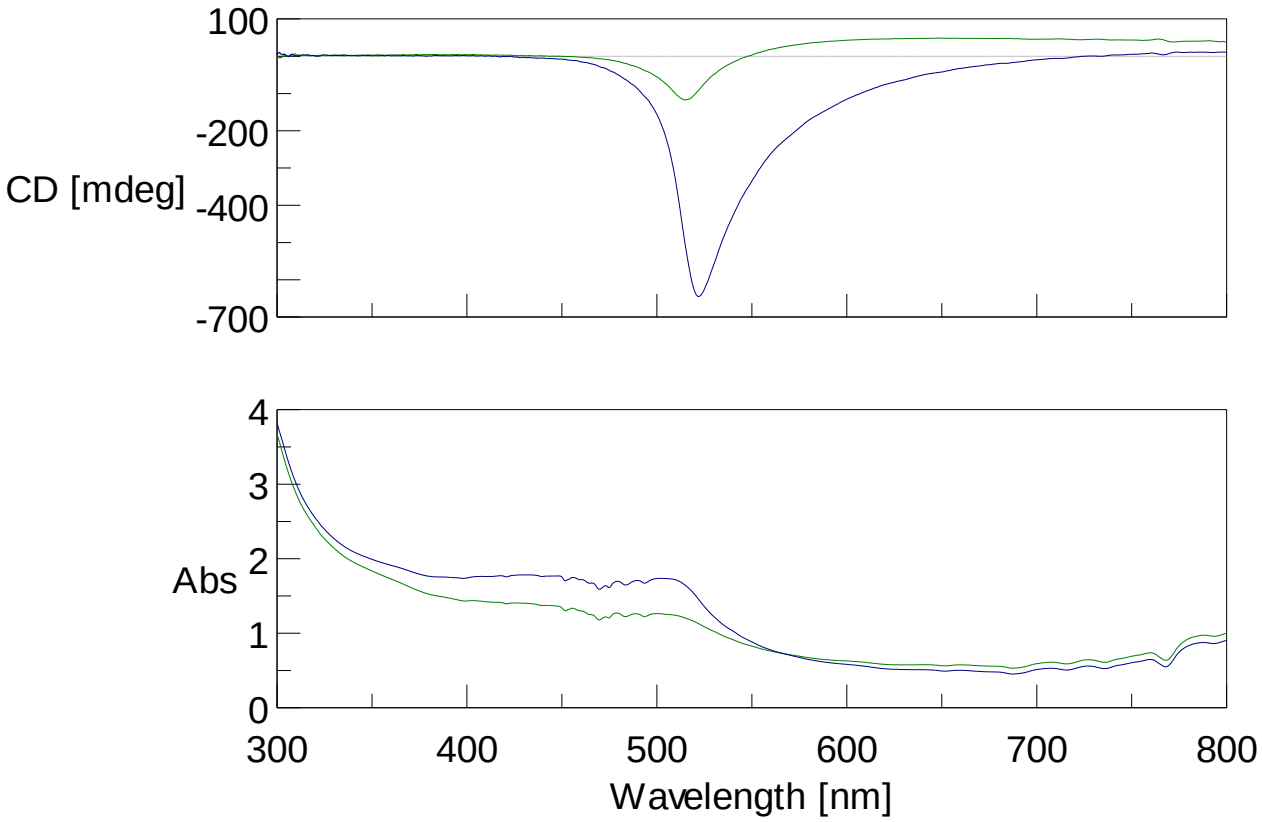

R-Limonene induced F8T2 measured at spot 1

R-Limonene induced F8T2 measured at spot 2

cPT sample 1

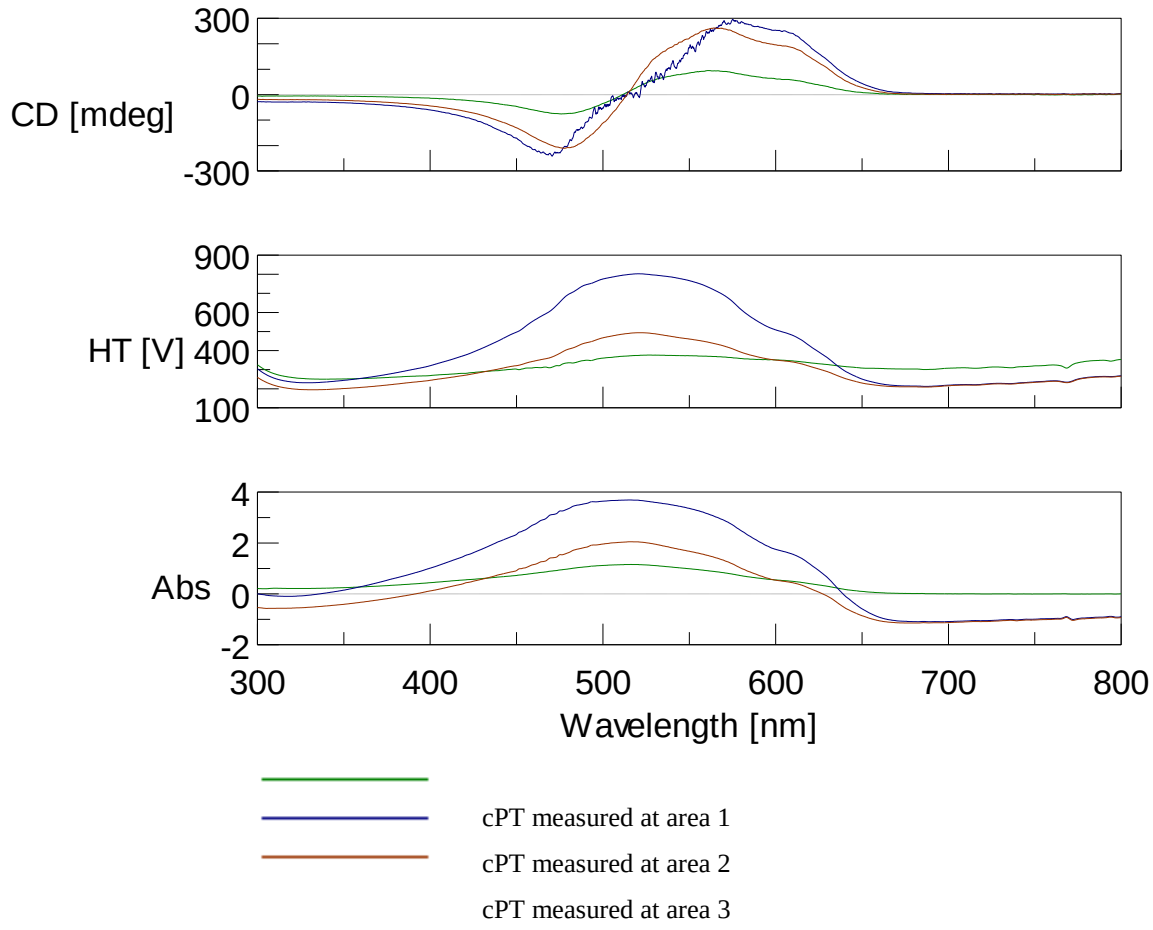
300
0
-300
CD [mdeg]
900
600
400
100
HT [V]
4
2
0
-2
Abs
300
400
500
600
700
800
Wavelength [nm]
cPT measured at area 1
cPT measured at area 2
cPT measured at area 3

cPT batch 2

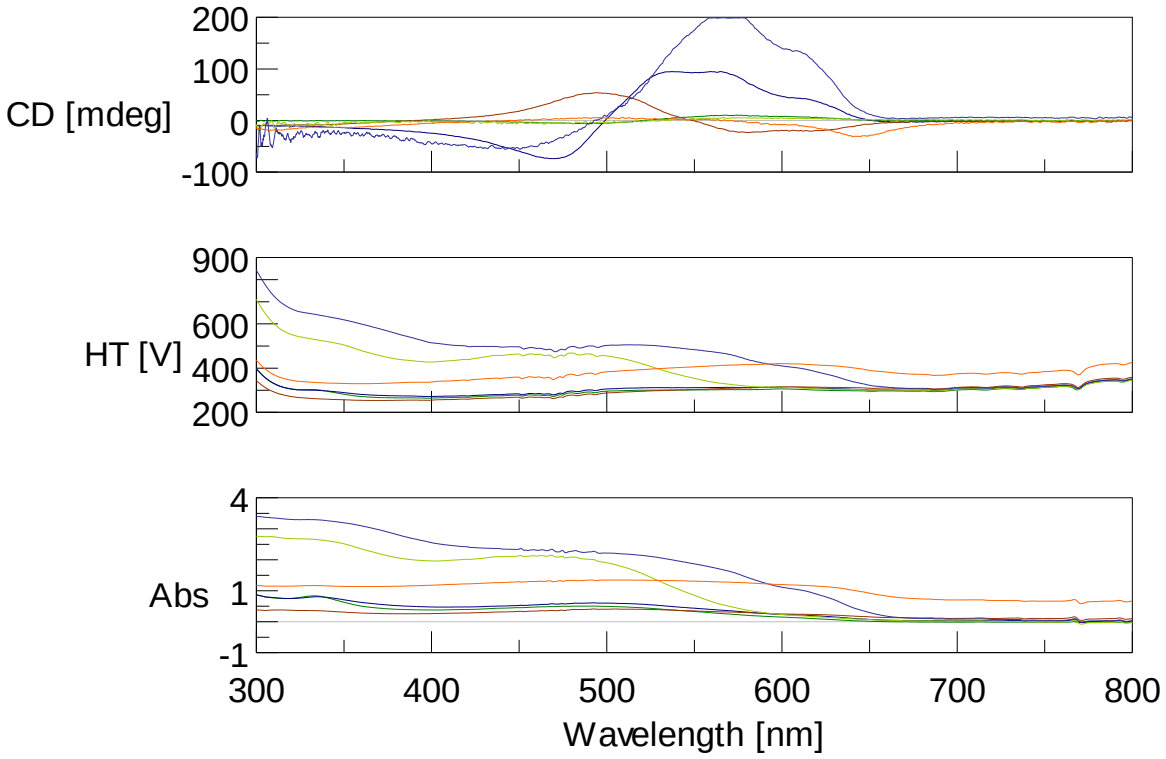

cPT as cast

cPT 120 C° annealed for 12 min

cPT 120 C° annealed for 30 min

cPT as cast

cPT 120 C° annealed for 5 min

cPT 120 C° annealed for 5 min, cools down to room temperature then 120 C° annealed for another 5 min